

*Exxon Valdez* Oil Spill  
Long-Term Monitoring Program (Gulf Watch Alaska) Final Report

Long-Term Monitoring of Oceanographic Conditions in Prince William Sound

*Exxon Valdez* Oil Spill Trustee Council Project 16120114-E  
Final Report

Robert W. Campbell

Prince William Sound Science Center  
300 Breakwater Ave., Box 705  
Cordova, AK, 99574

May 2018

The *Exxon Valdez* Oil Spill Trustee Council administers all programs and activities free from discrimination based on race, color, national origin, age, sex, religion, marital status, pregnancy, parenthood, or disability. The Council administers all programs and activities in compliance with Title VI of the Civil Rights Act of 1964, Section 504 of the Rehabilitation Act of 1973, Title II of the Americans with Disabilities Act of 1990, the Age Discrimination Act of 1975, and Title IX of the Education Amendments of 1972. If you believe you have been discriminated against in any program, activity, or facility, or if you desire further information, please write to: EVOS Trustee Council, 4230 University Drive, Suite 220, Anchorage, Alaska 99508-4650, or [dfg.evos.restoration@alaska.gov](mailto:dfg.evos.restoration@alaska.gov); or O.E.O., U.S. Department of the Interior, Washington, D.C. 20240.

*Exxon Valdez* Oil Spill  
Long-Term Monitoring Program (Gulf Watch Alaska) Final Report

Long-Term Monitoring of Oceanographic Conditions in Prince William Sound

*Exxon Valdez* Oil Spill Trustee Council Project 16120114-E  
Final Report

Robert W. Campbell

Prince William Sound Science Center  
300 Breakwater Ave., Box 705  
Cordova, AK, 99574

May 2018

# Long-Term Monitoring of Oceanographic Conditions in Prince William Sound

## *Exxon Valdez* Oil Spill Trustee Council Project 16120114-E Final Report

**Study History:** This project materially began as *Exxon Valdez* Oil Spill Trustee Council Project 10100132 of the Prince William Sound Herring Survey program (2009-2012), which included vessel surveys to the same stations occupied as part of this project. This project was approved by the *Exxon Valdez* Oil Spill Trustee Council in 2011, and funding began in February 2012. Fieldwork for this project began in 2013 and continued until December 2016, and the analysis of samples is ongoing. Annual reports were submitted in 2012 through 2015. Data from this project have been published in two manuscripts which are presented in this report as Appendices:

**Campbell, R.W.** 2018. Hydrographic trends in Prince William Sound, Alaska, 1960–2016. *Deep Sea Research II* 147:43-57. doi: 10.1016/j.dsr2.2017.08.014

McKinstry, C.A.E., and **R.W. Campbell.** 2018. Seasonal variation of zooplankton abundance and community structure in Prince William Sound, Alaska, 2009–2016. *Deep Sea Research II* 147:69-78. doi: 10.1016/j.dsr2.2017.08.016

**Abstract:** In order to track the bottom-up factors (environmental, biogeochemical and lower trophic level) that may be important for ecosystem function, regular surveys of the Prince William Sound region were conducted between 2013 and 2016, and consisted of basic oceanographic and biological measurements (temperature and salinity; chlorophyll-a, nitrate, and zooplankton concentrations). Additionally, an autonomous profiling mooring was deployed in central Prince William Sound, to capture high frequency variability in the surface layer. Analysis of a now 40-year long time series of temperature and salinity suggests that the region is experiencing a warming and a freshening trend in the surface waters, which may have enhanced horizontal transport mechanisms. The most recent years (2014 to present) have reflected a widespread warm anomaly throughout the Gulf of Alaska (aka “The Blob”). Biological measurements showed considerable year-to-year variability, although the basic trends in the biological cycles were consistent: a large spring phytoplankton bloom occurs each year in most locations, and also a less frequent autumn bloom. Zooplankton taxa broke out into several space/time groups, which corresponded with the physical and biological cycles, and appeared to be fairly consistent from year to year, although taxa shifts have been observed that are likely a reflection of the recent warm anomaly.

**Key words:** climate, oceanography, phytoplankton, Prince William Sound, salinity, temperature, zooplankton

**Project Data:** Data collected during this project includes conductivity, temperature, depth (CTD) casts, depth-specific chlorophyll concentrations, and zooplankton species composition and abundance. CTD data are in text files in the format produced by the software provided by the CTD manufacturer; all data processing steps are documented in

metadata headers within each file, as well as station metadata (station name, event number, longitude, latitude, date and time). Chlorophyll and zooplankton data are in flat text files. All of the data are publically available on the Alaska Ocean Observing System (AOOS) data portal (<http://portal.aos.org/gulf-of-alaska.php#metadata/fc5b0956-ef7c-49df-b261-c8e2713887fc/project>).

The custodian of the data is Robert Campbell, PWS Science Center, Box 705 Cordova, AK, [rcampbell@pwssc.org](mailto:rcampbell@pwssc.org).

The AOOS contact is Carol Janzen, 1007 W. 3rd Ave. #100, Anchorage, AK 99501, 907-644-6703, [janzen@aos.org](mailto:janzen@aos.org), <http://portal.aos.org/gulf-of-alaska.php>.

There are no limitations on the use of the data, however, it is requested that the authors be cited for any subsequent publications that reference this dataset. It is strongly recommended that careful attention be paid to the contents of the metadata file associated with these data to evaluate data set limitations or intended use.

**Citation:**

Campbell, R. W. 2018. Long term monitoring of oceanographic conditions in Prince William Sound. *Exxon Valdez* Oil Spill Trustee Council Project Final Report (Project 16120114-E), *Exxon Valdez* Oil Spill Trustee Council, Anchorage, Alaska.

## TABLE OF CONTENTS

Executive Summary.....	1
Introduction.....	2
Objectives.....	4
Methods.....	5
Results.....	7
Discussion.....	12
Conclusions.....	14
Acknowledgements.....	14
Literature Cited.....	14
Other References.....	16
Appendix A.....	<b>Error! Bookmark not defined.</b>
Appendix B.....	33

## LIST OF FIGURES

Figure 1. Prince William Sound, Alaska. The 12 stations occupied during the vessel surveys are indicated by the red dots, and the profiler was deployed at the “Mooring” site.....	5
Figure 2. A typical daily profile cycle done by the autonomous profiler. Most of the day is spent at a park depth (~60 m) in a low power state.....	6
Figure 3. Temperature time series measured by the autonomous profiler during each year of deployment in Prince William Sound, Alaska.....	8
Figure 4. Salinity time series measured by the autonomous profiler during each year of deployment in Prince William Sound, Alaska.....	8
Figure 5. Fluorescence time series measured by the autonomous profiler during each year of deployment in Prince William Sound, Alaska. Fluorescence is given as digital counts, which are linearly proportional to in situ chlorophyll-a fluorescence, and have been log <sub>10</sub> transformed. ....	9
Figure 6. Nitrate time series measured by the autonomous profiler during each year of deployment in Prince William Sound, Alaska.....	9
Figure 7. Temperature anomalies during each year of deployment in Prince William Sound, Alaska. Temperature observations were converted to anomalies by subtraction from the seasonally detrended annual average (see Campbell Appendix A). ....	11
Figure 8. Salinity anomalies during each year of deployment. Salinity observations were converted to anomalies by subtraction from the seasonally detrended annual average (see Campbell Appendix A). ....	11
Figure 9. Temperature climatology for central PWS. Redrawn from Campbell (Appendix A) Fig. 3 (region “CS”), with the axes rescaled to be comparable to Fig. 3 of this report. The color axis is identical to that of Fig. 3 of this report (i.e., the figures are directly comparable).....	13

Figure 10. Salinity climatology for central PWS. Redrawn from Campbell (Appendix A) Fig. 3 (region “CS”), with the axes rescaled to be comparable to Fig. 4 of this report. The color axis is identical to that of Fig. 4 of this report (i.e., the figures are directly comparable)..... 13

## **EXECUTIVE SUMMARY**

The goal of this program was to deliver an oceanographic monitoring program that would return useful information on temporal and spatial changes in the surface oceanography, biogeochemistry, and the planktonic ecosystem in the Prince William Sound (PWS) region. The data was depth-specific (because water column stability is important to ecosystem productivity), of high enough frequency to capture timing changes (changes that occur on order of weeks), and discover spatial variability in the region. Specific objectives included:

1. Install and maintain an autonomous profiling mooring in PWS to measure daily profiles of temperature, salinity, chlorophyll-a (as a proxy for phytoplankton biomass), turbidity and nitrate concentration in the surface layer (0-100 m).
2. Conduct regular surveys throughout PWS to tie in spatial variability to the high frequency time series provided by the mooring.
3. Support continued herring research by maintaining the existing time series (hydrography, plankton and nutrients) at the four bays previously targeted by the Sound Ecosystem Assessment (SEA) program.

The autonomous oceanographic profiler was purchased in 2012 and, following proving and test deployments in 2013, was operationally deployed at a site in central PWS in 2014 through 2016. The goal of the project was to deploy the profiler from spring through autumn to capture the evolution of the surface oceanography, plankton dynamics, and nutrient biogeochemistry over the growing season. The 2014 deployment ended early due to a hardware failure, but captured part of the spring bloom, which was extremely early that year. The 2015 and 2016 deployments covered late winter through autumn with unprecedented detail (with occasional small gaps caused by breakdowns and maintenance). The time series from the profiler showed widespread high temperatures (as much as 4°C above average), which corresponds to observations made throughout the Gulf of Alaska (known as “The Blob” warm anomaly). Phytoplankton bloom dynamics varied considerably among years, but it is difficult to attribute the effects of “The Blob” anomaly at present, because the profiler has only been deployed during warm anomaly years, and there is very little comparable data from other years.

The oceanographic observations from the vessel surveys were combined with a four-decade time series of temperature and salinity profiles within PWS and the immediately adjacent shelf that was compiled from numerous archives. Observations matched with recent cool (2007-2013) and warm (2013-onward) cycles observed recently in the region, and also showed an overall regional warming trend (0.1 to 0.2 °C per decade) that matches long-term increases in heat transport to the surface ocean. A cooling and freshening trend occurred in the near surface waters in some portions of PWS, particularly the northwestern margin which is also the location of most of ice sheets/glaciers, suggesting that those patterns are due to increased meltwater inputs. Increases in salinity at depth are consistent with enhanced entrainment of deep water by estuarine circulations, and by enhanced deep water renewal caused by reductions in downwelling-favorable winds. Estimates of mixed

layer depths shows a shoaling of the seasonal mixed layer over time by several meters, which may have implications for ecosystem productivity in the region.

The vessel surveys also sampled zooplankton at 12 stations in PWS and enumerated 188 species of zooplankton with *Oithona similis*, *Limacina helicina*, *Pseudocalanus* spp., and *Acartia longiremis* the most common species in 519 samples. Zooplankton communities remained low in abundance in the winter ( $894 \pm 112$  no. m<sup>-3</sup>) and were characterized by warm-water indicator species including *Mesocalanus tenuicornis* and *Calanus pacificus*. Zooplankton abundance peaked ( $38,784 \pm 10,106$  no. m<sup>-3</sup>) in the late spring/early summer. Community assemblages determined via hierarchical cluster analysis and indicator species analysis produced six distinct communities. Nonmetric multidimensional scaling using a Bray-Curtis dissimilarity matrix (3D stress = 0.17) corroborated these analyses. The winter assemblage diverged based on location into three communities characterized by small copepods, meroplanktonic larvae, and large calanoid copepods (*Neocalanus flemingeri*, *Eucalanus bungii*, *Calanus marshallae*) at open water stations. Large calanoid communities persisted into late summer and spread into PWS bays. In the early autumn, zooplankton communities sound-wide began to converge back into the winter community indicated by a transitional gelatinous carnivore community. Zooplankton abundance was significantly higher in 2010 ( $542$  ind. m<sup>-3</sup>  $\pm 55$ ) compared to all other years (ANOVA  $p < 0.05$ ) and lowest in 2013 ( $149$  ind. m<sup>-3</sup>  $\pm 12$ ). We also found significant relationships with mixed layer salinity, sea surface temperature, mixed layer depth, chlorophyll-a maximum (via CTD), depth of chlorophyll-a max, location, and bottom depth (BIOENV-BEST  $r = 0.24$ ,  $p < 0.05$ ).

## INTRODUCTION

Marine ecosystems are not static over time, they may change gradually from year to year or shift abruptly; those changes are in part driven by bottom up factors, such as environmental changes (e.g., temperature, salinity, turbidity), and biogeochemical interactions (the availability and recycling of nutrients). Long term monitoring of the spill-affected area is important, both in order to assess the recovery of resources, and to understand how the ecosystem is changing over time.

The ecosystems of the PWS region are influenced by physical environmental factors: metabolic and other vital rates for lower trophic species are generally temperature controlled, and water column production is ultimately limited by the amount of nitrogen made available to primary producers each year. Nitrogen availability is influenced by stratification (i.e., the onset of a seasonal thermocline or halocline) and mixing processes. These physical factors vary in space and in time, with different locations having different drivers (e.g., tidewater glaciers vs. riverine estuaries, watersheds of varying size), and those parameters also change both inter- and intra-annually. Superimposed over all those changes in the physical environment are myriad changes in the marine ecosystem, both in terms of the constituents (who is there) and abundance (how many there are, or their biomass). The phenology of ecosystem components (the timing of who appears) is also important, particularly concerning matches and mismatches between predators and prey.

The deep waters of the North Pacific are the terminus of the Great Ocean Conveyor (Broecker 1991), which accumulates remineralized nutrients from several centuries of detritus flux to depth. Those nutrient-rich deep waters are mixed onto the continental shelf, where they fuel very high primary productivity (Behrenfeld and Falkowski 1997) that is transferred up the food web to higher trophic levels (Ware and Thompson 2005).

Primary productivity in the Gulf of Alaska (GoA) is highly seasonal, and thought to be mediated by the availability of light and water column stability (Henson 2007). There is usually a large bloom each spring that depletes surface nutrients (primarily nitrate: Childers et al. 2005), a period of relatively low productivity through the summer months, and potentially a smaller autumn bloom as stability breaks down. The canonical hypothetical mechanism for spring bloom formation is the Critical Depth Hypothesis (CDH; Sverdrup 1953) whereby bloom initiation occurs after stability reaches a critical depth whereby growth exceeds losses. Recent work elsewhere has suggested that the CDH does not necessarily hold, and that bloom formation may occur in winter, leading to the Dilution-Recoupling Hypothesis of Behrenfeld (2010), which explicitly includes zooplankton grazing.

PWS is a large and complicated estuarine-fjord system with numerous sub-basins around its margins. It is separated from the GoA by several large islands, and surrounded on its three landward sides by the Chugach Mountains. The surface waters of PWS receive considerable freshwater inputs, from streams, rivers, and icefields, as well as considerable sediment loading. PWS is immediately downstream of the Copper River delta, the largest point source of fresh water to the GoA, which produces a turbid plume that travels westward along the coast into PWS through Hinchinbrook Entrance. PWS is also connected to shelf waters via the Alaska Coastal Current (ACC; Royer 1981), which may flow in through Hinchinbrook Entrance as well. Circulation in central PWS is usually cyclonic, and driven by local winds (Vaughan et al. 2001, Okkonen and Belanger 2008), although there may be occasional reversals (Niebauer et al. 1994). The depth of the main basin is approximately 350 m (although there are some basins in the western part that are 700 m deep), while the depth of the sill at Hinchinbrook Entrance is approximately 200 m deep. Deep water renewal events occur in PWS but are not well described, renewal is likely set up during the summer and autumn by the on-shelf movement of deep water (Weingartner 2005, Halverson et al. 2013).

Within PWS, variations in annual productivity have been posited to vary based on the variations in upwelling/downwelling and the track of the ACC (the River-Lake hypothesis of Cooney et al. 2001a). Some support was found for this hypothesis for some years (1981-1991), but not in others (Eslinger et al. 2001). During winter, nutrient availability is high, as deep, nutrient-rich water is mixed to the surface. Phytoplankton production during the winter is light-limited, with a vernal bloom following the onset of stratification in the spring. Stratification is driven by the balance between the stabilizing inputs of freshwater and heat and the destabilizing influence of wind and tidal mixing. PWS is destabilized by negative heat flux and tidal mixing in the winter, and stabilized by freshwater and heat inputs in the summer (Eslinger et al. 2001, Henson 2007). In general, the spring bloom starts in PWS in March to April (Weingartner 2005) and is temporally broad, occurring into

July (Henson 2007). PWS may also experience an autumn bloom, as stability breaks down and nutrients are moved to the surface (Eslinger et al. 2001).

The numerical and biomass dominant zooplankton in PWS is *Neocalanus* spp. (two closely related congeners, *N. plumchrus* and *N. flemingeri*), which overwinters at depths >300 m. In mid-winter (December onward), overwintering copepodids molt to adulthood and spawn at depth. Eggs and nauplii migrate to the surface, and development progresses rapidly (usually in conjunction with the spring bloom); upon reaching the penultimate copepodids stage, individuals descend to depth and enter a diapause state. Following the spring bloom, smaller bodied copepods predominate (*Pseudocalanus*, *Acartia*), and *Metridia* becomes more common in autumn (Cooney et al. 2001b). Several krill species are also present, but are less common and less easily sampled.

PWS is also a productive habitat for fish, including several forage fish species (Willette et al. 1997), including herring (*Clupea pallasii*), capelin (*Mallotus villosus*), sand lance (*Ammodytes hexapterus*), and several species important in commercial and subsistence fisheries including Pacific salmon (*Oncorhynchus* spp.), walleye Pollock (*Gadus chalcogrammus*), Pacific cod (*Gadus macrocephalus*), and Pacific halibut (*Hippoglossus stenolepis*). PWS is particularly important rearing habitat for juvenile pink salmon and herring, with pink salmon feeding on zooplankton during the spring bloom, and herring primarily in late summer/autumn (Cooney et al. 2001a).

Warming trends have been observed globally for many years (e.g., Levitus et al. 2001), and those trends have been observed in Alaska (Shulski and Wendler 2008, This report Appendix A). Much of the increased heat flux has been taken up by the ocean (Barnett et al. 2005), and warming trends have been observed in coastal Alaska at the regularly sampled GAK line near Seward, Alaska (Royer and Grosch 2006, Janout et al. 2010). Since late 2013, sea surface temperature anomalies throughout the GoA have been as much as 3-4°C above average; the leading hypothesis for that particular anomaly (colloquially referred to as “The Blob”) is a reduction in winter heat flux leading to residual heat being retained by the surface ocean (Bond et al. 2015). 2015-2016 was also the second strongest El Niño event on record (NOAA 2016), which generally correlates with higher than average surface temperatures.

## **OBJECTIVES**

The goal of this program was to deliver a monitoring program that would return useful information on temporal and spatial changes in physical, chemical, and biological oceanographic parameters at a reasonable cost, and with a reasonable amount of effort. The data should be depth-specific (because water column stability is important to ecosystem productivity), of high enough frequency to capture timing changes (changes that occur on order of weeks), and give an idea of spatial variability in the region. Specific objectives included:

1. Install and maintain an autonomous profiling mooring in PWS that will measure daily profiles of temperature, salinity, chlorophyll-a (as a proxy for phytoplankton biomass), turbidity and nitrate concentration in the surface layer (0-100 m).

2. Conduct regular surveys in PWS to tie in spatial variability to the high frequency time series provided by the mooring.

3. Support continued herring research conducted by the Herring Research and Monitoring Program (program 16120111) by maintaining the existing time series (hydrography, plankton and nutrients) at the four Sound Ecosystem Assessment (SEA) bays.

The results of Objectives 2 and 3 have been published in two peer-reviewed manuscripts (Appendix A, B); this portion of the report will focus on the results of objective 1, the autonomous profiling mooring.

## METHODS

A WETlabs Autonomous Moored Profiler (AMP) was purchased in 2013. The AMP was deployed at a site 9 km southeast of Naked Island, in 200 m water depth (Fig. 1); it is the same location of a biophysical buoy deployed by the University of Alaska Fairbanks in the 1990s as part of the *Exxon Valdez* Oil Spill Trustee Council-funded SEA program (see Eslinger et al. 2001).

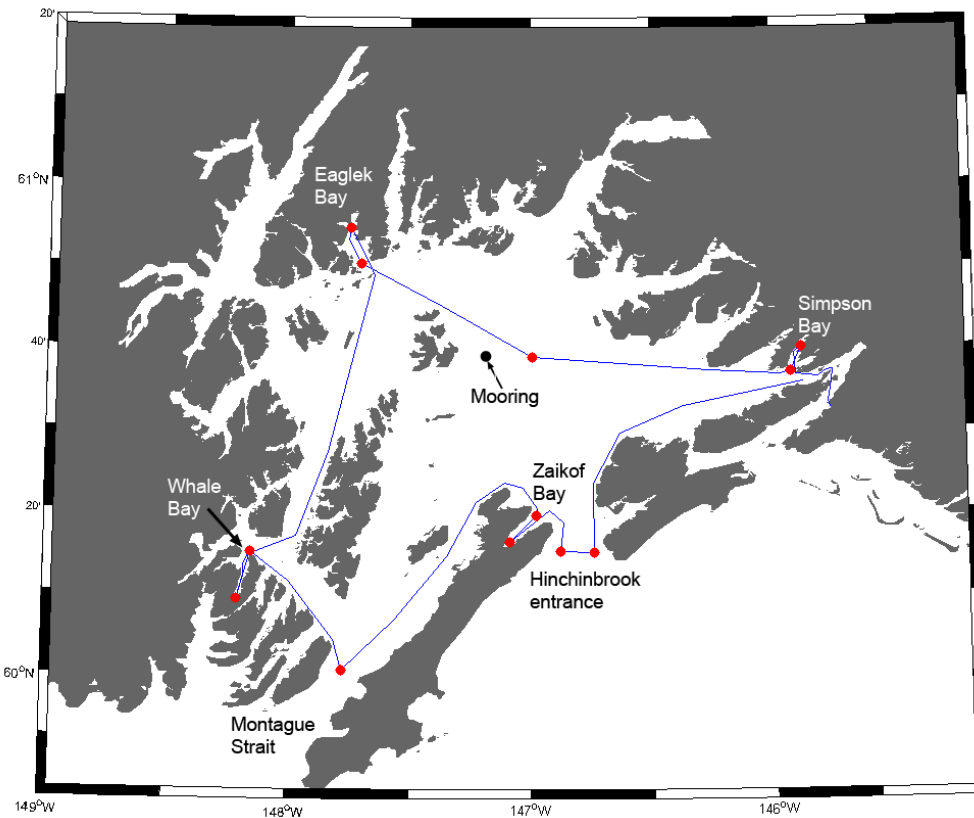


Figure 1. Prince William Sound, Alaska. The 12 stations occupied during the vessel surveys are indicated by the red dots, and the profiler was deployed at the “Mooring” site.

The AMP system is a surface piercing profiler that parks at depth and profiles from the park depth to surface at user specified intervals (Fig. 2). Once at the surface, the profiler connects to a server computer on land via a cellular data link for data and command/control telemetry, and then pulls itself back down the line to the park depth with a small onboard winch. The PWS AMP system includes a Seabird model 19 CTD, a WETLabs FLNTU chlorophyll-a fluorometer/backscatter turbidometer, and a Satlantic SUNA nitrate sensor, and is usually set to profile from 60 m depth to the surface. The system is powered by a 1.5kW lithium polymer battery manufactured by Bluefin Robotics for autonomous underwater vehicle use, and with the current instrument suite is capable of conducting approximately 60 profiles per charge.

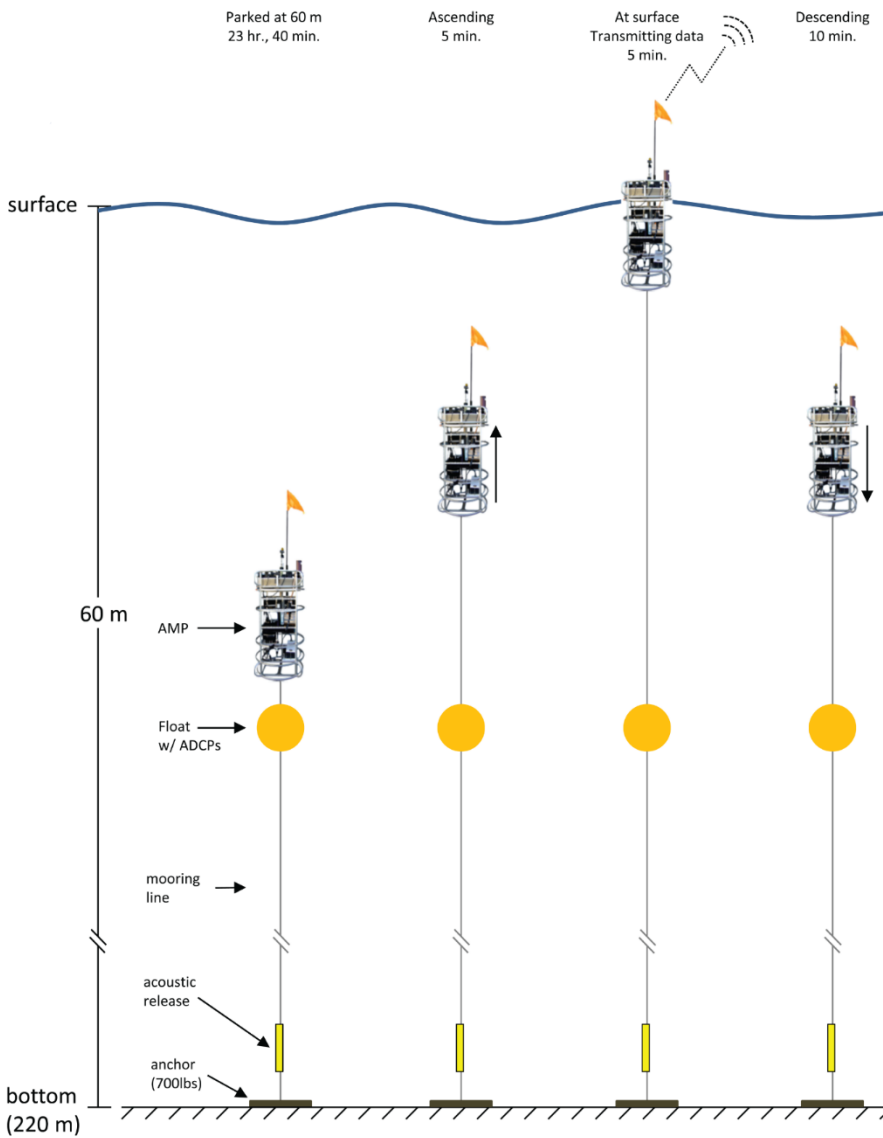


Figure 2. A typical daily profile cycle done by the autonomous profiler. Most of the day is spent at a park depth (~60 m) in a low power state.

The PWS AMP system arrived in late 2012 and was outfitted and tested in Nelson Bay near Cordova in late 2012 and early 2013. The first deployment at the Naked Island site was in June 2013. The AMP system is an emerging technology (the PWS AMP is the seventh such system built), and this deployment is the northernmost and most remote deployment done to date. Numerous issues were resolved in 2012 and 2013, including corrosion, floatation, and communications issues. The first operational deployment at the Naked Island site was done August 29 to September 30, 2013, and observed the disruption of the seasonal thermocline. The profiler was again deployed in April 2014, and observed the development of the subsurface spring bloom into May. The profiler was disabled by a hardware failure in late June 2014 and was returned to the manufacturer for service. The 2015 deployment began in late March, and the profiler was in place conducting daily profiles (with a small number of interruptions for service) until late October, thus capturing the annual evolution of the surface layer in PWS.

In 2015 the North Pacific Research Board approved a project submitted by R. Campbell to upgrade the profiler and develop and install an *in situ* plankton camera system. The profiler controller electronics were upgraded to the newest version, and a new cellular data modem installed. The camera was developed in 2015/16 in collaboration with the Jules Jaffe group at the Scripps Institution of Oceanography, and was integrated with the profiler in early 2016. The camera system images an approximately 10 x 10 x 6 cm volume of water at 4Hz, and has a pixel resolution of approximately 15  $\mu\text{m}$ , and is thus able to image large phytoplankton and most zooplankton. The 2016 deployment of the profiler system with the new camera was conducted from early April 4 to December 5, and profiles were done twice daily, with profiles done during solar maxima and minima (to observe diel migrant plankton that are active at night).

Temperature, salinity and pressure were measured directly by the CTD, which is mounted with the sampling duct at the top of the profiler. The nitrate sensor was plumbed after the CTD with a seabird 5T pump. The fluorometer/turbidometer was side-looking and mounted 35 cm below the CTD sampling duct. Nitrate and fluorescence observations were lagged in time relative to the CTD based on the ascent rate of the profiler to line up the observations. The winch motor turns at a constant rate, and the ascent rate decreases over the course of the profile as line is paid out.

To convert temperature measurements to anomalies, observations were subtracted from the long-term daily seasonal average. The long-term seasonal average is a second order cosine curve regressed over a 40 year CTD time series from the central sound ("CS region"; Appendix A). A detailed description of the method is included in Appendix A.

## **RESULTS**

The 2013 deployment was done very late in the year, and was done primarily as a trial deployment to operationally test the profiler. Thirty-three daily profiles were done during the deployment, and showed the deepening of the seasonal thermocline in temperature (Fig. 3) and salinity (Fig. 4). There was no indication of an autumn bloom in the fluorescence record (Fig. 5), and there was a pronounced nitricline (Fig. 6).

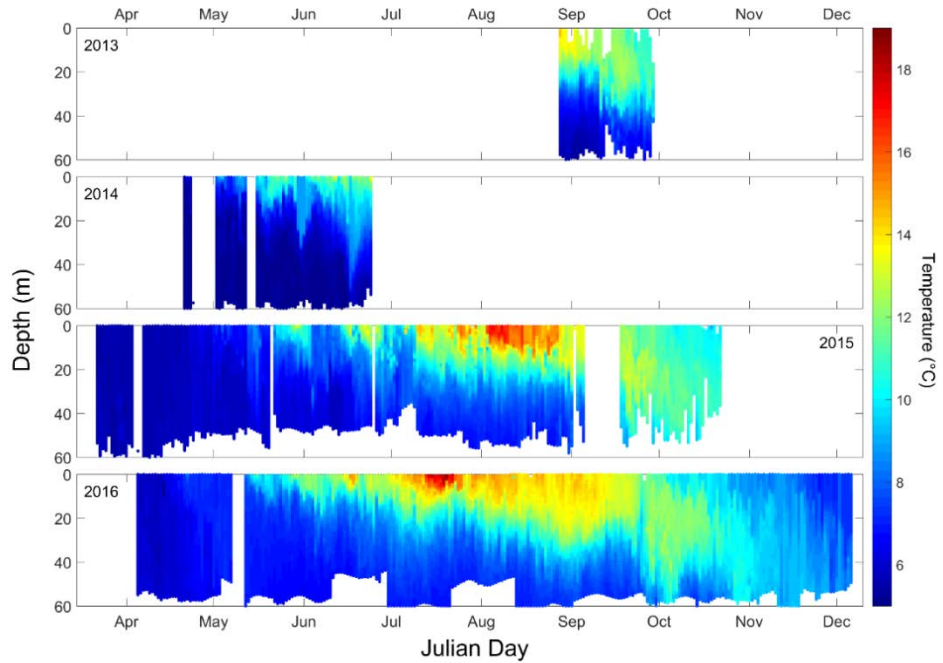


Figure 3. Temperature time series measured by the autonomous profiler during each year of deployment in Prince William Sound, Alaska.

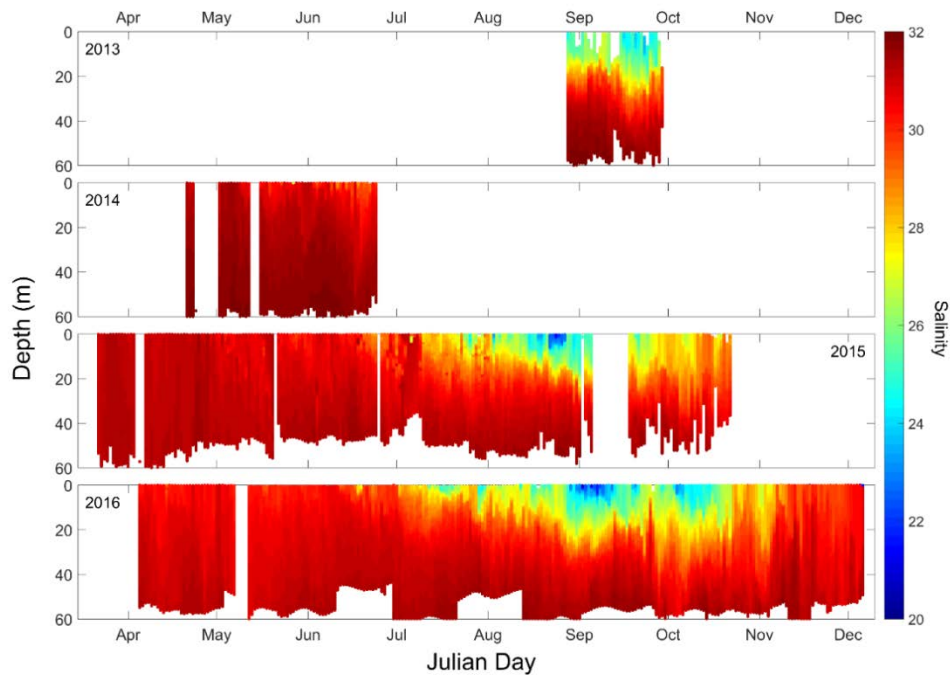


Figure 4. Salinity time series measured by the autonomous profiler during each year of deployment in Prince William Sound, Alaska.

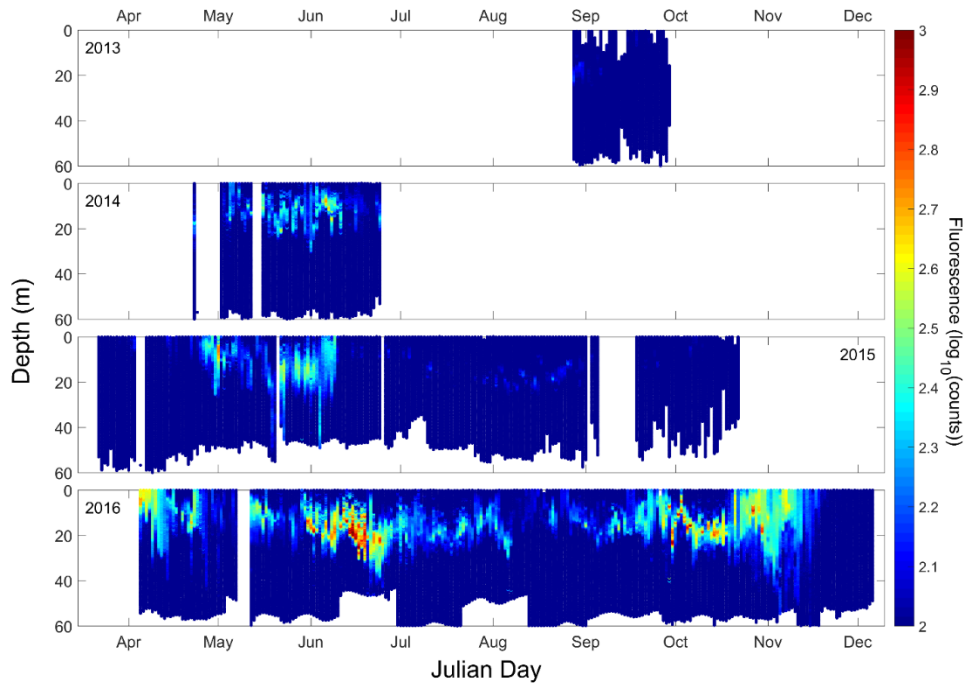


Figure 5. Fluorescence time series measured by the autonomous profiler during each year of deployment in Prince William Sound, Alaska. Fluorescence is given as digital counts, which are linearly proportional to in situ chlorophyll-a fluorescence, and have been  $\log_{10}$  transformed.

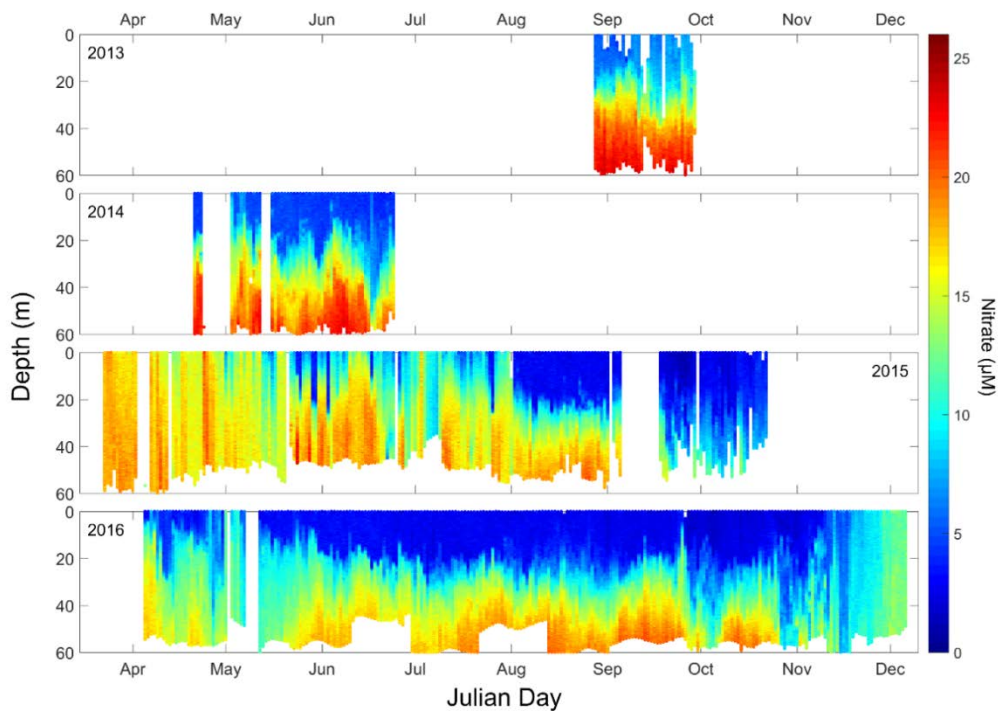


Figure 6. Nitrate time series measured by the autonomous profiler during each year of deployment in Prince William Sound, Alaska.

In 2014 the profiler was deployed on April 21. Although there was little indication that the spring thermocline had formed (Fig. 3), the spring bloom was already in progress, with a subsurface chlorophyll maximum, and significant draw-down of nitrate in the top 20 m of the water column. The 2014 deployment ended in late June following a hardware failure caused by a corrosion issue.

The 2015 deployment was started earlier in the year (March 22), and captured the development of the spring bloom, which began near-surface in late April and shifted towards a subsurface maximum into May (Fig. 5); the highest chlorophyll fluorescence at that time was located near the nitricline (Fig. 6). The seasonal thermocline developed in late April and into May, and was disrupted by large wind events in May and June that disrupted the thermocline (Fig. 3) and mixed nitrate towards the surface (Fig. 6). Near surface salinity began to decline in late June, and was also disrupted by a wind event in late July. Through July and August there was a chlorophyll maxima present at the nitricline (Figs. 5, 6), and there was not any indication of an autumn bloom during September and October when the seasonal pycnocline began to break down. However, there was about a two week gap where profiles were not recorded (the profiler was recovered after a software bug left it stuck at the surface, and weather prevented its redeployment for several days).

The start of the 2016 deployment was delayed by delays in the upgrades to the profiler at the factory, the need to test the new camera system, and an unexpected hardware failure when the electronics were initially returned. The profiler was deployed on April 4, and the spring bloom was already underway, with high chlorophyll fluorescence near-surface (Fig. 5) and nitrate depleted from the top 5 m of the water column (Fig. 6). The seasonal thermocline began to form in late April / early May, and broke down late September into October (Fig. 3). Near-surface salinity increased at approximately the same time (Fig. 4). There was again a chlorophyll maximum at the nitricline for much of the summer months, and a pronounced autumn bloom in late September and October, with high fluorescence occurring near-surface into November.

Deployments of the profiler began at approximately the same time as the initial genesis of “The Blob” anomaly in the central Gulf of Alaska, and temperature anomalies at the profiler site were almost always positive at the surface over the entire record (Fig. 7). Autumn (when observed) and winter temperatures were also characterized by positive anomalies. Temperatures were cooler than average underneath the seasonal thermocline. Near surface salinity anomalies were also generally below average (i.e., more fresh than the climatology; Fig. 8), and above average below the seasonal thermocline, at the same approximate depths and times that negative temperature anomalies occurred.

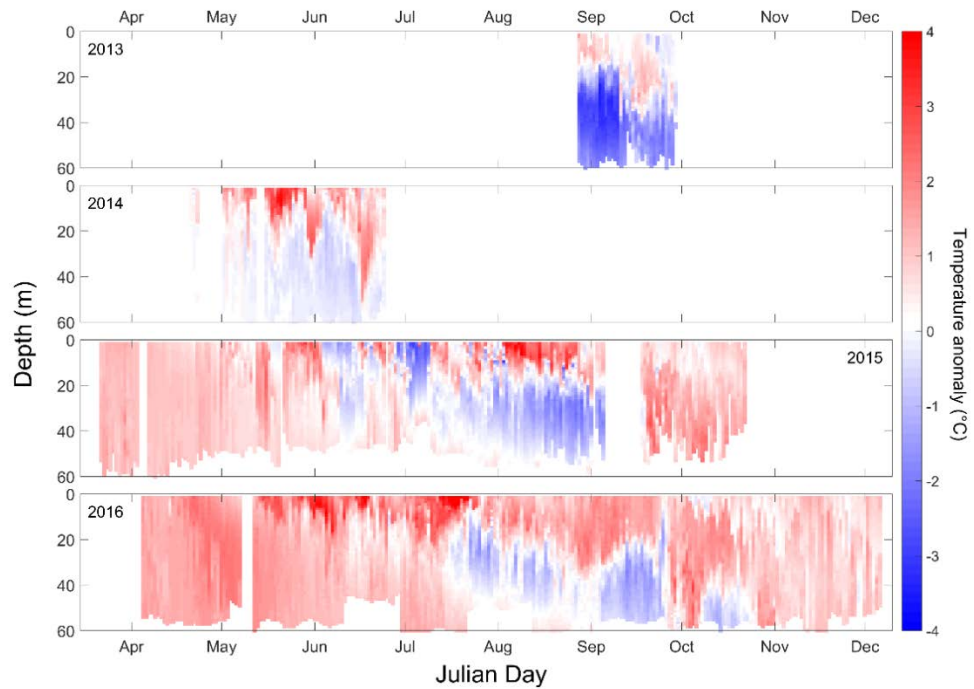


Figure 7. Temperature anomalies during each year of deployment in Prince William Sound, Alaska. Temperature observations were converted to anomalies by subtraction from the seasonally detrended annual average (Appendix A).

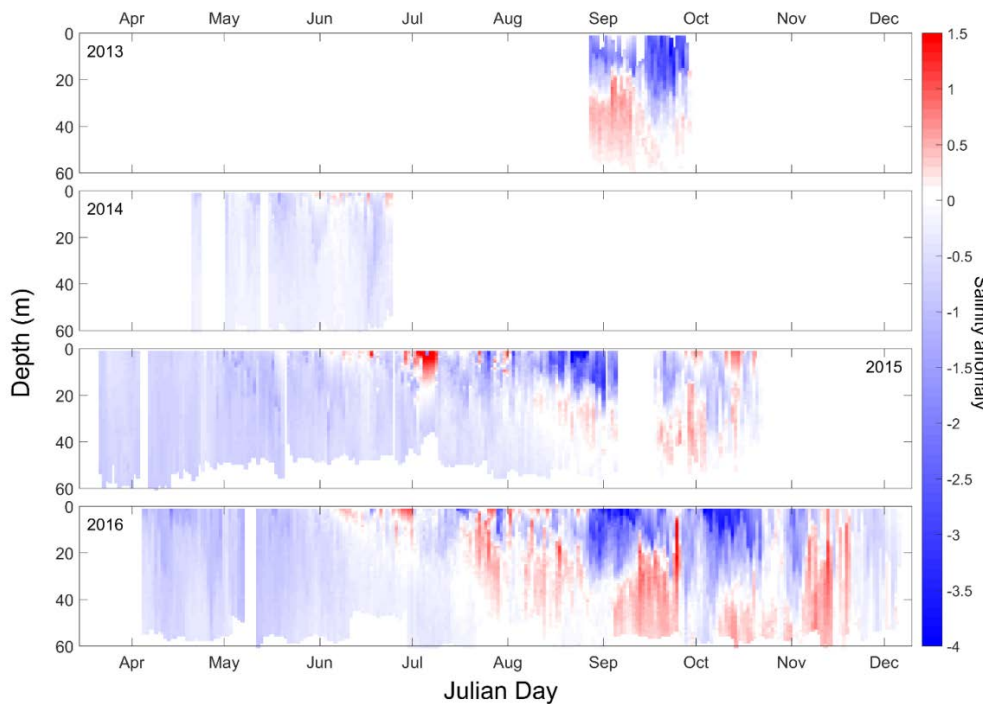


Figure 8. Salinity anomalies during each year of deployment. Salinity observations were converted to anomalies by subtraction from the seasonally detrended annual average (Appendix A).

## DISCUSSION

When it was purchased, the PWS AMP profiler was the seventh such system constructed in the world and the PWS deployment was the most remote, northerly, and coldest deployment location to date. There were numerous challenges to overcome, from working with the local telephone cooperatives to improve the reliability of the cellular network for data telemetry, to learning the various failure points of the system and developing best practices. Most of the initial issues have been worked out of the system, and the 2015/16 upgrades to the profiler (as well as upgrades done to the cellular network) have greatly improved the reliability of communications, both for control and data transmission. Although the 2014 deployment was shorter than desired, the 2015 and 2016 deployments have produced an unprecedented picture of the annual evolution of the surface layer oceanography and biogeochemistry in PWS.

All of the profiler deployments have been done during “The Blob” warm anomaly and surface temperature anomalies were almost universally positive throughout the time series (Fig. 7). It will remain uncertain for now just how unusual those years were, and continued observations moving forward will no doubt provide context on the impacts to the biogeochemistry and planktonic ecosystem. The warm near surface temperatures were not unexpected, given the positive anomalies observed basin-wide (Scannell et al. 2016). Negative salinity anomalies near surface were also not unexpected, given a freshening trend observed in PWS since the mid-1970s that is due in part to losses in ice mass by fringing ice sheets, and changes in precipitation patterns (Appendix A, and references therein).

The cool anomalies below the seasonal thermocline were accompanied by greater than average salinity (notable in 2015 and 2016: Figs. 7, 8). Those apparent anomalies appear to have been in part due to a thinning of the surface mixed layer, which is initially set up by temperature stratification, then reinforced by salinity stratification (Appendix A). The climatologies for temperature (Fig. 9) and salinity (Fig. 10) in Central PWS from Appendix A have been reproduced here, with the scaling of the axes adjusted to correspond with the depths sampled by the profiler (color axes are also identical). Comparison of the temperature time series (Fig. 3) to the climatology (Fig. 9) suggests that the spring thermocline set up earlier than average in 2014 through 2016, and that the thermocline was shallower than the climatology, particularly in 2015, resulting in the negative anomalies below the thermocline. The shoaling of density stratification in response to a warming signal has been observed in the central Gulf of Alaska (Li et al. 2005).

In contrast, salinity stratification in 2015 and 2016 (the only years that captured that time of the year well; Fig. 4) appears to have begun roughly on schedule, with salinity beginning to decline in late June, as it does in the climatology (Fig. 10). The near surface salinity minima was much lower than average near surface (Fig. 8), which would also serve to strengthen stratification. The higher than average subsurface salinity observed July through September may thus reflect changes to the overall synoptic oceanography. A long-term trend towards increasing salinity at depth was also observed, which appears likely to have been caused by changes in transport of more saline water at depth, both by

entrainment, and changes in deepwater renewal caused by changes in downwelling conditions on the adjacent shelf. Those mechanisms are described in detail in Appendix A.

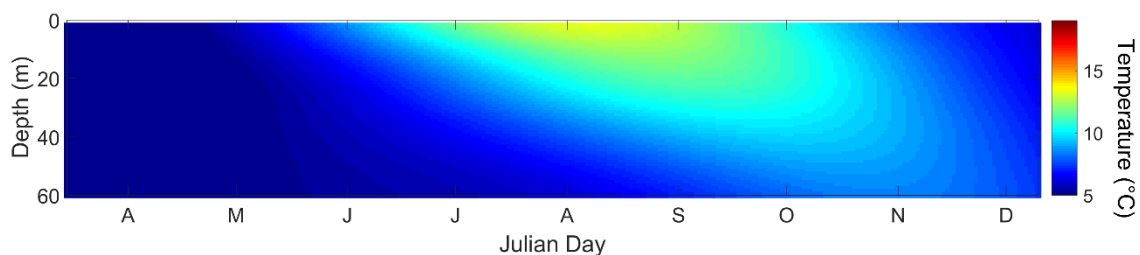


Figure 9. Temperature climatology for central PWS. Redrawn from Appendix A Fig. 3 (region “CS”), with the axes rescaled to be comparable to Fig. 3 of this report. The color axis is identical to that of Fig. 3 of this report (i.e., the figures are directly comparable).

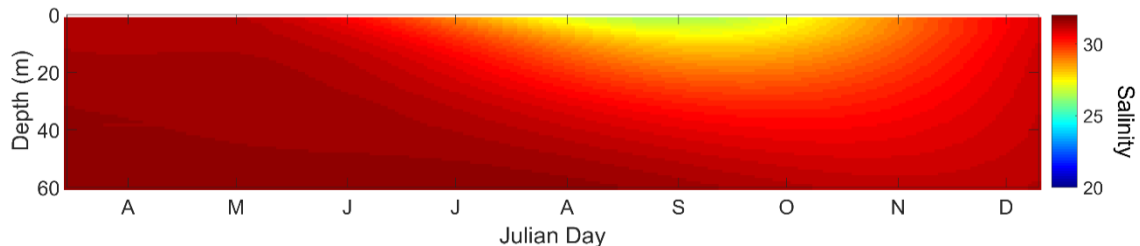


Figure 10. Salinity climatology for central PWS. Redrawn from Appendix A Fig. 3 (region “CS”), with the axes rescaled to be comparable to Fig. 4 of this report. The color axis is identical to that of Fig. 4 of this report (i.e., the figures are directly comparable).

The spring bloom in PWS has not been well described beyond a large scale satellite based study (Henson 2007) and a modeling effort done as part of the SEA project (Eslinger et al. 2001); chlorophyll-a and nitrate climatologies do not exist. The canonical picture that emerges from the prior studies is that the spring bloom usually initiates in late April into May, followed by an abrupt decline in early to mid-May when the surface nutrients are exhausted. Phytoplankton biomass remains low through the summer months (June-September), with a smaller autumn bloom occurring in October-November as stability breaks down and nutrients are mixed upward by equinoctial storms.

The observations made by this study were not fully in line with that canonical picture. The spring bloom occurred very early in 2014, with significant nitrate drawdown and low surface chlorophyll concentrations by mid-April (Figs. 5, 6). The 2016 bloom appears to have been early as well, with the bloom well underway in early April. The 2015 bloom began roughly on schedule, and chlorophyll concentrations declined in late May, although there were still relatively large concentrations of nitrate available near surface. An autumn bloom was only observed in 2016. Although analysis is ongoing, 2015 is emerging as something of an unusual year throughout the north Pacific with changes noted in many plankton species and mortality events in many vertebrates (Cavole et al. 2016). It is

entirely possible that the prolonged period of above average temperatures (up to 4°C above average) in 2014 and 2015 altered the phytoplankton community in such a way as to limit overall productivity. Phytoplankton species composition was not assessed by this project, but a small number of pilot samples were collected in 2016 and proposals have been submitted to add those observations in future. Changes in zooplankton taxa were discussed in detail in Appendix B.

## **CONCLUSIONS**

The PWS autonomous profiler is an in-development autonomous sampling platform and after some initial setbacks and lessons learned has documented the evolution of the surface oceanography and biogeochemistry of PWS much higher frequency than done previously (daily to twice-daily), and highlighted considerable year-to-year variability. The profiler observed the high temperature anomalies that occurred across the Gulf of Alaska as part of “The Blob” marine heat wave, as well as smaller scale salinity anomalies that are attributable to recent climatological changes (see Appendix A). Although the observations were confined to “Blob” years, there were large year-to-year differences in the timing of bloom events, overall productivity, and nutrient availability and drawdown. Ongoing deployments in future will put those observations into better context and permit a better understanding of the functioning of the surface oceanography and biogeochemistry of PWS. Ultimately, given an adequate time series, these data could be extremely useful for understanding changes in the abundance and productivity of higher trophic level organisms, including those that are commercially important.

## **ACKNOWLEDGEMENTS**

The author thanks Caitlin McKinstry, Lauren Bien, Hayley Hoover, Rachel Ertz, and Darren Roberts for assistance in the field; Bruce Rhoades at WETLabs Inc for his continual assistance with the profiler; and the staff at Cordova Wireless for their continued assistance with data telemetry issues. The donation of numerous train wheel anchors by the Alaska Railroad Corporation is gratefully acknowledged. The views expressed here are our own and do not necessarily represent those of the *Exxon Valdez* Oil Spill Trustee Council.

## **LITERATURE CITED**

- Barnett, T., D. W. Pierce, K. M. Achuta, Rao, P. J. Gleckler, B. D. Santer, J. M. Gregory, and W. M. Washington. 2005. Penetration of human-induced warming into the world's oceans. *Science*. 309:284-287.
- Behrenfeld, M. J. 2010. Abandoning Sverdrup's critical depth hypothesis on phytoplankton blooms. *Ecology* 91:977-989.
- Behrenfeld, M. J., and P. G. Falkowski. 1997. Photosynthetic rates derived from satellite-based chlorophyll concentration. *Limnological Oceanography* 42:1-20.

- Bond, N. A., M. F. Cronin, H. Freeland, and N. Mantua. 2015. Causes and impacts of the 2014 warm anomaly in the NE Pacific. *Geophysical Research Letters* 42:3414–3420. doi:10.1002/2015GL063306.
- Broecker, W. S. 1991. The great ocean conveyor. *Oceanography* 4:79-89.
- Cavole, L. M., A. M. Demko, R. E. Diner, A. Giddings, I. Koester, C. M. L. S. Pagniello, M.-L. Paulsen, A. Ramirez-Valdez, S. M. Schwenck, N. K. Yen, M. E. Zill, and P. J. S. Franks. 2016. Biological impacts of the 2013–2015 warm-water anomaly in the Northeast Pacific: Winners, losers, and the future. *Oceanography* 29(2):273–285, <http://dx.doi.org/10.5670/oceanog.2016.32>.
- Childers, A. R., T. E. Whitledge, and D. A. Stockwell. 2005. Seasonal and interannual variability in the distribution of nutrients and chlorophyll a across the Gulf of Alaska shelf: 1998–2000. *Deep Sea Research Part II* 52:193-216.
- Cooney, R. T., J. R. Allen, M. A. Bishop, D. L. Eslinger, T. Kline T, B. L. Norcross, C. P. Mcroy, J. Milton, J. Olsen, V. Patrick, A. J. Paul, D. Salmon, D. Scheel, G. L. Thomas, S. L. Vaughan, and T. M. Willette. 2001a. Ecosystem control of pink salmon (*Oncorhynchus gorbuscha*) and Pacific herring (*Clupea pallasii*) populations in Prince William Sound, Alaska. *Fisheries Oceanography* 10(Suppl. 1):1-13.
- Cooney, R. T., K. O. Coyle, E. Stockmar, and C. Stark. 2001b. Seasonality in surface-layer net zooplankton communities in Prince William Sound, Alaska. *Fisheries Oceanography*. 10(Suppl. 1):97-109.
- Eslinger, D. L., R. T. Cooney, C. P. McRoy, A. Ward, T. C. Kline, E. P. Simpson, J. Wang, and J. R. Allen. 2001. Plankton dynamics: observed and modeled responses to physical conditions in Prince William Sound, Alaska. *Fisheries Oceanography* 10(Suppl. 1):81-96.
- Halverson, M. J., C. Bélanger, and S. M. Gay. 2013. Seasonal transport variations in the straits connecting Prince William Sound to the Gulf of Alaska. *Continental Shelf Research* 63:S63–S78.
- Henson S. A. 2007. Water column stability and spring bloom dynamics in the Gulf of Alaska. *Journal of Marine Research* 65:715-736.
- Janout, M. A., T. J. Weingartner, T. Royer, and S. L. Danielson. 2010. On the nature of winter cooling and the recent temperature shift on the norther Gulf of Alaska shelf. *Journal of Geophysical Research* 115, C05023, doi:10.1029/2009JC005774
- Levitus, S. J., J. I. Antonov, J. Wang, T. L. Delworth, K. W. Dixon, and A. J. Broccoli. 2001. Anthropogenic warming of Earth’s climate system. *Science* 292:267-270.
- Li, M., P. G. Myers, and H. Freeland. 2005. An examination of historical mixed layer depths along Line P in the Gulf of Alaska. *Geophysical Research Letters* 32, L05613, doi:10.1029/2004GL021911

- Niebauer, H., T. Royer, and T. Weingartner. 1994. Circulation of Prince William Sound, Alaska. *Journal of Geophysical Research* 99:14113-14126.
- Okkonen, S., and C. Bélanger. 2008. A child's view of circulation in Prince William Sound, Alaska? *Oceanography* 21:62-65.
- Royer, T. C. 1981. Baroclinic transport in the Gulf of Alaska. Part II. Fresh water driven Alaska Coastal Current. *Journal of Marine Research* 39:251-266.
- Royer, T. C., and C. E. Grosch. 2006. Ocean warming and freshening in the northern Gulf of Alaska. *Geophysical Research Letters* 33, L16605. Doi:10.1029/2006GL026767
- Scannell, H. A., A. J. Pershing, M. A. Alexander, A. C. Thomas, and K. E. Mills. 2016. Frequency of marine heatwaves in the North Atlantic and North Pacific since 1950, *Geophysical Research Letters*, 43, 2069–2076, doi:10.1002/2015GL067308.
- Shulski, M., and G. Wendler. 2008. *The climate of Alaska*. University of Alaska Press, Fairbanks, Alaska, USA.
- Sverdrup H. U. 1953. On conditions for the vernal blooming of phytoplankton. *Journal du Conseil / Conseil Permanent International pour l'Exploration de la Mer* 18:287–295.
- Weingartner, T. 2005. Physical and geological oceanography: coastal boundaries and coastal and ocean circulation. Pages 35-48 in P. R. Mundy, editor, *The Gulf of Alaska: biology and oceanography*. Alaska Sea Grant, Fairbanks, USA.

## **OTHER REFERENCES**

NOAA Fisheries. El Niño/Southern Oscillation (ENSO) diagnostic discussion. Available: [http://www.cpc.ncep.noaa.gov/products/analysis\\_monitoring/enso\\_disc\\_jan2016/ensodisc.pdf](http://www.cpc.ncep.noaa.gov/products/analysis_monitoring/enso_disc_jan2016/ensodisc.pdf)

## **Scientific Presentations**

- Campbell, R.W. 2012. State of the Sound: Recent oceanographic conditions in Prince William Sound. Alaska Marine Science Symposium, Anchorage.
- Campbell, R.W. 2014. State of the Sound: Trends in the surface oceanography of Prince William Sound. Alaska Marine Science Symposium, January 2014.
- Campbell, R.W. 2015. Recent trends in the oceanography of Prince William Sound. Alaska Marine Science Symposium, Anchorage.
- Campbell, R.W. 2016. Effects of the 2013-2015 warm anomaly in Prince William Sound, Alaska. Pacific Anomalies Workshop 2, Seattle.
- Campbell, R.W. 2016. Surface layer and bloom dynamics observed with the Prince William Sound Autonomous Profiler. ASLO/AGO Ocean Sciences Meeting, New Orleans.

Campbell, R.W. 2017. Effects of the 2013-2016 warm anomaly in Prince William Sound, Alaska. Alaska Marine Science symposium, Anchorage.

**Public Presentations**

Campbell, R.W. 2015. State of the Sound: Oceanography, surface layer dynamics, and plankton blooms in PWS. PWSSC Pub Talk, Cordova.

Campbell, R.W. 2015. Oceanography, surface layer dynamics, and plankton blooms in PWS. PWS Regional Citizens' Advisory Council, Anchorage.

Campbell, R.W. 2015. State of the Sound: Oceanography, surface layer dynamics, and plankton blooms in PWS. PWSSC Lecture series, Cordova.



Contents lists available at ScienceDirect

## Deep-Sea Research Part II

journal homepage: [www.elsevier.com/locate/dsr2](http://www.elsevier.com/locate/dsr2)

## Hydrographic trends in Prince William Sound, Alaska, 1960–2016

Robert W. Campbell

Prince William Sound Science Center, Cordova, AK, USA



## A B S T R A C T

A five-decade time series of temperature and salinity profiles within Prince William Sound (PWS) and the immediately adjacent shelf was assembled from several archives and ongoing field programs, and augmented with archived SST observations. Observations matched with recent cool (2007–2013) and warm (2013-onward) periods in the region, and also showed an overall regional warming trend ( $\sim 0.1$  to  $0.2$  °C decade $^{-1}$ ) that matched long-term increases in heat transport to the surface ocean. A cooling and freshening trend ( $\sim -0.2$  °C decade $^{-1}$  and  $0.02$  respectively) occurred in the near surface waters in some portions of PWS, particularly the northwestern margin, which is also the location of most of the ice mass in the region; discharge (estimated from other studies) has increased over time, suggesting that those patterns were due to increased meltwater inputs. Increases in salinity at depth were consistent with enhanced entrainment of deep water by estuarine circulations, and by enhanced deep water renewal caused by reductions in downwelling-favorable winds. As well as local-scale effects, temperature and salinity were positively cross correlated with large scale climate and lunar indexes at long lags (years to months), indicating the longer time scales of atmospheric and transport connections with the Gulf of Alaska. Estimates of mixed layer depths show a shoaling of the seasonal mixed layer over time by several meters, which may have implications for ecosystem productivity in the region.

## 1. Introduction

Prince William Sound (PWS) is a large and complicated estuarine-fjord system with numerous sub-basins around its margins. It is separated from the Gulf of Alaska (GoA) by several large islands, and surrounded on its three landward sides by the Chugach mountains. The marine ecosystem in the PWS region is extremely productive, and supports several groundfish and salmon fisheries that are of considerable importance to the local economy. The region is also a locally important transport corridor for oil tankers travelling to and from the terminus of the Trans-Alaska Pipeline in Valdez, cruise ships, and cargo vessels.

The surface waters of the continental shelf adjacent to PWS are dominated by the relatively fresh Alaska Coastal Current and the Copper River, which is the largest point source of fresh water to the northern GoA (Stabeno et al., 2004). PWS is connected to the coastal GoA through two main entrances, Hinchinbrook Entrance (HE) and Montague Strait (MS), with surface waters generally entering through HE and exiting through MS, although reflux events do occur. Deepwater renewal events generally occur through HE during summer and autumn (Halverson et al., 2012). The surface waters of PWS also receive freshwater from countless streams, small rivers, and icefields along the periphery, as well as considerable sediment loading (Beamer et al., 2016; Feeley, 1979; Gay and Vaughan, 2001; Hill et al., 2015).

Precipitation in the region is prodigious, with order of  $95 \text{ km}^3$  of fresh water moving through the system each year, accounting for 11% of all freshwater discharge into the GoA (Neal et al., 2010; Beamer et al., 2016). Recent evidence (Arendt et al., 2013; Barclay et al., 2013; Beamer et al., 2016; Wiles et al., 1999) suggests that losses of ice mass in the GoA region have been considerable, which may have increased discharge into the coastal ocean. Over the continental shelf, near-surface salinity has been declining over time (Royer and Grosch, 2006).

Warming trends have been observed globally for many years (Levitus et al., 2001), and those trends have also been observed in Alaska (Shulski and Wendler, 2008). Much of the increased heat flux has been taken up by the ocean (Barnett et al., 2005), and warming trends have been observed in coastal Alaska at the regularly sampled GAK line near Seward, AK (Royer and Grosch, 2006; Janout et al., 2010). Since late 2013, sea surface temperature anomalies throughout the GoA have been as much as  $3\text{--}4$  °C above average; the leading hypothesis for that particular anomaly (colloquially referred to as “The Blob”) is a reduction in winter heat flux leading to residual heat being retained by the surface ocean (Bond et al., 2015). 2015–2016 was also the second strongest El Niño event on record (NOAA, 2016), which generally correlates with higher than average surface temperatures.

Although there is a well-maintained time series of the coastal GoA in the GAK line, there has not been a comparable coordinated long-term effort in Prince William Sound. Prior to the 1989 Exxon Valdez Oil Spill,

E-mail address: [rcampbell@pwssc.org](mailto:rcampbell@pwssc.org).<http://dx.doi.org/10.1016/j.dsr2.2017.08.014>

Available online 26 August 2017

0967-0645/ © 2017 The Author. Published by Elsevier Ltd. This is an open access article under the CC BY-NC-ND license (<http://creativecommons.org/licenses/by-nc-nd/4.0/>).

R. W. Campbell

Deep-Sea Research Part II 147 (2018) 43–57

oceanographic observations were sparse and scattered, with the Outer Continental Shelf Environmental Assessment Program (1974–1981) representing one of the few larger-scale efforts. Following the spill, there were several large field campaigns, including the Sound Ecosystem Assessment (1992–1998), Global Ocean Ecosystem Dynamics (1997–2004) and Gulf Watch Alaska projects (2009–present). However, sampling by those projects was also episodic, and in many cases visited different stations in different parts of PWS at different times. Given the trends observed elsewhere, it can be expected that there have been changes in the PWS region as well. It is therefore the goal of this study to assemble the many hydrographic (temperature and salinity) observations that have been made in the PWS region to produce a time series of observations, and to examine those time series to describe how the hydrography and oceanography of the region has changed, with reference to the oceanic and atmospheric forcing that drive the system.

## 2. Methods

### 2.1. Data sources

Profiles of temperature and salinity were collected from several sources. The database described by Musgrave et al. (2013) was used, which includes casts taken between 1973 and 2010 by several coordinated projects and various methods (STD, CTD, XCTD, XBT), which was merged with casts from the NOAA NODC World Ocean Database. Casts in the database were verified with automated methods to eliminate duplicate casts and to check for physically unlikely values ( $-2^{\circ}\text{C} < T < 25^{\circ}\text{C}$ ,  $0 < S < 35$ ); questionable casts were visually examined prior to being discarded.

Casts taken as part of recent oceanographic monitoring programs conducted by the author were also included. Those data were collected from 2009 to present at 12 standard stations in the PWS region with a Seabird Electronics SBE19 or SBE25 CTD. Casts were processed with the standard Seabird Data Processing routines (available from [www.seabird.com](http://www.seabird.com)) and calibrations were done annually. Salinity is reported on the Practical Salinity Scale (PSS-78). For analysis, the casts were grouped into four areas corresponding to the adjacent Gulf of Alaska Shelf (GoA), central Sound (CS), east (E) and northwest (NW) regions defined by Musgrave et al. (2013; Fig. 1). There were 2126, 3764, 540 and 4568 individual profiles within the GoA, CS, E and NW domains, respectively.

Profile data are often missing surface observations (profiles in the database usually began at 1 or 2 m depth, occasionally deeper), and it is at the surface that significant changes in atmospheric and freshwater forcing are most likely to occur; surface observations are more frequent, and also have a slightly longer time series available. For this study, Sea Surface Temperature (SST) from the International Comprehensive Ocean-Atmosphere Data Set (ICOADS) release 3.0 was used (National Centers for Environmental Information et al., 2016), with enhanced filtering tags set. SST data were sparse in the PWS region prior to 1960, and data prior to January 1st of that year were not used. The SST data were also assigned to the four spatial domains (see Fig. 1) and there were 590,598, 513,234, 1138 and 364,047 individual casts in the GoA, CS, E and NW domains, respectively.

The net turbulent heat flux (the sum of latent and sensible heat fluxes, which are highly correlated) was estimated from the nearest gridpoint of the National Centers for Environmental Prediction (NCEP) reanalysis (Kalnay et al., 1996), NCEP Reanalysis data were provided by the NOAA/OAR/ESRL PSD, Boulder, Colorado, USA (<http://www.esrl.noaa.gov/psd/>). Radiative heat fluxes were ignored because the turbulent terms dominate and for comparison with prior work (Janout et al., 2010). The grid point ( $60^{\circ}\text{N}$   $146^{\circ}\text{W}$ ) is approximately 44 km south of Hinchinbrook Entrance, on the adjacent shelf. Heat fluxes from the NCEP reanalysis were compared to heat flux estimates calculated at several National Data Buoy Center (NDBC) buoys in the region (buoys

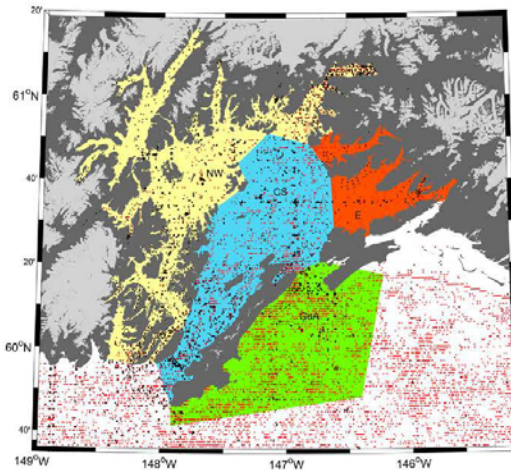


Fig. 1. Position of CTD casts in the CTD database (black dots) and ICOADS SST observations (red dots) used in this study, and geographic regions assigned to the casts. E = eastern (red) Prince William Sound NW = northwest PWS (yellow); CS = central PWS (blue); GoA = Gulf of Alaska (green). Glacier and ice sheet coverage over land from the Randolph Glacier Inventory (version 3.2) is shown in light grey; ice extent data was downloaded from [http://www.glims.org/RGI/rig132\\_d1.html](http://www.glims.org/RGI/rig132_d1.html). (For interpretation of the references to color in this figure legend, the reader is referred to the web version of this article.)

46,060, 46,061, 46,082, 46,085 and 46,076) using the TOGA-COARE algorithm (Fairall et al., 1996) and were found to be well correlated ( $r^2$  values of 0.60–0.67 with  $p < 0.05$ ). NCEP estimates were used in this study because they encompass the entire temporal range of the other datasets, while the buoy records begin in 1995 or later. Heat flux estimates were converted to seasonally detrended anomalies by subtracting observations from daily averages, and monthly averages calculated from the daily anomalies.

As a proxy for wind-driven transport into PWS (Halverson et al., 2012), the offshore component of the NOAA Pacific Fisheries Environmental Laboratory monthly upwelling index (<http://oceanwatch.pfel.noaa.gov/products/PFELData/upwell/monthly/upanoms.mon>) at  $60^{\circ}\text{N}$   $146^{\circ}\text{W}$  was used. The format of the upwelling index was the same as the heat flux estimates, and monthly anomalies were calculated with the same method.

Precipitation records in the PWS are sparse and there are few long-term time series. To estimate precipitation to the region, NOAA CMAP precipitation estimates provided by the NOAA/OAR/ESRL PSD, Boulder, Colorado, USA were used (<http://www.esrl.noaa.gov/psd/>; Xie and Arkin, 1997). Monthly averages at four grid points bracketing the PWS area (longitudes  $148^{\circ}$   $45^{\circ}\text{W}$  and  $151^{\circ}$   $15^{\circ}\text{W}$  and latitudes  $58^{\circ}$   $45^{\circ}\text{N}$  and  $61^{\circ}$   $15^{\circ}\text{N}$ ) were averaged, and anomalies calculated by subtracting the long-term mean (from 1981 to 2010, also provided by the NOAA PSD). Freshwater discharge estimates into PWS were taken from Beamer et al. (2016) available at (<http://www.aocs.org>). Discharge in each coastal cell within PWS (i.e. the CS, E and NW regions) was summed for each model day, converted to a daily anomaly, and averaged monthly.

In order to relate the conditions within PWS to larger scale climatic trends, cross correlations were determined between temperature and salinity and large-scale climate indices. The Pacific Decadal Oscillation (PDO: Mantua et al., 1999) is the first principal component of North Pacific SST and was downloaded from the University of Washington JISAO PDO page (<http://research.jisao.washington.edu/pdo/>). The North Pacific Gyre Oscillation (NPGO: Di Lorenzo et al., 2008), the second principal component of sea surface height anomaly, is

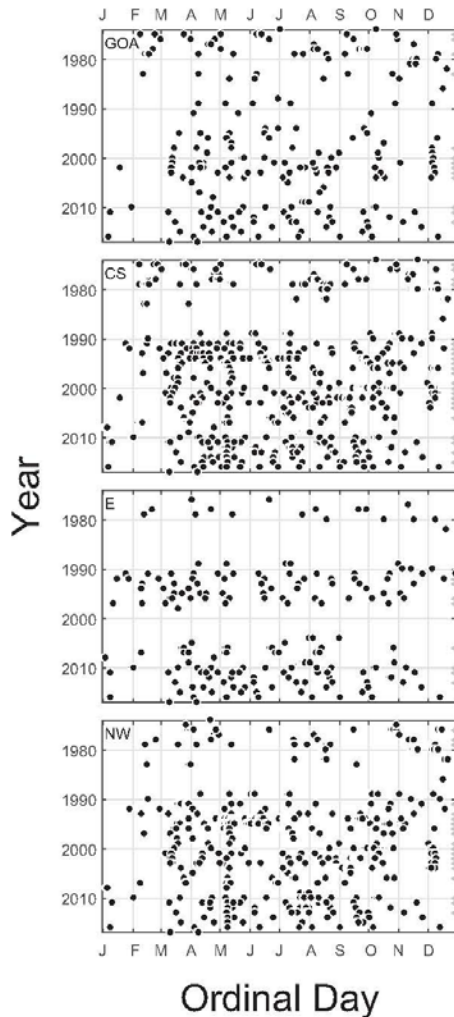


Fig. 2. Inter- and intra-annual coverage of the CTD casts used in this study, broken out into the four Prince William Sound geographic regions (Fig. 1). Each dot denotes a cast. Years that were found to have an adequate number of casts to define the annual cycle (> 6 observations, with an observation in each quarter, see text) are denoted with triangles along the ordinate.

uncorrelated with the PDO, and reflects changes in the intensity of gyre circulations in the North Pacific. Values of the NPGO index were obtained from <http://www.o3d.org/npgo/>.

2.2. Data analysis

The datasets used in this study presented a number of analysis challenges caused by the spatial and temporal heterogeneity of the samples, as is to be expected when using archived data from numerous different projects with different goals. Assigning the observations into spatial domains attempts to remove the effect of spatial heterogeneity in the dataset by combining stations that can be expected to be similar (a discussion of the choice of the regions is given by Musgrave et al.,

2013). The observations in the dataset were also temporally scattered (Fig. 2), which created a challenge for standard time series and frequency domain methods that require a regularly sampled time series. Breaking the observations up into categorical time categories (i.e. weekly, monthly) is undesirable, because the region has large seasonal changes in hydrographic properties (e.g. Xiong and Royer, 1984; Wang et al., 2001; Royer, 2005), and thus the date and time an observation was made has value. It was therefore decided to use a simple regression and harmonic analysis that explicitly includes time to examine trends (Wilks, 2011).

All regressions calculated in this study were by nonlinear least squares using a Trust Region Reflective algorithm (Branch et al., 1999), with a termination tolerance of  $10^{-6}$ . No constraints were set on the number of iterations, but they were always < 600. Initial parameter estimates were set to zero, except for constants ( $\bar{y}$  and  $\beta_0$ , see below) which were initialized as the mean of all observations being fit. Confidence intervals were calculated at the 95% level.

If not already binned, casts were averaged into 1-m depth bins starting with the 2-m bin. Depth specific fits to the entire dataset showed that a second order cosine curve of the following form tended to describe the seasonal cycle in temperature and salinity reasonably well:

$$H_z(t) = \bar{y} + \sum_{k=1}^2 C_k \cos \left[ \frac{2\pi kt}{365} - \varphi_k \right] \quad (1)$$

where H is the hydrographic quantity of interest (temperature or salinity, for a specific depth, z), t is the day of the year (i.e. a number between 1 and 365.25) and  $\bar{y}$ ,  $C_k$  and  $\varphi_k$  are fitted parameters. The constant,  $\bar{y}$ , may be thought of as the seasonally detrended average, while  $C_k$  and  $\varphi_k$  describe the amplitude and phase respectively of the components. With  $k = 1$  and 2, the model contains an annual and a semiannual component. Prior work in the region (e.g. Royer et al., 2001) have used a first order equation (e.g.  $k = 1$  only), but it was found with the current dataset that a second order model gave a better fit (as diagnosed with an F-test), particularly in the upper part of the water column; a third order model was not a significant improvement (F-test  $p = 1.0$ , at all depths).

Fitting the data by depth bins for the entire dataset (and within each spatial domain) thus produces a climatological annual cycle for that depth that may be put together into a depth-specific climatological annual cycle (Fig. 3). Similarly, seasonal climatologies were produced for MLD, surface heat flux, and the NOAA upwelling index (Fig. 4).

Eq. (1) may also be extended to a simple regression model that may be fit to the entire time series, again for each depth:

$$H_z(d) = \beta_0 + \beta_1 t + \sum_{k=1}^2 C_k \cos \left[ \frac{2\pi kd}{365} - \varphi_k \right] \quad (2)$$

where d is the date number, a fractional number of days from an arbitrary date and time (in this study, the reference date number was set such that date number 1 was January 1, 0000),  $\beta_0$  is the constant,  $\beta_1$  the linear trend, and the rest of the parameters are as in Eq. (1). The advantage of this regression method is that it can span gaps in the time series; the disadvantage is that the parameters of the harmonics are fit for the entire dataset, and may in fact change over time (e.g. changes in minimum or maximum temperatures, or the timing of the annual cycle).

To incorporate interannual variability in the timing and the magnitude of the annual cycle, Eq. (1) was also fit to individual years (January 1 through December 31). Because the data are patchy in time, individual years were included in the analysis only if (1) there were > 6 observations made over the course of the year, and (2) the observations were distributed such that there were observations made within each quarter of the year. The choice of quarters was arbitrary, and was intended to ensure that there was a good enough temporal spread of observations over the year to reasonably describe the annual cycle.

## Appendix A

Open Access manuscript available at <https://doi.org/10.1016/j.dsr2.2017.08.014>

R.W. Campbell

Deep-Sea Research Part II 147 (2018) 43–57

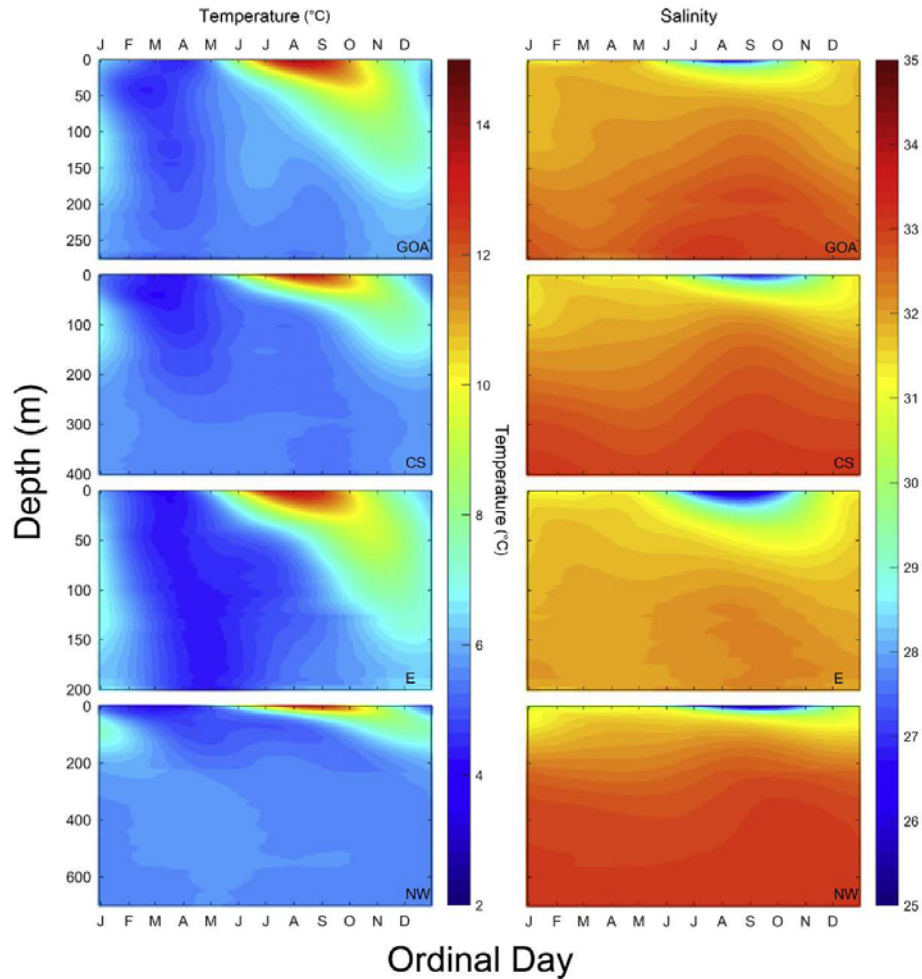


Fig. 3. Climatological annual temperature ( $^{\circ}\text{C}$ , left panels) and salinity (right panels) cycles in each of the Prince William Sound geographic regions (Fig. 1). Each annual cycle was created by fitting Eq. (1) to each depth bin in a stepwise fashion, (see text). Note that the scaling of the ordinate changes among regions.

Temporal coverage was best at the surface and tended to decline at depth. After fitting Eq. (1) to each depth bin in each spatial domain, the changes in  $\bar{y}$ ,  $C_k$  and  $\phi_k$  were regressed over time to test for trends. This analysis is referred to as an “annual” analysis, because parameters were calculated for each entire year that met the data density criteria.

Changes in the depth of the surface mixed layer have been observed in time series elsewhere in the GoA (Li et al., 2005; Weingartner, 2007), although not on the nearby coastal shelf (Sarkar et al., 2005); changes in heat or freshwater fluxes might result in changes in PWS. In this study, mixed layer depth (MLD) was estimated with a simple threshold method (Thomson and Fine, 2003; Musgrave et al., 2013) based on the differences in potential density at the surface versus at depth. MLD was defined as the depth ( $z$ ) where the difference in potential density ( $\Delta\rho_p = \rho_p(z) - \rho_p(z_0)$ ) at depth and the surface ( $z_0$ ) exceeded  $0.125 \text{ kg m}^{-3}$ . The threshold was selected to be an estimate of the depth of the seasonal pycnocline (Thomson and Fine, 2003). MLD is much more susceptible to short term-variations by wind mixing, was much more variable than temperature and salinity measurements, and did not have

as coherent a seasonal structure. MLD estimates were seasonally detrended and converted to anomalies by subtracting observations from a 10-day moving average of MLD versus ordinal day from the entire dataset, then combined into quarterly averages.

Lag-lead relationships between hydrographic properties (T and S anomalies) and the large-scale climatic indices (PDO, NPGO) and Lunar Nodal Cycle (LNC; see below) were examined with cross correlations (Pearson’s). Cross correlations were estimated for each 1-m depth bin within each geographic region. The PDO and NPGO indices are reported monthly, and anomalies (calculated from the entire dataset) were assigned to calendar months for each correlation. LNC lags were computed from the time associated with each observation. The significance of each correlation was assessed with simulated probability distribution functions (10,000 permutations) of correlation coefficients generated from two red noise time series estimated from the anomalies and indexes (Di Lorenzo et al., 2008).

The ICOADS SST observations are complementary to the cast data, but are of difference provenance (and longer temporal resolution), so

R. W. Campbell

Deep-Sea Research Part II 147 (2018) 43–57

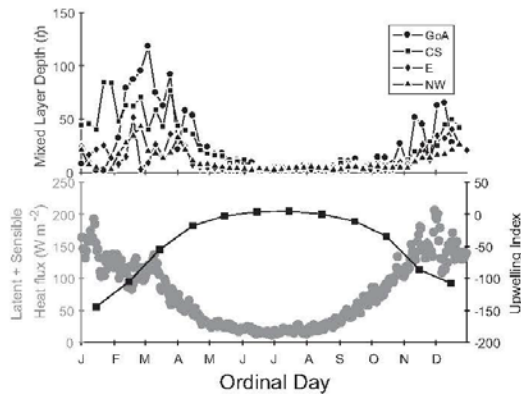


**Fig. 4.** Annual climatologies of mixed layer depth (MLD; top panel) and surface heat flux (bottom panel, grey symbols, left axis) in Prince William Sound and the nearest NOAA upwelling index (bottom panel, black symbols, right axis). Daily MLD averages were linearly interpolated to weekly values to reduce clutter to better allow comparison among the geographic regions. A positive upwelling index indicates coastal upwelling, a negative index indicates downwelling.

were treated separately in this analysis. SST was converted to anomalies by subtracting observations from the long-term climatology (Eq. (1)) and regressed over time with a linear model (which is equivalent to fitting Eq. (1)).

### 2.3. Lunar nodal tide

As well as long term trends that can be expected to follow as a result of global and basin scale changes, it has been shown that there is a low frequency component to air and sea surface temperatures set up by the 18.6-year lunar declination cycle (Loder and Garrett, 1978; Royer, 1993; McKinnell and Crawford, 2007). As well as linear fits to the parameters, the progression of the 18.6-year nodal tide was estimated with the cosine of the negative of the longitude of the Moon's ascending node,  $N'$  (Doodson, 1921):

$$N' = 100^{\circ}0.8432 + 1934^{\circ}0.1420T - 0^{\circ}0.0021T^2 \quad (3)$$

where  $T$  is time, based on a Julian century of 36,525 solar days, with time zero at 00:00 January 1, 1900; the cosine of  $N'$  shall be referred to as the Lunar Nodal Cycle (LNC). The LNC was cross correlated with temperature and salinity to determine the dominant lags.

## 3. Results

### 3.1. CTD time series

The slope of the simple regression model (Eq. (2)) applied to the cast data in each 1-m depth bin indicated a significant warming trend in the GoA region at all depths, and a warming trend at depth in central PWS and the NW region (Fig. 5). Near-surface and near-bottom trends in the E region had confidence intervals that spanned zero, and thus were not significant (the E region had the smallest number of casts and the poorest temporal coverage); there was a significant warming trend in the mid-depths. There was a significant cooling trend in the NW region between 3 and 23 m. There was a trend toward increasing salinity at depth in the GoA and CS regions, and at mid-depths (~100 to 250 m) in the NW region (Fig. 6). Regression models incorporating an 18.6-year component resulted in fits with confidence intervals for the coefficients that spanned zero and are not shown.

The trends in the parameters from the annual model fits returned similar results with significant trends in the  $\bar{y}$  term, also indicating a

warming trend at depth in the GoA region, and over most depths in the CS region (Fig. 7, left panel); there were few significant trends in salinity: there was near-surface freshening in the NW region and a trend towards higher salinity at depth in the CS region (and ~205 to 225 m in the GoA region). The annual amplitude component ( $C_1$ , corresponding to the mid-summer temperature maximum or salinity minimum) had a significant positive temperature trend in the near surface in the NW region (Fig. 8, left panel), and a significant negative trend in salinity at the surface in the GoA and NW regions (Fig. 8, right panel). There were few significant trends in the phase term ( $\phi_1$ ) for temperature. There was a negative trend in salinity at the surface in the GoA region, and a positive trend in the top-most depth bins in the NW region (Fig. 9, right panel). A trend of 0.025 rad corresponds to a time shift of just under 1.5 days, which indicates a shift of the annual salinity minima to earlier timing (about 1 week earlier over the course of the entire dataset) in the GoA region, and to a later timing (4–5 days) in the NW region.

Mixed layer depth anomalies over time indicated a shallowing trend in the depth of the seasonal thermocline in all but the E region (Fig. 10; negative anomalies imply a MLD thinner than average). The slopes of the anomalies suggest a shoaling of the seasonal pycnocline within PWS of slightly more than 3 m decade<sup>-1</sup>. Although there were long-term trends, there was also considerable year-to-year variability, with several stanzas having similar mixed layer depths. There was no indication of consistent seasonal changes in MLD.

Temperatures were out of phase with the 18.6-year nodal tide (LNC) with a 4–5-year lag, with the strongest correlations ( $r = 0.4–0.5$ ,  $p < 0.05$ ) at depths greater than 100 m in all regions except E (Fig. 11). Because the LNC is an oscillation, the figures repeat on an 18.6-year cycle and the high positive correlations at long lags (13–14 years) are equivalent to a lead time of 4–5 years. Lagged correlations with salinity showed broadly similar patterns, although the correlations were not as strong (excepting the E region, with the lowest data density).

The PDO index lead temperatures in the top 200 m in all regions by 3–12 months, with longer leads in the deeper waters of the NW region (Fig. 12). Salinity was weakly correlated with the PDO at short time scales, though there were not consistent patterns among the regions. Cross correlations between NPGO and temperature also varied among the regions (Fig. 13), the strongest correlations were with temperature at depth at long lags in the NW region (and to a lesser degree the GoA region). Salinity was broadly positively correlated to NPGO at all depths in the GoA, and at 100–200 m in the CS and E regions. NPGO was not well correlated with salinity in the NW region.

The mechanisms driving PDO and NPGO might be related to the LNC, and a cross correlation was done between both indices and the LNC (not shown). NPGO was uncorrelated with the LNC ( $p < 0.05$  at every lag), and PDO was weakly correlated, with significant ( $p < 0.05$ ) correlation peaks of  $r = -0.18$  and  $0.18$  at 23 and 135 months, respectively.

### 3.2. SST

SST trends varied among the regions, with a long-term slope that was not significantly different from zero in the CS and E regions (Fig. 14). There was a small but significant cooling trend in SST in the NW region (slope:  $-0.09$  °C decade<sup>-1</sup>, 95% CI:  $-0.017$  to  $-0.010$ ) and a warming trend in the GoA region (slope:  $0.08$  °C decade<sup>-1</sup>, 95% CI:  $0.03–0.14$ ).

### 3.3. Surface heat flux, upwelling, precipitation and discharge

Surface heat flux anomalies were primarily positive at the beginning of the time series, with a negative trend; positive anomalies became more prevalent in the late 1970s/early 1980s (Fig. 14). The NCEP convention of positive heat flux is from the ocean to the atmosphere was used, indicating an increase in heat flux to the surface ocean over

# Appendix A

Open Access manuscript available at <https://doi.org/10.1016/j.dsr2.2017.08.014>

R. W. Campbell

Deep-Sea Research Part II 147 (2018) 43–57

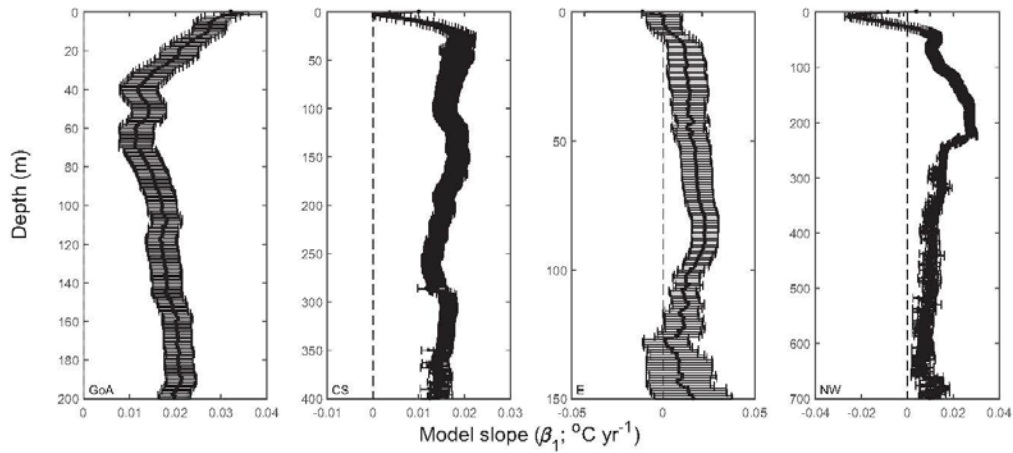


Fig. 5. Profiles of  $\beta_1$  (i.e. the long term slope in Eq. (2)) fit to temperature, in the four Prince William Sound geographic regions (Fig. 1). Error bars indicate 95% confidence intervals for the parameter. Note that both axes change among figures.

time.

Upwelling index anomalies did not show a long-term trend on a monthly basis (the slope was not significantly different from zero), and did not exhibit significant 18.6-year periodicity (Fig. 14). Spectral analysis of the upwelling time series identified a main peak in the power spectral density at  $\sim 12$  months, with a second smaller peak at  $\sim 6$  months. An annual upwelling index, calculated as the sum of all the monthly anomalies in each calendar year, showed a significantly positive trend over time. Heat flux was positively correlated with the PDO (at lags up to 7 months) but not the NPGO; the upwelling index was not significantly correlated with the climate indices.

The precipitation and discharge time series were the best available but the shortest records employed in this analysis, beginning in 1979 (Fig. 15). There was no long-term trend in precipitation. There was a small but positive trend in discharge anomaly.

## 4. Discussion

### 4.1. High vs low frequency variability

The trends observed in this study were of much lower magnitude than the considerable inter- and intra-annual variability in temperature and salinity. There is no doubt considerable high frequency temporal and spatial variability in the region: Vaughan et al. (2001), for instance, highlighted the spatial and temporal variability in temperature and salinity in central PWS that is caused by smaller scale oceanographic processes (and all the data used by Vaughan et al., 2001 is included in this study). This type of analysis cannot account for that high frequency variability, and it is assumed that the considerable variability surrounds the mean. Most prior work in the North Pacific has been from a small number of regularly visited stations (e.g. Royer, 1993; Royer and Grosch, 2006; Royer et al., 2001), but there has not been a similar coordinated effort undertaken in the PWS region. It can be expected

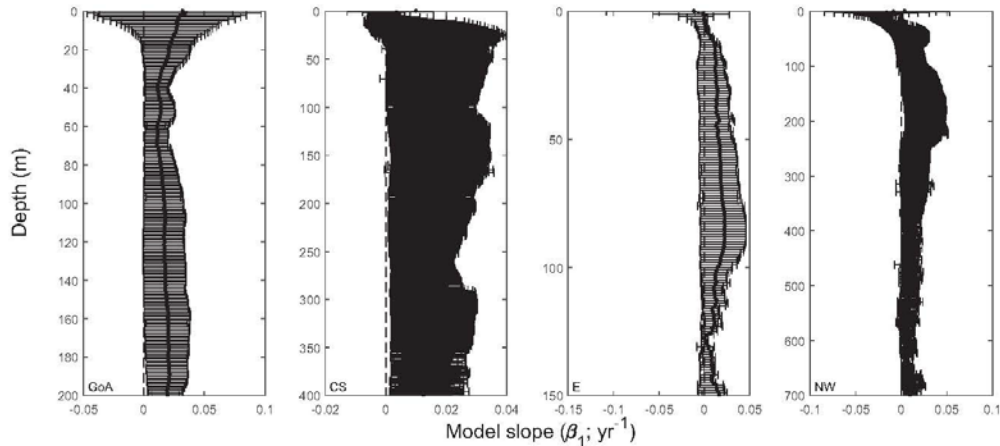


Fig. 6. Profiles of  $\beta_1$  (i.e. the long term slope in Eq. (2)) fit to salinity, in the four Prince William Sound geographic regions. Error bars indicate 95% confidence intervals for the parameter. Note that both axes change among figures.

## Appendix A

Open Access manuscript available at <https://doi.org/10.1016/j.dsr2.2017.08.014>

R. W. Campbell

Deep-Sea Research Part II 147 (2018) 43–57

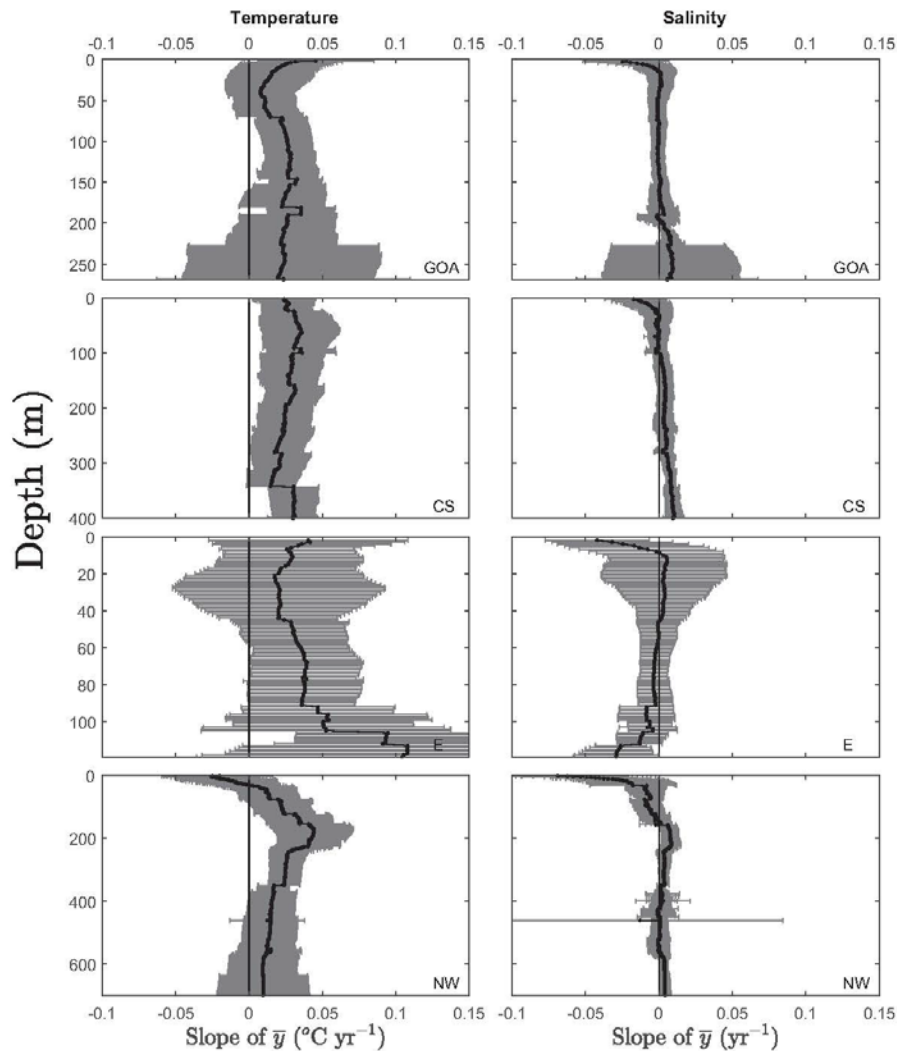


Fig. 7. Profiles of the slope of  $\bar{F}$  ("annual mean") over time in the four Prince William Sound geographic regions (Fig. 1) for temperature (left panel) and salinity (right panel). Bars indicate 95% confidence intervals. Note that the scaling of the ordinate differs among regions.

that using ensembles of stations in this way will increase the likelihood of type II errors and will therefore likely fail to detect some existing patterns. For this reason, several complementary methods and models were used, but they did not always agree, leading to some ambiguity in the interpretations.

#### 4.2. Climatological annual cycles

The climatological annual cycle that emerges from this analysis is similar from region to region and similar to that of Xiong and Royer (1984): following winter minima in February–April, surface temperatures begin to warm in May, with warming largely confined to the upper 25 m of the water column (Fig. 3). The thermocline begins to break down in September and heat is mixed downward into the water

column. The salinity cycle is similar, with surface salinity beginning to decrease in late May, decreasing over the summer, and being mixed downward in autumn (Fig. 3). Salinity also tends to increase at depth during the summer months (June–Sept), as deep-water renewal occurs. Halverson et al. (2012) observed annual renewal events at moorings in Hinchinbrook Entrance during that same time between 2005 and 2010.

The MLD climatology presented here (Fig. 4) also matches the canonical pattern for the region described previously (Henson, 2007; Musgrave et al., 2013; Weingartner, 2007). MLD was deepest in off-shore locations (GoA and CS) in autumn/winter and shoaled in spring. More protected locations (E and NW) experienced an earlier return to stability and retained a shallower MLD longer into autumn, as would be expected from enhanced stability from near shore freshwater inputs and comparatively less wind mixing in protected locations with less fetch.

## Appendix A

Open Access manuscript available at <https://doi.org/10.1016/j.dsr2.2017.08.014>

R. W. Campbell

Deep-Sea Research Part II 147 (2018) 43–57

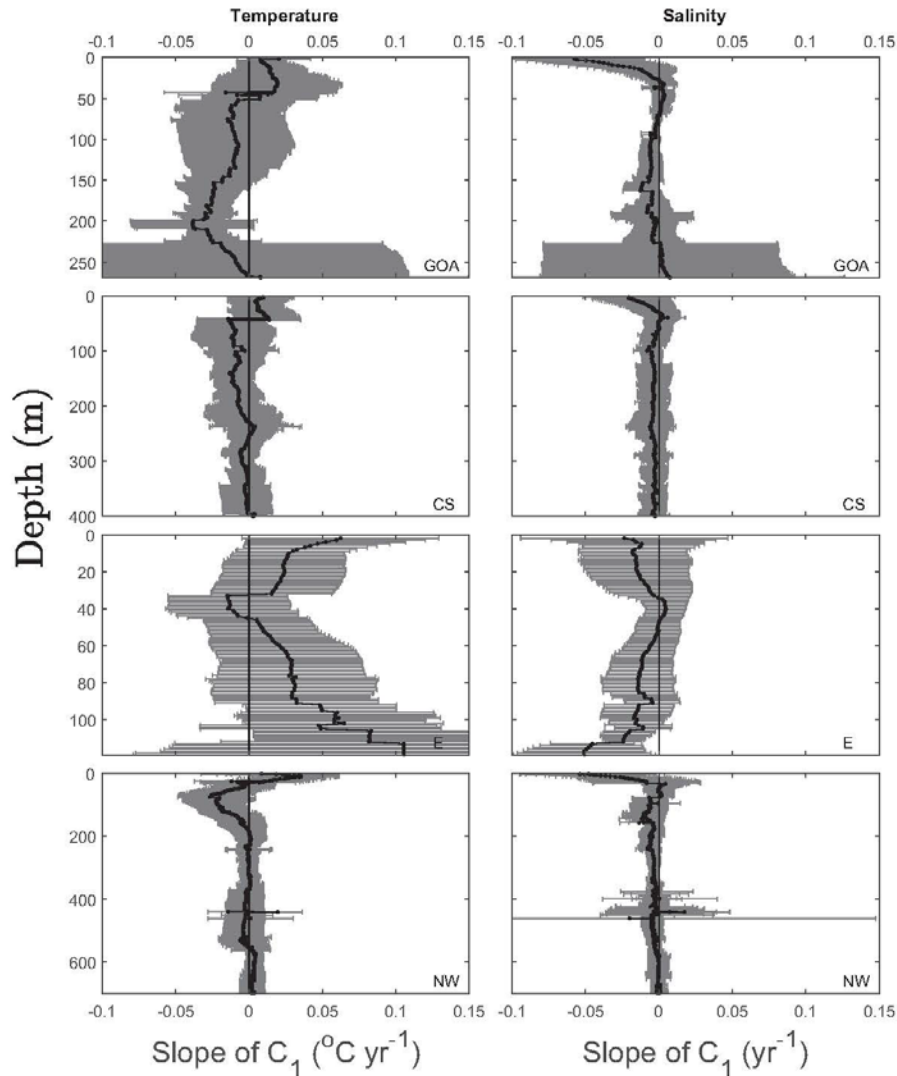


Fig. 8. Profiles of the slope of  $C_1$  (amplitude) over time in the four Prince William Sound geographic regions (Fig. 1) for temperature (left panel) and salinity (right panel). Bars indicate 95% confidence intervals. Note that the scaling of the ordinate differs among regions.

On the shelf adjacent to PWS, latent and sensible heat fluxes were on average a net loss from the ocean to the atmosphere (Fig. 4), with the highest fluxes in winter, as is to be expected for the region (Janout et al., 2010; Bond et al., 2015). The upwelling index climatology (Fig. 4) showed weak upwelling in the summer, peaking in June/July and coinciding with the increase in salinity at depth (Fig. 3) likely caused by deep-water renewal (Halverson et al., 2012). Downwelling predominated during the winter months.

### 4.3. Long term trends in the PWS region

In the waters adjacent to PWS (GoA), there was a warming trend in the last 40 years of  $\sim 0.2$  to  $0.3$   $^{\circ}\text{C}$  per decade, with most warming at

the surface (Figs. 5, 7 and 14), similar to the trends observed as part of a larger pattern of warming throughout the region (Royer and Grosch, 2006; Wu and Li, 2007). Beyond an overall increase in temperature, the annual model fits did not suggest any meaningful changes in the magnitude of the annual peak or in timing.

At depth ( $> 150$  m), there was a decrease in the amplitude of the annual temperature maximum (Fig. 8). The freshening trend observed by Royer and Grosch (2006) at the GAK1 site off Seward, AK was less evident in the shelf region (GoA) included here, but their site, in the mouth of Resurrection Bay, was nearshore and downstream of PWS and may have thus reflected, in part, the outflows from NW PWS (as well as the rest of the coastal margin upstream of Resurrection Bay). A freshening trend at the surface from the annual analysis of casts occurred

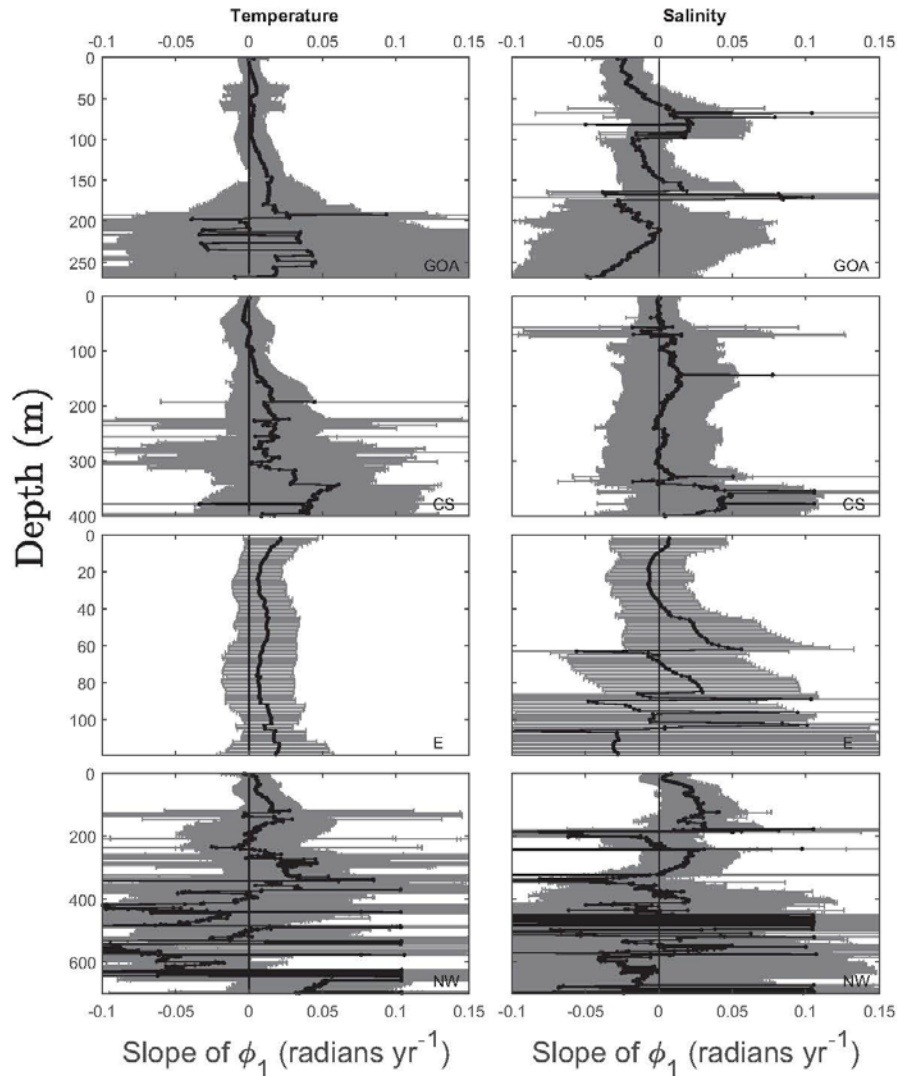


Fig. 9. Profiles of the slope of  $\phi_1$  (phase) over time in the four Prince William Sound geographic regions (Fig. 1) for temperature (left panel) and salinity (right panel). Bars indicate 95% confidence intervals. Note that the scaling of the ordinate differs among regions.

near surface in the NW region (Fig. 6), but with a trend towards higher salinities at depth. These observations suggest an enhancement in deep-water renewal events over time, with more cool, salty water transported shoreward during the deep-water renewal season, which could account for the observed reduction in the annual maximum. An enhancement in deep-water renewal could also be expected to accompany decreases in surface runoff because enhanced surface transport will cause entrainment of more saline water at depth (Royer, 2005; see below).

In central PWS there was also a warming trend of similar magnitude to GoA at most depths identified by both the simple and annual regression models, there was again no evidence for changes in timing or the magnitude of the summer maximum. Trends in salinity were similar to the GoA region, with an increase at depth and non-significant

increase at the surface. The interpretation for those trends is essentially the same as the GoA region: PWS may be considered to be a large estuary (e.g. Vaughan et al., 2001), and enhanced outflowing freshwater fluxes at the surface can be expected to increase entrainment and be compensated by inflowing higher salinity water at depth (see below). The eastern portion of PWS (area E) also generally showed the same trends, although they were less likely to be detectable (i.e. significantly different from zero), presumably due to the comparatively lower data density there (rather than combining the region with CS, it has been left separate to preserve the regions used by Musgrave et al., 2013).

In northwestern PWS, the simple regression model showed declining temperatures near surface and a warming trend at depth; annual regressions had a similar pattern in annual mean temperature near

R. W. Campbell

Deep-Sea Research Part II 147 (2018) 43–57

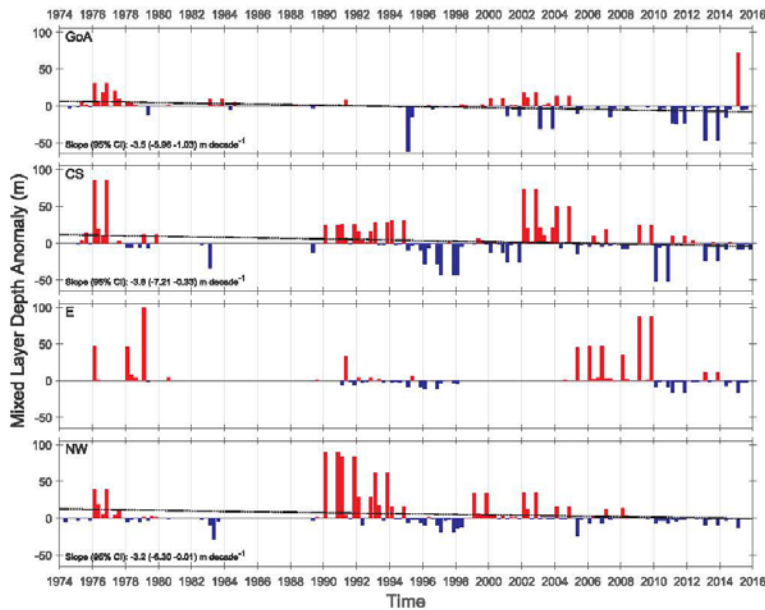


Fig. 10. Quarterly averages of the mixed layer depth (MLD) anomaly time series in the four Prince William Sound geographic regions (Fig. 1). Long term slopes are only reported for regions where the slope of the line was significantly different from zero.

surface, but the 95% CI spanned zero (Fig. 7). There was also a negative trend in the annual maximum temperature parameter ( $C_1$ ; Fig. 8), which suggests that the annual temperature maximum has been declining in that region (both overall, and in terms of the maximum temperature reached). Annual regressions (which are more conservative, since years with few observations are dropped) also found a non-significant negative trend in annual mean temperature.

There was also a trend towards declining salinity at the surface in the NW region, but no significant trend at depth (Fig. 6, Fig. 7). The overall picture suggests a general cooling and freshening at the surface, and warming and increasing salinity trends at depth. A freshening trend can be the result of enhanced inputs of freshwater through precipitation and/or runoff, and a cooling trend will be the result of reduced surface heat flux or transport. The estimates of heat flux from the adjacent shelf suggest that surface fluxes from the atmosphere to the ocean have been increasing in the region (Fig. 14).

The hydrologic connections between the atmosphere, land, and surface ocean in Prince William Sound are not well described. The region is poorly gaged, has sparse weather observations, and consists of numerous small watersheds (e.g. see Beamer et al., 2016). Precipitation in the region is considerable (Shulski and Wendler, 2008), but earlier hydrological models (Royer, 1982; Royer, 2005; Wang, 2004; Hill et al., 2015) did not show long-term trends in discharge. The available precipitation and discharge estimates used here suggest that precipitation has not changed significantly in the region in recent decades, while there has been a modest increase in discharge. Recent estimates of ice mass in the GoA region suggest a negative mass balance in the region (Arendt et al., 2013), and declines in watershed storage (Hill et al., 2015; Beamer et al., 2016), and that discharge may thus represent freshwater derived from ice storage. Most of the ice mass in PWS is concentrated on the western side (i.e. the NW region, Fig. 1), and the freshening trend observed there may reflect inputs from ice ablation. The Beamer et al. (2016) discharge estimates do not include inputs from tidewater glaciers (which are also largely receding in the PWS region, e.g. Colgan et al., 2012) that represent another potential source of freshwater and negative heat inputs.

The cooling and freshening trend near surface in the NW region thus could be the combination of two mechanisms: At the surface ( $\sim 0$  to 10 m, the depth of the seasonal thermocline; Fig. 4), increased discharge of freshwater of glacial origin would lead to reductions in the average temperature and salinity. The increased discharge would also increase entrainment of deep water (generally cooler and more saline than surface water). The resulting circulation of cool deep water towards the surface would then be responsible for the reduction of temperature just below the surface layer, to a depth of  $\sim 30$  m (Fig. 5). At depths well away from the surface layer, salinity has increased over time, which is most likely a reflection of the overall enhanced movement of deep water into PWS from the shelf.

Exchange between PWS and the adjacent shelf is primarily northward through Hinchinbrook Entrance (Niebauer et al., 1994; Halverson et al., 2012) and is driven in part by wind (Niebauer et al., 1994). In winter, westward winds drive near-surface transport, and in summer and autumn the relaxing of wind driven downwelling allows a flux of slope water along the bottom into the basins of PWS (Ladd et al., 2005; Weingartner et al., 2005). The upwelling anomaly index used here (Fig. 14) is a proxy for that transport (Halverson et al., 2012). The northern GoA shelf is a primarily downwelling system, upwelling is generally weak at best (Stabeno et al., 2004; Halverson et al., 2012). The positive trend in “upwelling” observed here on the shelf (Fig. 14) is thus best viewed as a reduction in downwelling, rather than increased upwelling: most of the positive upwelling anomalies, particularly since the 1990s, occurred during the winter months, when downwelling predominates (Fig. 4). Reduced downwelling would tend to lead to enhanced deep-water renewal during late summer/autumn. That is also the time of maximal freshwater inputs to the surface (Fig. 3) and when entrainment could be expected to be highest as well.

#### 4.4. Long term changes attributable to large scale drivers

Several long-term trends and oscillations have been identified in the North Pacific at varying time scales, from 50 to 70 years (Minobe, 1997), 23 years (Gedalof and Smith, 2001), the 18.6-year lunar nodal

## Appendix A

Open Access manuscript available at <https://doi.org/10.1016/j.dsr2.2017.08.014>

R.W. Campbell

Deep-Sea Research Part II 147 (2018) 43–57

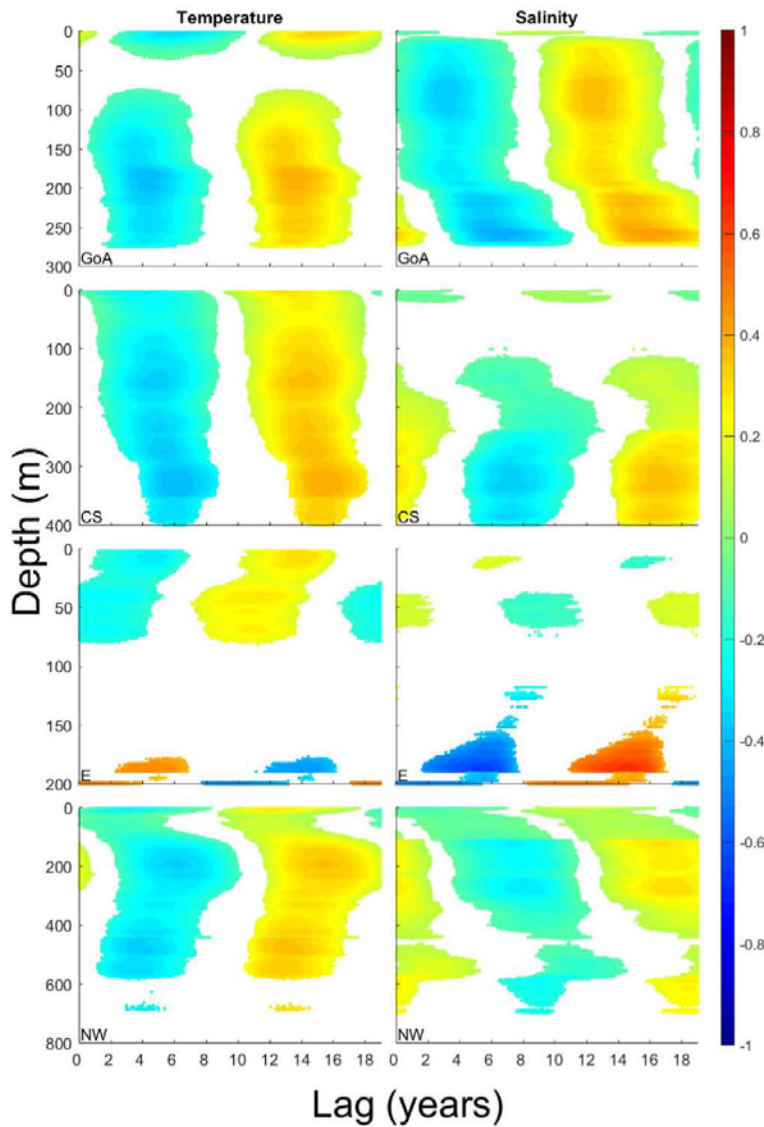


Fig. 11. Cross correlations (lags only) between the Lunar Nodal Cycle (LNC) and temperature (left panels) and salinity (right panels) in the four Prince William Sound geographic regions (Fig. 1). Note that the scaling of the ordinate differs among regions. Only significant correlations ( $p < 0.05$ , from 10,000 simulated probability distribution functions) are shown.

tide (Royer, 1993) and quasi-decadal (Mantua et al., 1997; Di Lorenzo et al., 2008); this analysis has focused on the latter three, given the length of the time series. There was some correspondence between conditions in PWS and the North Pacific in general terms: there was a switch from cool to warm SST in 1977 (Fig. 14, top panel), which corresponds to the basin-wide regime shift that occurred around that time (Hare and Mantua, 2000), although SST did not stay positive into the 1980s in PWS as they did elsewhere. Negative surface heat flux anomalies became more prominent at approximately the same time (Fig. 14). PWS also experienced a cool phase beginning in 2006 that corresponds to the cool period identified on the GoA shelf off Seward, Alaska (Janout et al., 2010), and switched toward positive anomalies in late 2013, as did the central GoA (the “Blob” anomaly of Bond et al.,

2015). Both of those contemporary stanzas appear to have been in part due to winter cooling processes (which are varied and complex, e.g. Janout et al., 2010), which manifested immediately south of PWS as well: the upwelling anomaly (Fig. 14, bottom panel) suggests that winter winds were strongly downwelling in 2006–2007, and less so from 2011 onward.

The PDO is the first principal component of SST in the North Pacific (Mantua et al., 1997), and is also correlated with sea surface height (Di Lorenzo et al., 2008), it describes the dominant spatial and temporal patterns of SST in the northeastern Pacific Ocean. The PDO pattern is not a monolithic climatic mode, it is the sum of several drivers including variations in surface heat flux and wind-driven transport, oceanic thermal inertia, and decadal variations in the Oyashio/

## Appendix A

Open Access manuscript available at <https://doi.org/10.1016/j.dsr2.2017.08.014>

R.W. Campbell

Deep-Sea Research Part II 147 (2018) 43–57

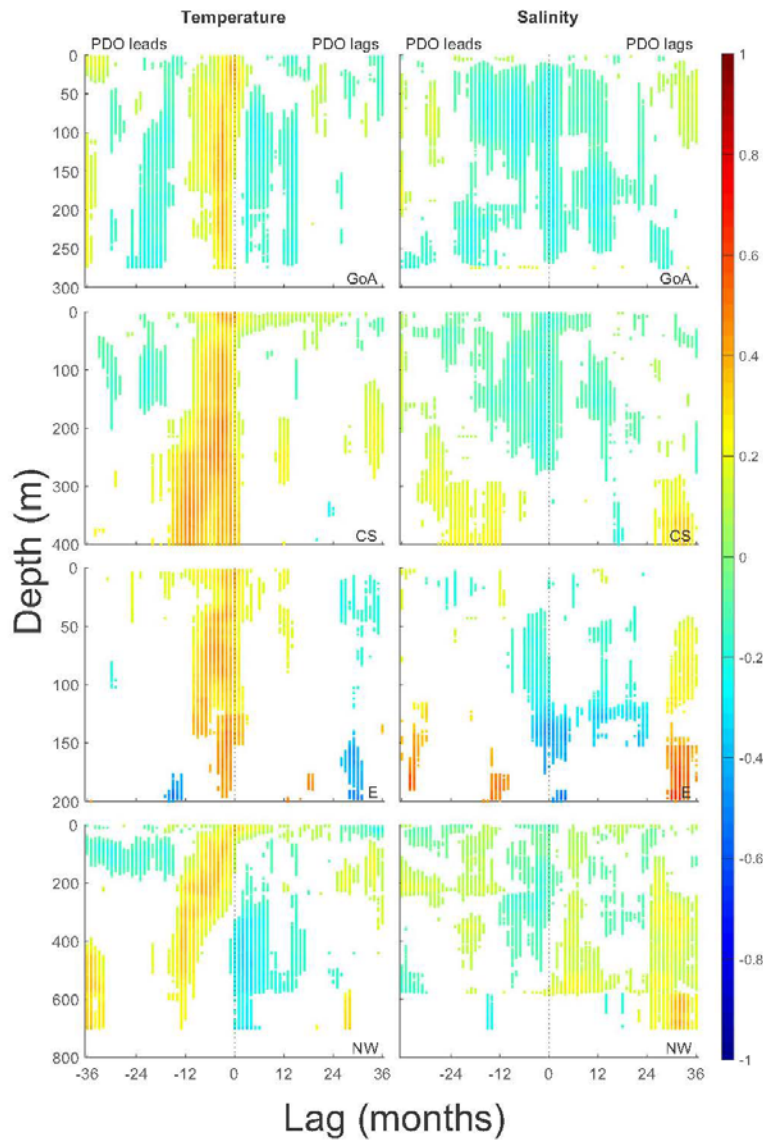


Fig. 12. Cross correlations between the Pacific Decadal Oscillation (PDO) and temperature (left panels) and salinity (right panels) in the four Prince William Sound geographic regions (Fig. 1). Note that the scaling of the ordinate differs among regions. Only significant correlations ( $p < 0.05$ , from 10,000 simulated probability distribution functions) are shown.

Kuroshio extension (Newman et al., 2016). The PDO pattern also reflects variability driven by the El Niño Southern Oscillation (ENSO) and correlates with ENSO indices. The NPGO is the second principal component of sea surface height, and reflects changes in geostrophic circulations in the North Pacific; a positive NPGO is associated with a strengthening of the Alaska Current (Di Lorenzo et al., 2008).

Cross correlations of the PDO and NPGO with temperature and salinity highlight the connections between large-scale patterns in the Gulf of Alaska and PWS. Temperature at most depths lagged the PDO (Fig. 12), presumably caused by lags attributable to transport time and mixing. Salinity also lagged the NPGO (Fig. 13) and was correlated at much broader temporal ranges, perhaps reflecting the longer-term

changes in circulation (indexed by the NPGO) versus shorter term atmospheric variability (indexed in part by the PDO). Flushing times of PWS vary seasonally, with a minimum in summer ( $> 500$  days) and maximum in autumn/winter (120–300 days; Niebauer et al., 1994; Halverson, 2012) and vary by depth (e.g. most transport during summer months is at depth). The relatively long lags of NPGO relative to salinity may also reflect long-term oscillations. Although the correlations indicate that the indexes account for a relatively small proportion of the variance, they are consistent with correlations done at regional scales (Di Lorenzo et al., 2008; Newman et al., 2016).

An 18.6-year periodicity is a common feature of geophysical time series of adequate length (Currie, 1996) and has been observed in SST

## Appendix A

Open Access manuscript available at <https://doi.org/10.1016/j.dsr2.2017.08.014>

R.W. Campbell

Deep-Sea Research Part II 147 (2018) 43–57

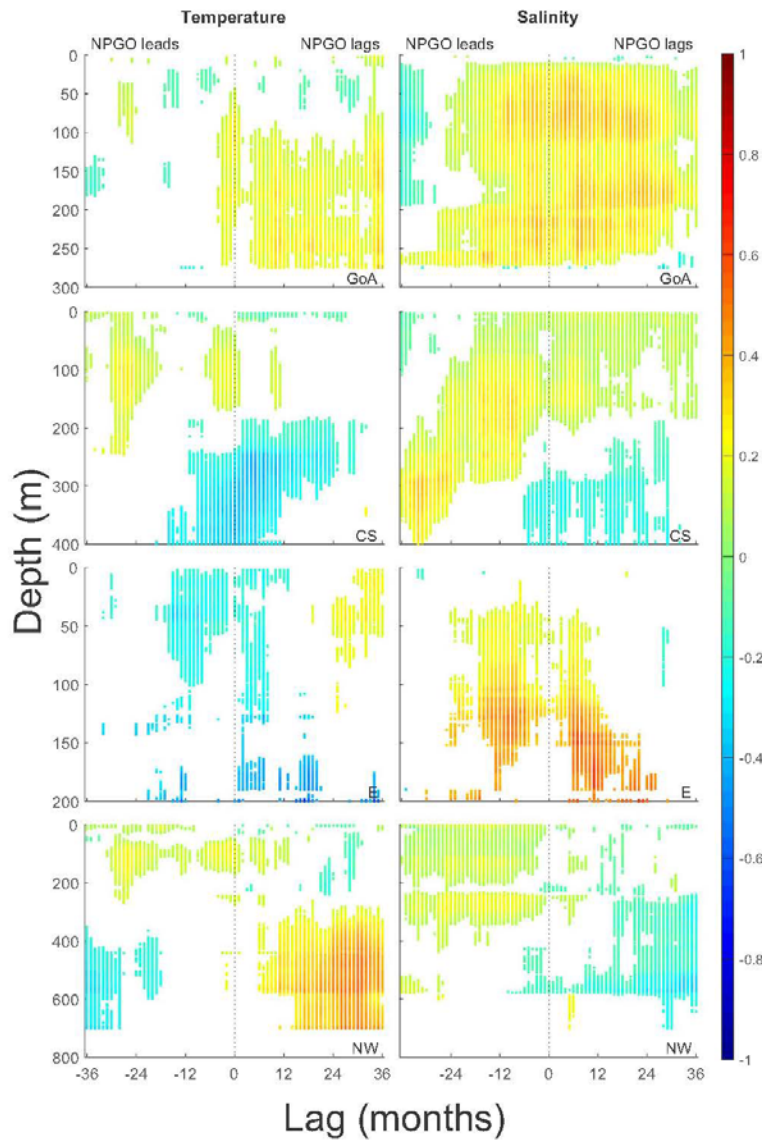


Fig. 13. Cross correlations between the North Pacific Gyre Oscillation (NPGO) and temperature (left panels) and salinity (right panels) in the four Prince William Sound geographic regions (Fig. 1). Note that the scaling of the ordinate differs among regions. Only significant correlations ( $p < 0.05$ , from 10,000 simulated probability distribution functions) are shown.

records from coastal Alaska (Royer, 1993) and British Columbia (Loder and Garrett, 1978; McKinnell and Crawford, 2007). The mechanisms by which the lunar declination cycle alter surface temperature are unclear, it has been hypothesized that changes in tidal mixing or ocean-atmosphere heat flux are responsible (Loder and Garrett, 1978; McKinnell and Crawford, 2007). The latter authors used SST data from British Columbia and noted a two-year lag correlation between the LNC signal and the Pacific North America teleconnection index, which is an indicator of low-frequency variability in atmospheric circulation in the North Pacific (Barnston and Livezey, 1987). This suggests that the effect is likely part of much larger circulation patterns in the hemisphere (the cross-correlation pattern between temperature and the PNA index in

the data used here was very similar to the PDO index, but correlation coefficients were lower). The lag observed here was of similar magnitude.

Cross correlations with profile data showed the LNC leading temperature and salinity by 4–5 years and that temperature and salinity patterns were broadly similar. Coupling with temperature near surface would tend to support the notion that atmospheric forcing is, in part, responsible for the oscillation, but correlation at depth and with salinity would also tend to implicate mixing processes. A weak but significant correlation between the LNC and PDO suggests a possible atmospheric link. However, the independence between NPGO and the LNC, but with significant cross correlations between salinity and the LNC, suggests

# Appendix A

Open Access manuscript available at <https://doi.org/10.1016/j.dsr2.2017.08.014>

R. W. Campbell

Deep-Sea Research Part II 147 (2018) 43–57

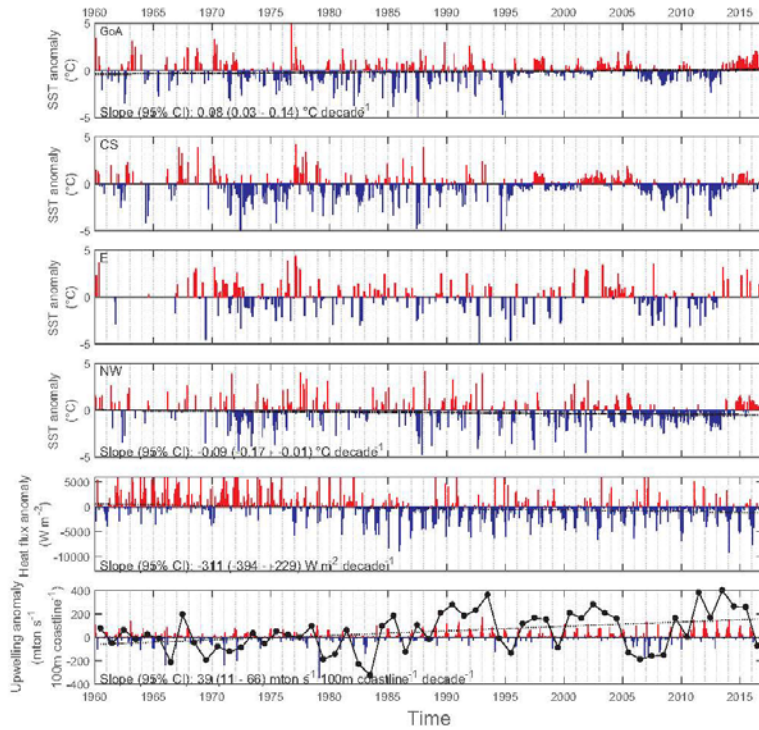


Fig. 14. Top four panels: Monthly average SST anomaly in the Prince William Sound regions (Fig. 1). Fifth panel: Heat flux anomaly (latent + sensible heat flux) at NCEP reanalysis point at 60°N 146°15'W (see text). The dashed line is the long-term trend fit by linear regression, slope and 95% CI are shown. Bottom panel: NOAA PFEL Upwelling anomaly (offshore component only) at 60°N 146°W. Bars are monthly anomalies and solid line and points are annual sums of anomalies (see text). The dashed line indicates the long-term trend of annual anomalies and the text indicates the slope and 95% CI.

two modes of salinity variability in the region, related to transport (NPGO) and mixing (LNC).

## 5. Conclusions

The overall picture that emerges from the data assembled here is a regional warming trend, with indications of enhanced freshwater inputs at the surface that in some regions are accompanied by a reduction in temperature attributable to inputs from melting ice. As well as generally higher average temperatures, there was a trend towards higher maximum temperatures during the summer maximum, but little in the

way of changes in timing. At depth, the trend was towards warmer and more saline water, which is consistent with increased entrainment of deep water caused by enhanced surface circulation and deep-water transport. Both trends can be expected to enhance stability in near-surface waters, which can be seen by the shoaling of the seasonal mixed layer by several meters during the 40-year span examined here. Annual productivity is controlled in part by the timing and depth of the onset of stratification in spring (e.g. Sverdrup, 1953), and reductions in the depth of the seasonal mixed layer may result in reductions in overall seasonal productivity that may cascade in unpredictable ways to higher trophic levels (e.g. Benson and Trites, 2002).

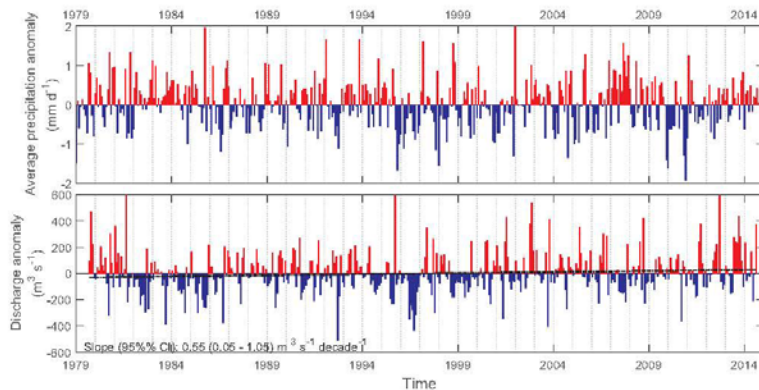


Fig. 15. Top panel: CMAP precipitation anomaly time series in the PWS region (1979–2015). Bottom panel: Discharge anomaly time series in the PWS region (i.e. along the periphery of PWS), from Beamer et al. (2016).

## Acknowledgements

The research described in this paper was supported by the Exxon Valdez Oil Spill Trustee Council (Project 12120114-E). However, the findings and conclusions presented by the author are his own and do not necessarily reflect the views or position of the Trustee Council.

## References

- Arendt, A., Luthcke, S., Gardner, A., O'Neil, S., Hill, D., Moholdt, G., et al., 2013. Analysis of a GRACE global masscon solution for Gulf of Alaska glaciers. *J. Glaciol.* **59**, 913–924. <http://dx.doi.org/10.3189/2013JG12J197>.
- Bartley, D.J., Yager, E.M., Graves, J., Kloczko, M., Calkin, P.E., 2013. Late Holocene glacial history of the Copper river Delta, coastal south-central Alaska, and controls on valley glacier fluctuations. *Quat. Sci. Rev.* **81**, 74–89.
- Barnett, T., Pierce, D.W., AchutaRao, K.M., Gleckler, P.J., Santer, B.D., Gregory, J.M., et al., 2005. Penetration of human-induced warming into the world's oceans. *Science* **309**, 284–287.
- Barnston, A.G., Livezey, R.E., 1987. Classification, seasonality and persistence of low-frequency atmospheric circulation patterns. *Mon. Weather Rev.* **115**, 1083–1126.
- Beamer, J.P., Hill, D.F., Arendt, A., Liston, G.E., 2016. High-resolution modeling of coastal freshwater discharge and glacier mass balance in the Gulf of Alaska watershed. *Water Resour. Res.* **52**, 3888–3909. <http://dx.doi.org/10.1002/2015WR018457>.
- Benson, A.J., Trites, A.W., 2002. Ecological effects of regime shifts in the Bering Sea and eastern North Pacific Ocean. *Fish. Fish.* **3**, 95–113.
- Bond, N.A., Cronin, M.F., Freeland, H., Mantua, N., 2015. Causes and impacts of the 2014 warm anomaly in the NE Pacific. *Geophys. Res. Lett.* **42**, 3414–3420. <http://dx.doi.org/10.1002/2015GL063306>.
- Branch, M.A., Coleman, T.F., Li, Y., 1999. A Subspace, interior, and conjugate gradient method for large-scale bound-constrained minimization problems. *SIAM J. Sci. Comput.* **21**, 1–23.
- Colgan, W., Pfeffer, W.T., Rajaram, H., Abdalati, W., Balog, J., 2012. Monte Carlo ice flow modeling projects a new stable configuration for Columbia Glacier, Alaska, c. 2020. *Cryosphere* **6**, 1395–1409. <http://dx.doi.org/10.5194/tc-6-1395-2012>. (2012).
- Currie, R.G., 1996. Variance contribution of luni-solar (Mn) and solar cycle (Sc) signals to climate data. *Int. J. Climatol.* **16**, 1343–1364.
- Doodson, A.T., 1921. The harmonic development of the tide-generating potential. *Proc. R. Soc. Lond. A* **100**, 305–329.
- Di Lorenzo, E., Schneider, N., Cobb, K.M., Chhak, K., Franks, P.J.S., Miller, A.J., et al., 2008. North Pacific Gyre Oscillation links ocean climate and ecosystem change. *Geophys. Res. Lett.* **35**, L08607. <http://dx.doi.org/10.1029/2007GL032838>.
- Fairall, C.W., Bradley, E.F., Rogers, D.P., Edson, J.B., Young, G.S., 1996. Bulk parameterization of air-sea fluxes for tropical ocean global atmosphere coupled-ocean atmosphere response experiment. *J. Geophys. Res.* **101**, 3747–3764.
- Feeley, R.A., 1979. Processes affecting the distribution and transport of suspended matter in the northeast Gulf of Alaska. *Deep Sea Res.* **26**, 445–464.
- Gay, S.M., Vaughan, S.L., 2001. Seasonal hydrography and tidal currents of bays and fjords in Prince William Sound, Alaska. *Fish. Oceanogr.* **10** (Suppl. 1), S159–S193.
- Gedalof, Z., Smith, D.J., 2001. Interdecadal climate variability and regime-scale shifts in Pacific North America. *Geophys. Res. Lett.* **24**, 1515–1518.
- Hare, S.R., Mantua, N., 2000. Empirical evidence for North Pacific regime shifts in 1977 and 1989. *Prog. Oceanogr.* **47**, 103–145.
- Halverson, M.J., Belanger, C., Gay, S.M., 2012. Seasonal variations in the transport through the straits connecting Prince William Sound to the Gulf of Alaska. *Cont. Shelf Res.* <http://dx.doi.org/10.1016/j.csr.2012.06.017>.
- Henson, S.A., 2007. Water column stability and spring bloom dynamics in the Gulf of Alaska. *J. Mar. Res.* **65**, 715–736.
- Hill, D.F., Bruhis, N., Calos, S.E., Arendt, A., Beamer, J., 2015. Spatial and temporal variability of freshwater discharge into the Gulf of Alaska. *J. Geophys. Res.* **120**, 634–646. <http://dx.doi.org/10.1002/2014JC010395>.
- Janout, M.A., Weingartner, T.J., Royer, T., Danielson, S.L., 2010. On the nature of winter cooling and the recent temperature shift on the northern Gulf of Alaska shelf. *J. Geophys. Res.* **115**, C05023. <http://dx.doi.org/10.1029/2009JC005774>.
- Kalnay, E., Kanamitsu, M., Kistler, R., Collins, W., Deaven, D., Gandin, F., et al., 1996. The NCEP/NCAR 40-year reanalysis project. *Bull. Am. Met. Soc.* **77**, 437–471.
- Ladd, C., Stabeno, P., Cokolet, E.D., 2005. A note on cross-shelf exchange in the northern Gulf of Alaska. *Deep Sea Res.* **52**, 667–669. <http://dx.doi.org/10.1016/j.dsr2.2004.12.022>.
- Levitus, S.J., Antonov, J.I., Wang, J., Delworth, T.L., Dixon, K.W., Broccoli, A.J., 2001. Anthropogenic warming of Earth's climate system. *Science* **292**, 267–270.
- Li, M., Myers, P.G., Freeland, H., 2005. An examination of historical mixed layer depths along Line P in the Gulf of Alaska. *Geophys. Res. Lett.* **32**, L05613. <http://dx.doi.org/10.1029/2004GL021911>.
- Loder, J.W., Garrett, C., 1978. The 18.6-year cycle of sea surface temperature in shallow seas due to tidal mixing. *J. Geophys. Res.* **83**, 1967–1970.
- Mantua, N.J., Hare, S.R., Zhang, Y., Wallace, J.M., Francis, R.C., 1997. A Pacific interdecadal climate oscillation with impacts on salmon production. *Bull. Am. Meteorol. Soc.* **78**, 1069–1079. [http://dx.doi.org/10.1175/1520-0477\(1997\)078<1069:APICOW.2.0.CO;2](http://dx.doi.org/10.1175/1520-0477(1997)078<1069:APICOW.2.0.CO;2).
- McKinnell, S.M., Crawford, W.R., 2007. The 18.6-year lunar nodal cycle and surface temperature variability in the northeast Pacific. *J. Geophys. Res.* **112**, C02002. <http://dx.doi.org/10.1029/2006JC003671>.
- Minobe, S., 1997. A 50–70 year climatic oscillation over the North Pacific and North America. *Geophys. Res. Lett.* **24**, 683–686.
- Musgrave, D.L., Halverson, M.J., Pegau, W.S., 2013. Seasonal surface circulation, temperature, and salinity in Prince William Sound, Alaska. *Cont. Shelf Res.* **53**, 20–29.
- National Centers for Environmental Information/NESDIS/NOAA/U.S. Department of Commerce, Research Data Archive/Computational and Information Systems Laboratory/National Center for Atmospheric Research/University Corporation for Atmospheric Research, Earth System Research Laboratory/NOAA/U.S. Department of Commerce, Cooperative Institute for Research in Environmental Sciences/University of Colorado, National Oceanography Centre/Natural Environment Research Council/United Kingdom, Met Office/Ministry of Defence/United Kingdom, Deutscher Wetterdienst (German Meteorological Service)/Germany, Department of Atmospheric Science/University of Washington, and Center for Ocean-Atmospheric Prediction Studies/Florida State University, 2016, updated monthly. International Comprehensive Ocean-Atmosphere Data Set (ICOADS) Release 3, Individual Observations. Research Data Archive at the National Center for Atmospheric Research, Computational and Information Systems Laboratory. <http://dx.doi.org/10.5065/D6Z52T33> (Accessed 20 September 2016).
- Neal, E.G., Hood, E., Smikrud, K., 2010. Contribution of glacier runoff to freshwater discharge into the Gulf of Alaska. *Geophys. Res. Lett.* **37**, L06404. <http://dx.doi.org/10.1029/2010GL042385>.
- Newman, M., Alexander, M.A., Ault, T.R., Cobb, K.M., Deser, C., Di Lorenzo, E., et al., 2016. The Pacific decadal oscillation, revisited. *J. Climate* **29**, 4399–4427.
- Niebauer, H.J., Royer, T.C., Weingartner, T.J., 1994. Circulation of Prince William Sound, Alaska. *J. Geophys. Res.* **99**, 14113–14126.
- NOAA El Niño/Southern Oscillation (ENSO) Diagnostic Discussion. Available: [http://www.cpc.ncep.noaa.gov/products/analysis\\_monitoring/ensio\\_disc\\_jan2016/ensiodisc.pdf](http://www.cpc.ncep.noaa.gov/products/analysis_monitoring/ensio_disc_jan2016/ensiodisc.pdf).
- Royer, T.C., 1982. Coastal fresh water discharge in the Northeast Pacific. *J. Geophys. Res.* **87**, 2017–2021.
- Royer, T.C., 1993. High latitude oceanic variability associated with the 18.6-year nodal tide. *J. Geophys. Res.* **98**, 4639–4644.
- Royer, T.C., 2005. Hydrographic responses at a coastal site in the northern Gulf of Alaska to seasonal and interannual forcing. *Deep. Res. II* **52**, 267–288.
- Royer, T.C., Grosch, C.E., 2006. Ocean warming and freshening in the northern Gulf of Alaska. *Geophys. Res. Lett.* **33**, L16605. <http://dx.doi.org/10.1029/2006GL026767>.
- Royer, T.C., Grosch, C.E., Mysak, L.A., 2001. Interdecadal variability of Northeast Pacific coastal freshwater and its implications on biological productivity. *Prog. Oceanogr.* **49**, 95–111.
- Sarker, N., Royer, T.C., Grosch, C.E., 2005. Hydrographic and mixed layer depth variability on the shelf in the northern Gulf of Alaska, 1974–1998. *Cont. Shelf Res.* **25**, 2147–2162.
- Stabeno, P.J., Bond, N.A., Hermann, A.J., Kachel, N.B., Mordy, C.W., Overland, J.E., 2004. Meteorology and oceanography of the Northern Gulf of Alaska. *Cont. Shelf Res.* **24**, 859–897.
- Shuiski, M., Wendler, G., 2008. *The Climate of Alaska*. University of Alaska Press, Fairbanks, pp. 216.
- Sverdrup, H.U., 1953. On conditions for the vernal blooming of phytoplankton. *J. Cons. Int. Explor. Mer.* **18**, 287–295.
- Thomson, R.E., Fine, L.V., 2003. Estimating mixed layer depth from oceanic profile data. *J. Atmos. Ocean. Tech.* **20**, 319–329.
- Vaughan, S.L., Mooers, C.N.K., Gay, S.M., 2001. Physical variability in Prince William Sound during the SEA Study (1994–98). *Fish. Oceanogr.* **10** (Suppl. 1), 58–80.
- Wang, J., Jin, M., Patrick, V., Allen, J.R., Eslinger, D.L., Mooers, C.N., et al., 2001. Numerical simulations of the seasonal circulation patterns and thermohaline structures of Prince William Sound, Alaska. *Fish. Oceanogr.* **10** (Suppl. 1), 132–148.
- Wang, J., Jin, M., Musgrave, D., Ikeda, M., 2004. A hydrological digital elevation model for freshwater discharge into the Gulf of Alaska. *J. Geophys. Res.* **109**, C07009. <http://dx.doi.org/10.1029/2002JC001430>.
- Weingartner, T., 2007. *Atmosphere and ocean*. In: Spies, R.B. (Ed.), *Long Term Ecological Change in the Gulf of Alaska*. Elsevier B.V. Amsterdam, pp. 266–273.
- Weingartner, T.J., Danielson, S.L., Royer, T.C., 2005. Freshwater variability and predictability in the Alaska Coastal Current. *Deep Sea Res.* **52**, 169–191.
- Wiles, G.C., Bartley, D.J., Calkin, P.E., 1999. Tree-ring dated 'Little Ice Age' histories of maritime glaciers from western Prince William Sound, Alaska. *Holocene* **9**, 163–173.
- Wilks, D.S., 2011. *Statistical Methods in the Atmospheric Sciences*. Elsevier, Oxford.
- Wu, L., Li, C., 2007. Warming of the North Pacific Ocean: local Air-Sea coupling and remote climatic impacts. *J. Clim.* **20**, 2581–2601. <http://dx.doi.org/10.1175/JCLI4117.1>.
- Xie, P., Arkin, P.A., 1997. Global precipitation: a 17-year monthly analysis based on gauge observations, satellite estimates, and numerical model outputs. *Bull. Am. Meteorol. Soc.* **78**, 2539–2558.
- Xiong, Q., Royer, T.C., 1984. Coastal temperature and salinity in the northern Gulf of Alaska. *J. Geophys. Res.* **89**, 8061–8066.



Contents lists available at ScienceDirect

## Deep-Sea Research Part II

journal homepage: [www.elsevier.com/locate/dsr2](http://www.elsevier.com/locate/dsr2)

## Seasonal variation of zooplankton abundance and community structure in Prince William Sound, Alaska, 2009–2016



Caitlin A.E. McKinstry\*, Robert W. Campbell

Prince William Sound Science Center, 300 Breakwater Avenue, Cordova, AK 99574, USA

## ARTICLE INFO

**Keywords:**  
Zooplankton  
Indicator species  
Community composition  
Marine ecology  
Copepods  
Prince William Sound  
Alaska  
Warm-water species

## ABSTRACT

Large calanoid copepods and other zooplankters comprise the prey field for ecologically and economically important predators such as juvenile pink salmon, herring, and seabirds in Prince William Sound (PWS). From 2009–2016, the Gulf Watch Alaska program collected zooplankton 5–10 times each year at 12 stations in PWS to establish annual patterns. Surveys collected 188 species of zooplankton with *Oithona similis*, *Limacina helicina*, *Pseudocalanus* spp., and *Acartia longiremis* as the most common species present in 519 samples. Generalized additive models assessed seasonal abundance and showed peak abundance in July (mean: 9826 no. m<sup>-3</sup> [95% CI: 7990–12,084]) and lowest abundance in January (503 no. m<sup>-3</sup> [373 to 678]). Significantly higher zooplankton abundance occurred in 2010 (542 no. m<sup>-3</sup> ± 55 SE) and lowest in 2013 (149 no. m<sup>-3</sup> ± 13). The species composition of communities, determined via hierarchical cluster analysis and indicator species analysis, produced six distinct communities based on season and location. The winter community, characterized by warm-water indicator species including *Mesocalanus tenuicornis*, *Calanus pacificus*, and *Corycaeus anglicus*, diverged into four communities throughout the spring and summer. The first spring community, characterized by copepods with affinities for lower salinities, occurred sound-wide. The second spring community, comprised of planktonic larvae, appeared sporadically in PWS bays in 2011–2013. Spring and summer open water stations were defined by the presence of large calanoid copepods. A summer community including the most abundant taxa was common in 2010 and 2011, absent in 2013, then sporadically appeared in 2014 and 2015 suggesting interannual variability of zooplankton assemblages. The zooplankton community shifted to a uniform assemblage characterized by cnidarians in the early autumn. Community assemblages showed significant correlations to a set of environmental variables including SST, mixed layer depth, location, depth of chlorophyll-*a* max, mixed layer average salinity, chlorophyll-*a* maximum, and bottom depth ( $\rho = 0.24$ ,  $p < 0.05$ ). The disappearance of the summer community coincided with the appearance of the Gulf of Alaska warm water anomaly known as “The Blob”. A shift in zooplankton community composition during critical grazing periods for predators such as juvenile Pacific herring (*Clupea pallasii*) could have energetic consequences for overwintering success.

## 1. Introduction

Located at the northernmost part of the Gulf of Alaska (GOA), Prince William Sound (PWS) is a large estuary defined by numerous marginal fjords, containing approximately 3300 km of shoreline (Grant and Higgins, 1910). This small inland sea, approximately the size of Massachusetts (17,700 km<sup>2</sup>), has experienced drastic oceanic and atmosphere changes over the past 30 yrs including several ENSO cycles, the recent marine heat wave known as “The Blob” (Hermann et al., 2016; Bond et al., 2015), and the Exxon Valdez oil spill, which still has measurable impacts (Boufadel et al., 2016). However, little is known about the structure of the PWS zooplankton community and overall zooplankton abundance during such environmental changes.

In the northern GOA and PWS, large lipid-rich copepods, mainly *Calanus marshallae*, *Neocalanus plumchrus*, *Neocalanus flemingeri*, *Eucalanus bungii*, and *Neocalanus cristatus*, constitute the majority of zooplankton biomass during the critical grazing period of the spring phytoplankton bloom and are thus the most thoroughly described species in this region in regards to life histories and abundance (Cooney, 1986; Cooney et al., 2001b; Coyle and Pinchuk, 2003, 2005; Coyle et al., 2013; Sousa et al., 2017). These species and other zooplankters comprise the prey field for ecologically and economically important predators such as juvenile pink salmon (Willette, 2001), herring (Foy and Norcross, 1999), juvenile walleye pollock, gelatinous carnivores (Purcell and Sturdevant, 2001), and other fishes, seabirds, and marine mammals.

\* Corresponding author.

E-mail address: [cmckinstry@pwssc.org](mailto:cmckinstry@pwssc.org) (C.A.E. McKinstry).<http://dx.doi.org/10.1016/j.dsr2.2017.08.016>

Available online 21 September 2017

0967-0645/ © 2017 The Authors. Published by Elsevier Ltd. This is an open access article under the CC BY-NC-ND license (<http://creativecommons.org/licenses/by-nc-nd/4.0/>).

## Appendix B

Open Access manuscript available at <https://doi.org/10.1016/j.dsr2.2017.08.016>

C.A.E. McKinstry, R.W. Campbell

Deep-Sea Research Part II 147 (2018) 69–78

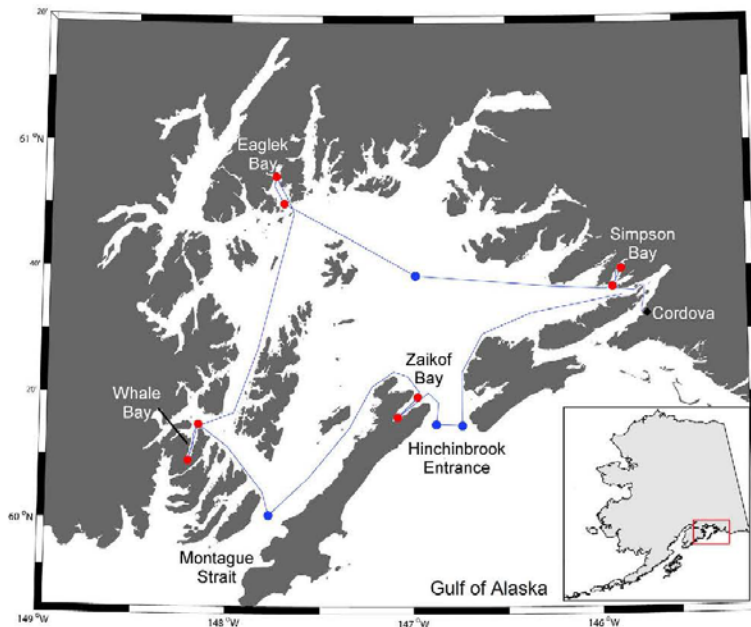


Fig. 1. Gulf Watch Alaska sampling stations within Prince William Sound, AK encompassing four bays (red dots), the two main entrances of PWS, and a central sound location. Blue dots signify stations considered here as “open water”. The blue line indicates the travel path during each monthly cruise. (For interpretation of the references to color in this figure legend, the reader is referred to the web version of this article.)

In the years following the oil spill, the Sound Ecosystem Assessment (SEA) program (1994–1997) examined the causes of PWS herring and pink salmon declines including the role zooplankton stocks played in the ecology of these planktivores. Cooney et al., 2001b described the cyclical abundance and biomass of the major zooplankton taxa found in PWS during SEA. A total of 88 zooplankton species were reported, but no multivariate analysis of the overall community structure of zooplankton assemblages or correlations to environmental variables was included.

On the northern GOA continental shelf (the Seward, or GAK line) the Northeast Pacific GLOBEC Program (1997–2004) investigated the effects of climate change and atmospheric anomalies on coastal phytoplankton and zooplankton productivity and included some western PWS stations. These results showed clear differences in species abundance based on atmospheric forcing between the open waters of the continental shelf and the protected inner waters of PWS (Coyle et al., 2013; Coyle and Pinchuk, 2005; Doubleday and Hopcroft, 2015). For example, *Neocalanus plumchus* and *Neocalanus flemingeri* peak in abundance earlier in the spring in PWS than on the shelf (Coyle and Pinchuk, 2005). Also, pteropod abundance (*Limacina helicina*) on the continental shelf exhibited strong relationships with large scale climate patterns including the Pacific Decadal Oscillation (PDO) and the North Pacific Gyre Oscillation (NPGO), although these relationships did not occur with *Limacina helicina* from PWS (Doubleday and Hopcroft, 2015).

Indicator species can reflect environmental conditions and community shifts resulting from those environmental conditions that may otherwise go unnoticed if the focus resides on only the most abundant taxa. First, a thorough description of community taxa is required for such an analysis (Dufrene and Legendre, 1997; Keister et al., 2009; Keister and Peterson, 2003; Morgan et al., 2003; Peterson and Keister, 2003). Zooplankton are often indicators of particular water masses based on correlations with water mass physical properties such as temperature, salinity, and stability of the mixed layer. Off the coast of Oregon, on-shelf zooplankton community structure characterized by

three northern cold-water associated copepods supported the hypothesis that the source of the water mass was from the GOA (Morgan et al., 2003). Examination of southern warm-water associated species as indicators also described how ENSO shifts the zooplankton community to a more subtropical structure (Keister and Peterson, 2003; Peterson and Keister, 2003). Zooplankton community structure (along with abiotic variables) gave further evidence of changes in mesoscale circulation patterns in this region (Keister et al., 2009). In PWS, community structure and an examination of indicator species has not been thoroughly investigated.

The environmental drivers component of the Gulf Watch Alaska (GWA) program has collected zooplankton and oceanographic data in PWS approximately monthly during the annual production cycle since late 2009. In this study, our primary objective was to explore the characteristics of PWS zooplankton assemblages based on seasonal abundance, species composition, and the underlying environmental variables driving these communities. To do this, we used ANOVA to evaluate among-year zooplankton abundance differences, and multivariate techniques to describe patterns in the zooplankton community including indicator species analysis (ISA), non-metric multidimensional scaling (NMDS), and the BIO-ENV “Best” procedure to assess correlations between environmental variables and zooplankton community structure. A clear knowledge of how abundance and composition of zooplankton communities vary seasonally and interannually is an essential prerequisite to assess how they may be impacted by anthropogenic factors such as future oil spills or climate change.

## 2. Methods

### 2.1. Field collection

A total of 12 stations were selected for the GWA monitoring program based on prior sites occupied during the SEA program (Fig. 1). These sites included four bays around the periphery of PWS, the primary entrances, and a central sound station (PWS). For the purposes of

this study, the three entrance stations at Montague Strait and Hinchinbrook Entrance, and the central sound station will be referred to as “open water” stations in contrast to the more protected, inshore bay stations. Within each of the four bays (Simpson, Zaikof, Whale, and Eaglek), stations were occupied at the mouth and head of the bay. At each station a suite of oceanographic and biological measurements were collected including plankton nets and a CTD cast. All data were collected during daylight hours. Descriptions of the methods used for measurements of temperature and salinity, and the estimation of mixed layer depths are described in Campbell (this issue). *In situ* chlorophyll-*a* concentration was estimated from a WET Labs FLNTU fluorometer mounted on a Seabird Electronics SBE19 or SBE25 plus CTD. The fluorometer was factory calibrated annually, and compared against extracted chlorophyll-*a* measured from bottle samples.

Zooplankton were collected with a 0.6 m bongo net (202  $\mu\text{m}$  mesh) equipped with a calibrated one-way flowmeter (Hydro-Bios Altenholz, Germany) to estimate the sampled volume. The bongo net was lowered to 50 m or just above the bottom (depending on depth) then hauled vertically ( $-0.75 \text{ m s}^{-1}$ ) to the surface. All samples were preserved in a buffered 3–5% formalin-seawater solution. The side lacking the flowmeter was enumerated to reduce potential net avoidance by larger zooplankters. Samples were subsampled using a Folsom splitter (McEwen et al., 1954) until approximately 200 individuals of the dominant taxa were reached. This subsample was then enumerated for species composition to the finest taxonomic scale possible under a stereomicroscope (Leica ML25, Wetzlar, Germany). Individual plankters were identified to species where practical and to coarser taxonomic levels when difficult, poorly described, or time intensive. For all analyses, *Neocalanus plumchrus* and *N. flemingii* were combined because earlier life stages could not be resolved to species (Sousa et al., 2017). Less abundant, larger taxa (e.g. euphausiids, *N. cristatus*, ichthyoplankton) present in higher subsamples were also identified and counted. Species names and hierarchical classifications were reviewed for accuracy using the Integrated Taxonomic Information System (1996).

## 2.2. Statistical analyses

Sea surface temperature (SST) and salinity (SSS) were taken from the top (0 or 1 m) bin from the CTD casts. SST and SSS anomalies were calculated by subtracting observations from the climatology at each site as estimated with a second order cosine curve (methods are described in Campbell, this issue). Mixed layer depth (MLD) was estimated as the depth where the potential density exceeded a threshold relative to the surface (described in Campbell, this issue); here a density threshold of  $0.125 \text{ kg m}^{-3}$  was used, which is the threshold usually used to denote the annual pycnocline (Thomson and Fine, 2003). Integrated chlorophyll-*a* concentrations measured by the fluorometer were calculated from 50 m or bottom to the surface using the Trapezoidal Rule.

Patterns in community assemblages of zooplankton were analyzed using the statistical package R (R Development Core Team, 2005). The high amount of variation in our abundance data and the relatively short time period of our data collection prohibited us from producing a robust time series analysis for this initial study. Therefore, abundance data were assessed, independent of year, using generalized additive models (GAM) with day-of-year as the explanatory variable (Hastie and Tibshirani, 1986) via the R package mgcv (Wood, 2004). This technique allows for flexibility in cases of nonlinear relationships. Strong temporal correlations were expected, and the use of GAMs in these analyses were for illustrative purposes only to demonstrate the average seasonal trends in zooplankton abundance. GAMs were run using a Gaussian distribution and identity link function. The four most frequently encountered zooplankton taxa along with *Calanus marshallae*, *Neocalanus* spp., and *Eucalanus bungii* were aggregated for individual GAMs. To evaluate trends among groups of similar species, large calanoid copepod abundance (comprised of *C. marshallae*, *Neocalanus* spp., and *E.*

*bungii*) and small copepod abundance (small copepods included in the ISA; see below) were aggregated. Abundance data were  $\log_{10}$  transformed to stabilize variance prior to GAM analysis except in the cases of *Eucalanus bungii*, *Calanus marshallae*, and large calanoid copepods. These data required further transformation by  $\log_{10}(n + 0.1) + 1$  (Keister et al., 2009, 2011) to stabilize variance.

To determine if yearly abundances were similar, a one-way Analysis of Variance (ANOVA) was carried out on annual mean abundances with a significance level of  $\alpha = 0.05$ . A Tukey's post hoc test further examined inter-annual differences ( $\alpha = 0.05$ ). Only years with full coverage were included (2010–2015).

Taxa present in < 5% of samples were omitted from multivariate analyses (Peterson and Keister, 2003; Keister et al., 2003; Morgan et al., 2003; Keister et al., 2011). Abundance data were transformed [ $\log(n + 0.1) + 1$ ] to stabilize variance of dominant species (Keister et al., 2011). Using Ward's agglomerative method with Euclidean distances, a hierarchical cluster analysis (HCA) produced distinct sample-group clusters based on species assemblage per sample (Manley, 1994).

An Indicator Species Analysis (ISA; Dufrene and Legendre, 1997) examined which species were indicative of each sample-group's zooplankton community (R package “indispecies”: De Caceres and Legendre, 2009). ISA determines how consistently present taxa are in their sample-group based on overall taxa abundance and frequency of occurrence. ISA produces an Indicator Species Value (ISV) that ranges from 0 (absent) to 1 (present in all samples of a particular group). Species that are considered the “best” indicators of a group are those with scores closest to 1 meaning they are found within their group only and do not occur anywhere else. Thus, abundance is not necessarily the most highly weighted factor in this analysis. Indicator species with ISVs of less than 0.25 were omitted; the association at this level is considered too weak (Dufrene and Legendre, 1997). Unequal size groupings within sample-groups were accounted for following De Caceres (2013). Permutation tests ( $n = 999$ ) were carried out to determine the significance of species as indicator ( $\alpha = 0.05$ ).

Non-Metric Multidimensional Scaling (NMDS) with a Bray-Curtis dissimilarity matrix was used to determine zooplankton community similarities based on abundance (R package “vegan”: Oksanen et al., 2016). These tests were run with two and three dimensional scaling to examine strength of correlations and goodness of fit (stress). To assess the environmental variables influencing the community compositions, continuous environmental variables were tested against the Bray-Curtis matrix using a modified version of the BIO-ENV BEST model (Clarke and Ainsworth, 1993; Oksanen et al., 2016). This analysis uses a set of environmental variables to determine which combination “best” explains the maximum amount of variation seen in the zooplankton community structure produced by NMDS. These variables included SST, SSS, MLD, average temperature and salinity of MLD, extracted integrated chlorophyll-*a* concentration, maximum extracted chlorophyll-*a* concentration, integrated chlorophyll-*a* concentration, maximum chlorophyll-*a* concentration, depth of chlorophyll-*a* maximum, latitude, longitude, and bottom depth. A Mantel test based on Spearman's rank correlation coefficient ( $\rho$ ) was used to verify the significance of the BIO-ENV BEST correlations (Legendre and Legendre, 2012). For the sake of brevity, only those environmental variables with significant correlations are included in the subsequent text.

## 3. Results

### 3.1. Oceanography

PWS stations were sampled 5–10 times per calendar year starting in November 2009 through May 2016. SST and mixed layer average salinity (MLDS) varied seasonally with a temperature maximum (and salinity minima) in July/August. A full discussion of seasonal cycles in temperature and salinity is given in Campbell (this issue). Both SST and MLDS varied considerably from seasonal averages; temperatures were

## Appendix B

Open Access manuscript available at <https://doi.org/10.1016/j.dsr2.2017.08.016>

C.A.E. McKinstry, R.W. Campbell

Deep-Sea Research Part II 147 (2018) 69–78

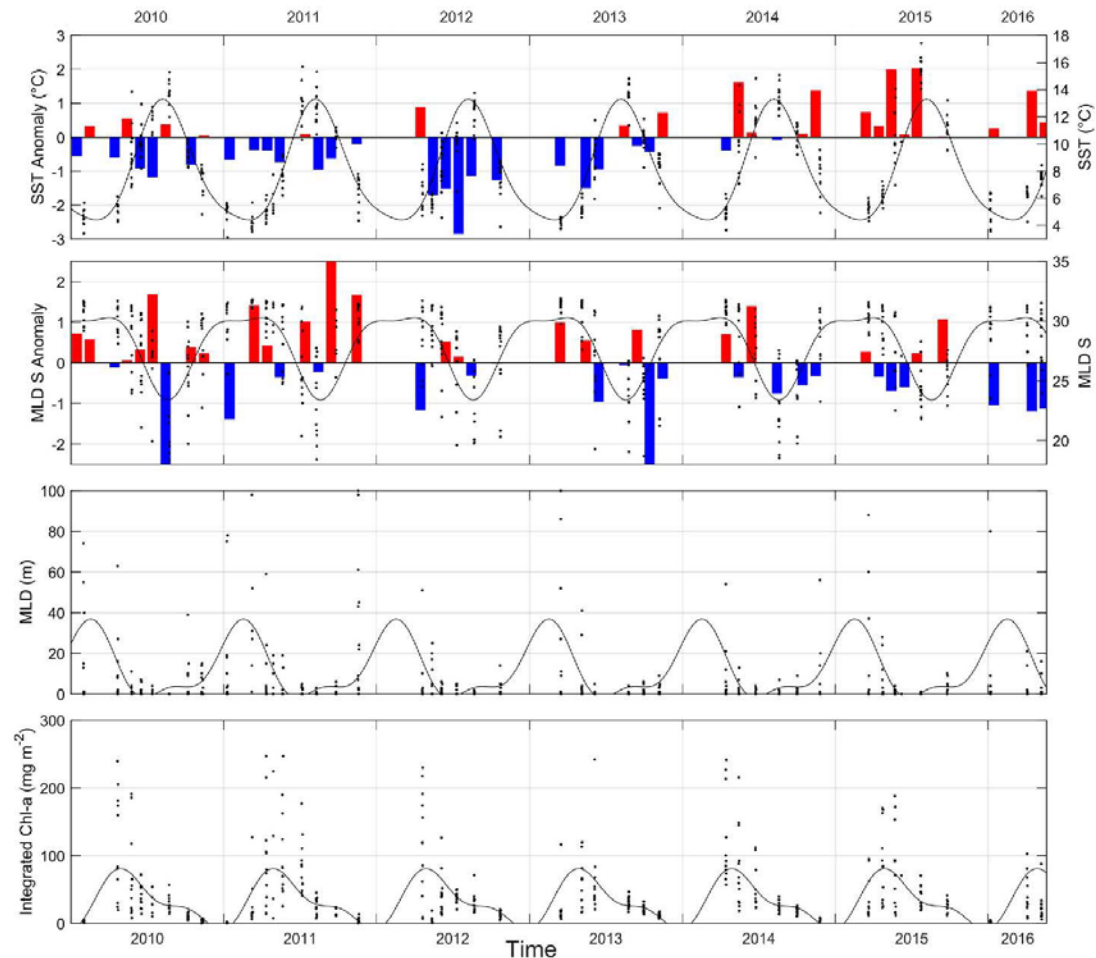


Fig. 2. Oceanographic variables measured in Prince William Sound during this study, including sea surface temperature (SST, top panel), sea surface salinity (SSS, second panel), mixed layer depth (MLD, third panel), and integrated chlorophyll-*a* concentration (fourth panel). Black dots indicate observations, and bars indicate anomalies. The black line indicates the annual cycle, as fit by a second order cosine curve. Note the change in y-axes between plots.

generally below average prior to late 2013, and above average after (Fig. 2, top panel). MLDS also varied considerably from averages presented in Fig. 2. Late summer/autumn MLDS were above or near average prior to 2013, and below average after.

MLD displayed wide variation during autumn and winter months (0–289 m; Fig. 2). In the spring, MLD range began to decrease and remained relatively shallow and stable (0–25 m) into the summer. Integrated chlorophyll-*a* showed consistent seasonality with peak concentrations declining from the spring bloom into the winter months (Fig. 2). We did not observe increases in chlorophyll-*a* during autumn months that would signify a bloom of phytoplankton production.

### 3.2. Zooplankton abundance

A total of 519 zooplankton samples were analyzed. Of the 188 unique taxonomic groups and categories of zooplankton (Supplemental Table 1), *Oithona similis*, *Limacina helicina*, *Pseudocalanus* spp. and *Acartia longiremis* were the most consistently observed species (> 95%).

Overall, copepods were the most frequently observed taxa followed by copepod/euphausiid nauplii, meroplanktonic larvae, and larvaceans.

GAMs of log-transformed abundance were applied to the four most abundant zooplankton taxa (*Oithona similis*, *Pseudocalanus* spp., *Limacina helicina*, and *Acartia longiremis*), *Neocalanus* spp. (*N. flemingii* and *N. plumchris* combined), *Calanus marshallae*, *Eucalanus bungii*, large calanoid copepod abundance, small copepod abundance, and total zooplankton abundance of all taxa encountered (Fig. 3). In all instances, day-of-year significantly correlated to zooplankton abundance ( $p < 0.05$ ). The degree to which time was a predictive variable ranged from 18.8% (*Calanus marshallae*) to 59.4% (Small Copepods; Fig. 3). Overall zooplankton abundance displayed consistent seasonal variation over the course of this study (Fig. 3). Abundance remained low during the winter (January: 503 no.  $m^{-3}$  [95% CI: 373–678]) then increased in the spring (May: 6312 no.  $m^{-3}$  [5408 to 7367]) and peaked in the summer (July: 9826 no.  $m^{-3}$  [7990 to 12,084]). This peak was followed by a steady decline throughout the late summer and into the autumn (November: 933 no.  $m^{-3}$  [664 to 1310]). Small copepod

# Appendix B

Open Access manuscript available at <https://doi.org/10.1016/j.dsr2.2017.08.016>

C.A.E. McKinstry, R.W. Campbell

Deep-Sea Research Part II 147 (2018) 69–78

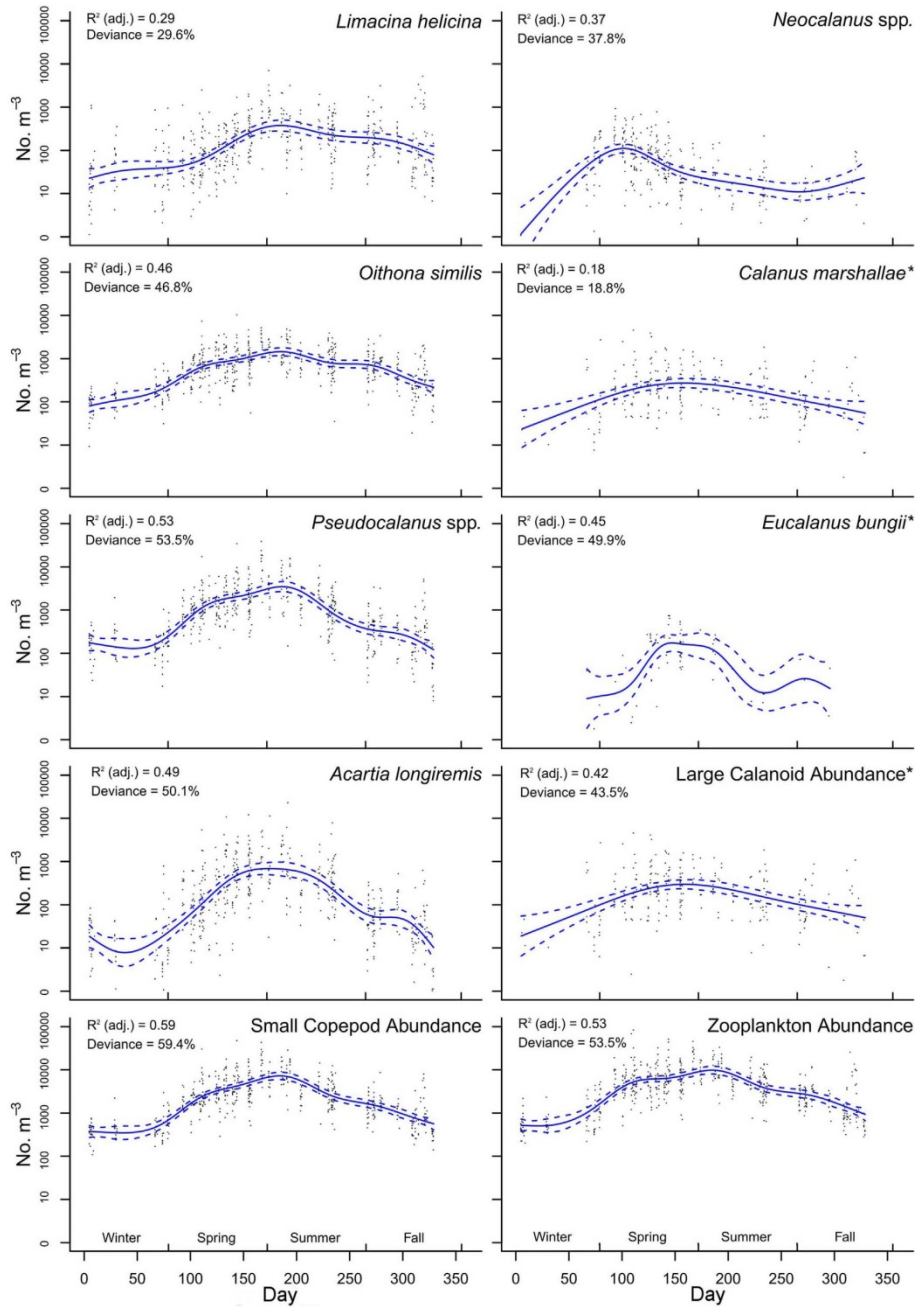


Fig. 3. Seasonal abundance of zooplankton in Prince William Sound with GAM best-fit models (blue line) and 95% confidence intervals (blue dashed line) for selected taxa and categories. GAM adjusted  $R^2$  values and deviance explained (%) are included ( $p < 0.05$ ). Black dots indicate observations. Titles with (\*) indicate  $\log_{10}(n + 0.1) + 1$  data. *Neocalanus* spp. includes both *N. plumchurs* and *N. flemingeri*. Large calanoid abundance combines *Neocalanus* spp., *Calanus marshallae*, and *Eucalanus bungii* data. Small copepod abundance combines small copepods included in the ISA. These species are identified with a (+) in Supplemental Table 1. (For interpretation of the references to color in this figure legend, the reader is referred to the web version of this article.)

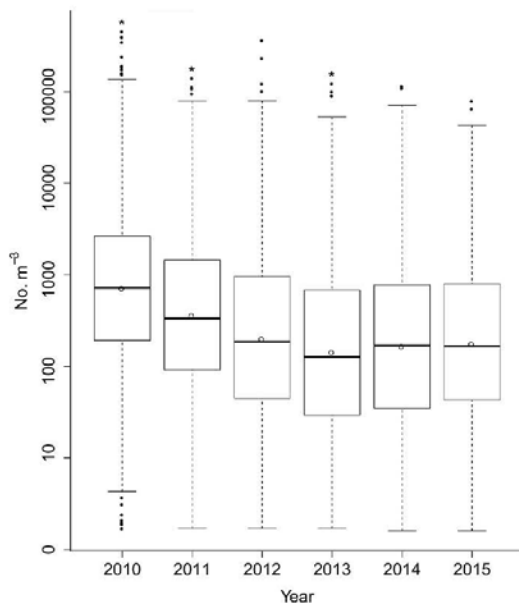


Fig. 4. Box-and-whisker plot of  $[\log_{10}(n + 0.1) + 1]$  yearly zooplankton abundance with outliers (dots) and means (circles). Boxes show 25th and 75th percentiles. Bars represent 90th and 10th percentiles. The (\*) indicates significance differences in log-transformed yearly abundance based on ANOVA and Tukey's test.

abundance comprised the majority of overall zooplankton abundance and mirrored this seasonal trend. Some species varied from the overall seasonal abundance pattern and were more common in spring. Large calanoid copepod assemblages including *Neocalanus* spp., *Calanus marshallae*, and *Eucalanus bungii* were largely absent from PWS during the winter then appeared suddenly and peaked early in the spring (Fig. 3). The abundance of *Oithona similis*, *Limacina helicina*, *Pseudocalanus* spp., *Acartia longiremis* and other small copepods (Fig. 3) peaked in the late spring/early summer, with lower abundances observed during autumn and winter.

ANOVA results showed that log-transformed yearly means were not equal during 2010–2015 ( $p < 0.05$ , Fig. 4). Tukey's post hoc test revealed that mean zooplankton abundance  $\pm$  SE was highest in 2010 followed by 2011 (Fig. 4) compared to all other years ( $p < 0.05$ ). 2013 had significantly fewer zooplankton than all other years of this study except 2014 ( $p < 0.05$ ).

### 3.3. Community composition

For the below multivariate analyses, the 70 taxa occurring in  $> 5\%$  of samples were used. *Neocalanus cristatus*, a fairly common GoA shelf/slope calanoid (Cooney, 1986) was not as common in the upper 50 m of the water column in PWS (present in 4.81% of samples) so was excluded from multivariate analyses.

HCA produced six monotonic clusters (Fig. 5A) with a cophenetic correlation coefficient of 0.39 ( $p < 0.05$ ) based on a dissimilarity matrix of 519 samples by 70 taxa. Sample-group clustering produced considerable overlap but did generally cohere to seasonal and spatial patterns (Fig. 5B). The winter group disappeared in the early spring and was replaced with three distinct communities. Some of these communities persisted through the summer, but others quickly shifted to different communities as the season progressed. By early autumn, PWS communities began shifting to the winter community structure with a

transitional community made up of carnivorous gelatinous taxa. Based on these seasonal patterns and the ISA relationships, zooplankton communities will simply be referred to in the subsequent text as follows: winter, spring, larval spring, open water, summer, and autumn groups (Fig. 5C).

The winter group, the most frequent group overall (23% of observations), appeared every year mainly from November through January; during Alaska's shortest photoperiod. The larval spring group was the smallest group overall (12%). The presence of this group increased from 2011 (3%) to 2015 (27%) and first appeared in April 2011 in Zaikof and Whale Bays. From 2012 onward, the larval spring group was common in PWS bays and in 2014 appeared at open water stations. This rise of the larval spring group coincided with a decline in the summer group (2010: 29% to 2015: 3%). The summer group comprised the majority of the groups in 2011 and 2012 from May to August but was absent in 2013. The summer group appeared sporadically in June 2014 and only twice in 2015. The open water group (16% overall) was most frequently observed at Hinchinbrook Entrance, Montague Strait, and central PWS (61%) compared to bay mouths (35%) or heads (4%). The spring group (17%) primarily occurred during the first field survey each year (March/April) and was consistent throughout the stations with the exception of the heads of Simpson and Whale bays. The autumn group (18%) occurred between late August and October preceding the appearance of the winter group.

No individual species were perfect indicators of their respective HCA group (i.e. ISV = 1). The ISA identified 60 out of 70 taxa with ISVs  $> 0.25$  as significant indicators ( $p < 0.05$ ) of sample-groups (Fig. 5C). The winter community was characterized by four species of copepods, two cnidarians, and ostracods. Four indicator species described the spring, which included three copepods and fish eggs. The larval spring group was defined by the most indicator species (20 taxa) and was dominated by larval stages of holo- and meroplankton. Two species of large calanoid copepods along with several other larger mesozooplankton represented the open water group. The summer group indicator species included all four of the most abundant taxa (Fig. 3) along with both cladoceran species resident in PWS. Only one species of meroplankton appeared in the summer group (bivalve veliger). The autumn group contained the majority of ctenophores and cnidarians included in the ISA.

Two dimensional (stress = 0.23, nonmetric fit  $R^2 = 0.95$ ) and three dimensional (0.16, 0.97) NMDS ordination further supported seasonal clustering based on changes in community structure (Fig. 6). This clustering was most pronounced and distinct for the autumn and winter groups. Spring, larval spring, open water, and summer groups showed the most overlap and further supported the conclusion that seasonality produces the most community variation. The BIO-ENV BEST analysis and Mantel tests found a significant correlation ( $\rho = 0.24$ ,  $p < 0.05$ ) based on the combination of seven variables. SST ( $\rho = 0.13$ ) contributed the most to the correlation followed by MLD ( $\rho = 0.06$ ), longitude ( $\rho = 0.03$ ), depth of chlorophyll-*a* max ( $\rho = 0.01$ ), MLDS ( $\rho = 0.01$ ), chlorophyll-*a* maximum ( $\rho = 0.003$ ), and bottom depth ( $\rho = 0.0001$ ). The seasonal changes of these environmental variables dictate much of the overlap appearing in the spring, larval spring, open water, and summer groups (Fig. 6). Winter environmental conditions of low SST, low chlorophyll-*a* max, high average salinity in the mixed layer, and deep mixed layer depth correspond to the winter group of the NMDS plot. As the seasons progress and environmental variables display increasing variation, the different complex site-groups began to diverge in tandem.

### 4. Discussion

There was considerable seasonal and temporal variation in zooplankton abundance and community structure in the protected inner shelf waters of PWS. Indicator species showed seasonal, temporal, and spatial shifts in community composition and then abundance of

# Appendix B

Open Access manuscript available at <https://doi.org/10.1016/j.dsr2.2017.08.016>

C.A.E. McKinstry, R.W. Campbell

Deep-Sea Research Part II 147 (2018) 69–78

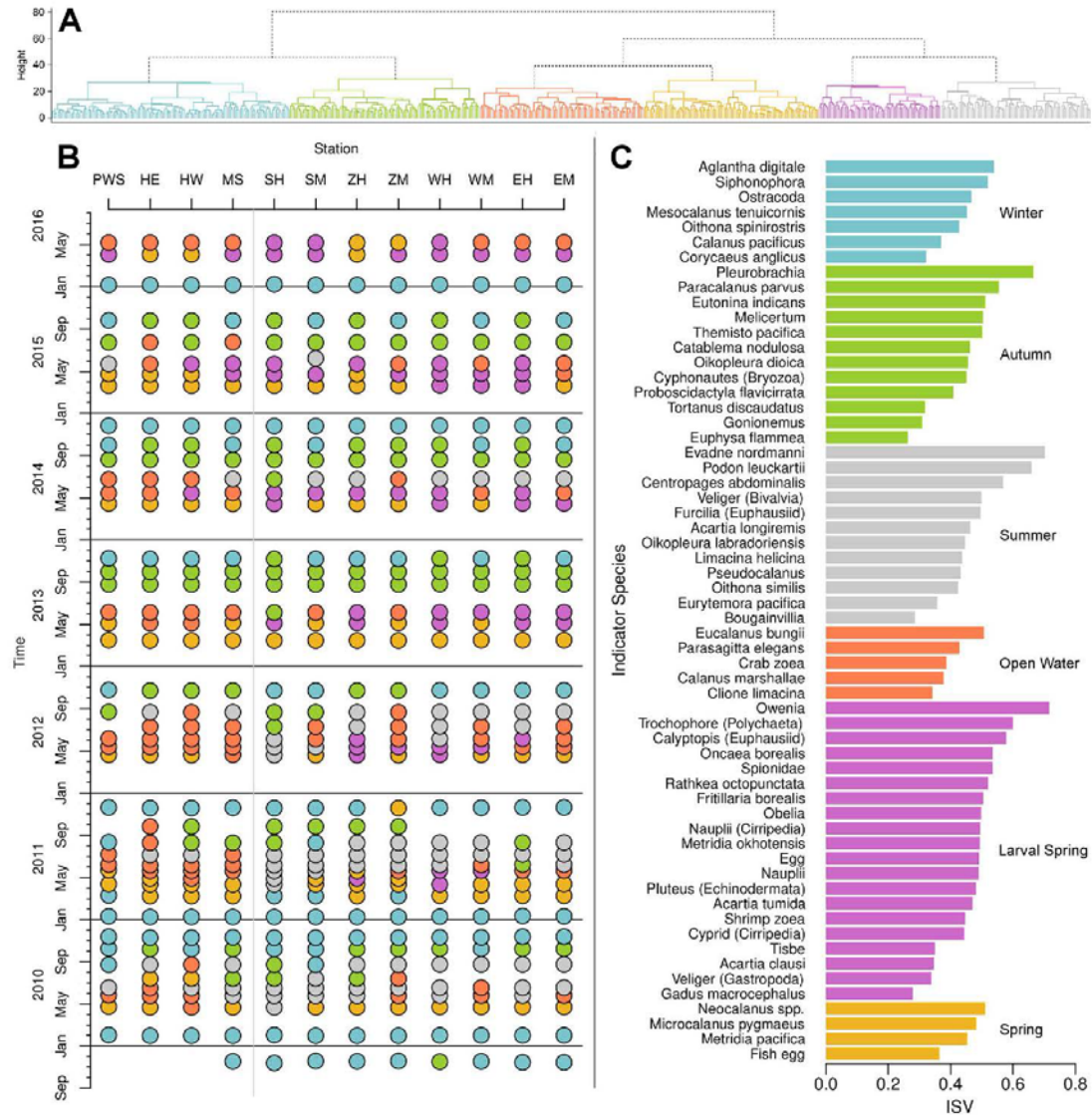


Fig. 5. A) Dendrogram of sample-groups produced by the hierarchical cluster analysis using Ward's agglomerative method. Clusters were cut at a height of 38. The y-axis indicates agglomeration node heights in Euclidian distance. B) Dot matrix plot showing HCA cluster (sample-group) assignment by date and station. The colors correspond to the sample-group cluster. These colors are standard for all other figures in the present study to facilitate comparison. C) Graph of the 60 significant ( $p < 0.05$ ) Indicator species determined as indicative of the six sample-group clusters and respective values (ISV). Sample-groups are indicated by (#) under the group name. Colors coincide with Fig. 6.

individual zooplankton taxa. Communities remained relatively uniform throughout PWS in the winter, diverged into four distinct assemblages during the spring and summer, then merged back to a uniform community observed sound-wide in autumn. The 2014 and 2015 spring/summer season showed an absence of the “summer” community defined by the most abundant copepod taxa (Fig. 5). These shifts were driven by environmental conditions based on SST, characteristics of the mixed layer, primary production, and geography of PWS. This suggests that the seasonality and structure of the zooplankton community reacts to anomalous fluctuations in oceanographic conditions, particularly

SST, such as those observed in PWS and the GOA in recent years.

### 4.1. Seasonal patterns

During the winter months, zooplankton abundance stayed relatively low and was comprised of several copepod species that remained active in the upper 0–50 m of the water column (Fig. 5). Chlorophyll- $\alpha$  and SST also remained low (Fig. 2) but began to increase as the season progressed and the photoperiod lengthened. The PWS community was defined by the consistent and uniform presence of small copepods

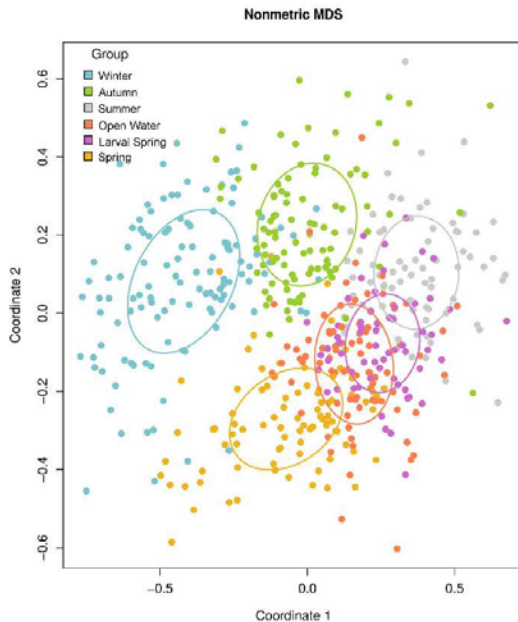


Fig. 6. NMDS plot of zooplankton species composition in Prince William Sound based on the Bray-Curtis dissimilarity ordination (3D stress = 0.16). Ellipses around the clusters indicate the standard deviation of point scores based on sample-group clusters. Colors of the ellipses correspond to sample-groups in Fig. 5.

including *Oithona spinirostris* and the warm-water associated species *Mesocalanus tenuicornis*, *Corycaeus anglicus*, and *Calanus pacificus*, which are prominent in southern regions off the coast of Oregon and Washington (Keister and Peterson, 2003; Peterson and Keister, 2003).

The vernal phytoplankton bloom in PWS usually corresponds to increased stability from both radiation and freshwater inputs, begins in April–May, and peaks within approximately two weeks (Eslinger et al., 2001; Henson, 2007); a similar pattern was observed in this study (Fig. 2). Following the spring bloom, the PWS zooplankton community increased in species richness and abundance. From the uniform winter assemblage, three distinct spring community assemblages began to diverge based on location. The first and most uniform spring community was characterized by the presence of *Microcalanus pygmaeus*, a euryhaline species (Abramova and Tuschling, 2005), *Neocalanus* spp. and *Metridia pacifica*. The latter two copepods have a negative association with high salinity habitats (Coyle and Pinchuk, 2005; Sousa et al., 2017), which would explain their ISA assignment to this group during the lowest salinities of the year. The second larval spring community emerged sporadically in 2011 and 2012 then became the common spring group sound-wide in 2013 onward. The indicator species of this group were mainly meroplanktonic larvae. Of the 17 meroplanktonic species included in the ISA, 13 described this larval spring group. Larval stages of polychaetes had the highest fidelity to this group.

The third spring open water community of large calanoid copepods (*Calanus marshallae*, and *Eucalanus bungii*) first occupied open water stations in the late spring before spreading to the protected inner bays through late summer. *C. marshallae* and *E. bungii* reached peak abundance shortly after *Neocalanus* spp. in the late spring as seen in prior years in both PWS (Cooney et al., 2001b) and the shelf (Cooney, 1986; Coyle et al., 2013; Coyle and Pinchuk, 2003, 2005). *E. bungii* has an affinity for higher salinity habitats (> 31.5; Coyle and Pinchuk, 2005; Sousa et al., 2017) such as those found at the open water stations. These

stations are located away from bays and areas of terrestrial freshwater run-off. In the GOA, *E. bungii* is often found between the surface thermocline and the permanent halocline (~40–150 m) where it is thought to feed on sinking particles (Coyle and Pinchuk, 2003; Mackas et al., 1993). The appearance of *E. bungii* in summer may indicate transport into PWS at depth by the deep-water renewal events that occur in summer (Campbell, this issue; Halverson et al., 2012).

After the spring bloom, chlorophyll-*a* levels subsided and remained low during the summer, while SST continued to increase into the summer and peaked mid-summer (Fig. 2). The salinity of the mixed layer continued its decline to its lowest point a few weeks after the peak in SST. As chlorophyll-*a* levels declined and large-bodied spring copepods left the upper water column, smaller bodied copepods became dominant. Zooplankton able to efficiently ingest smaller particles (Frost, 1993) during the period of lower productivity were present in the summer community, which was comprised of both cladoceran species and the four most abundant taxa whose peak abundance occurred in the summer (*Oithona similis*, *Limacina helicina*, *Pseudocalanus* spp., and *Acartia longiremis*; Fig. 3).

Western PWS encompasses areas of deep water (+700 m) that harbor overwintering large calanoid copepods numerous enough to give rise to the subsequent year's copepod stocks for PWS and the shelf (Cooney et al., 2001a; Coyle and Pinchuk, 2005; Damkaer, 1977). The degree of connection between PWS and the adjacent shelf likely varies over time (embodied by the “river/lake” hypothesis of Cooney et al., 2001b). In general, water flows into PWS through Hinchinbrook entrance and out through Montague Strait (Halverson et al., 2012; Niebauer et al., 1994). This process allows transfer of *Neocalanus plumchrus/flemingeri* between PWS and the shelf (Cooney et al., 2001b; Coyle et al., 2013; Eslinger et al., 2001), which may account for the peak abundance in PWS *Neocalanus plumchrus/flemingeri* generally preceding that of the shelf (Coyle and Pinchuk, 2005).

In autumn, SST continued to decline toward winter low temperatures after the mid-summer peak. During this time, daylight hours shorten while chlorophyll-*a* levels also continued to drop. The salinity of the mixed layer increased while the mixed layer depth decreased as the autumn storm cycle stimulated vertical mixing (see 4.2 for further details). Although this mixing can induce small ephemeral phytoplankton blooms (Eslinger et al., 2001), observed chlorophyll-*a* concentrations did not suggest that this occurred during our study (Fig. 2). Zooplankton abundance continued to decline during this time. Sound-wide, the variable summer communities converged into a uniform zooplankton assemblage characterized by gelatinous carnivores including ctenophores, cnidarian medusae, and larvaceans. The SEA program also reported an increase in biomass of these plankters during the autumn (Cooney et al., 2001b).

#### 4.2. Climatic shifts and zooplankton variation

This 8-year study spans a wide range of environmental conditions that may explain the large interannual variability in zooplankton abundance (Fig. 4). From spring 2010 through 2013, the Pacific Decadal Oscillation index (PDO; Mantua et al., 1997) was negative, which usually corresponds to cooler than average temperatures in the GOA. Temperatures in PWS were also cooler than average during this time (Fig. 2) and coincided with the three years of highest zooplankton abundance (2010–2012, Fig. 4). In January 2014, the PDO index became positive and very large temperature anomalies, as much as 3 °C above average, were observed in the central GOA (Bond et al., 2015). The post-2013 warm water anomaly is hypothesized to be the result of an inhibition in winter storm mixing by a persistent atmospheric high pressure ridge (Swain, 2015) and has coincided with numerous changes to the marine ecosystems of the North Pacific including changes in the abundance and species composition of plankton populations (Batten et al., 2017). Zooplankton abundance in PWS in 2014 and 2015 was significantly lower than years prior to the change in PDO. Temperature

anomalies in PWS shifted towards positive at the same time (Fig. 2) presumably under the same forcing. Severe ENSO events, such as the 2014/2015 event (NOAA NWFSC, 2015), also contributed to warmer than average temperatures in the GOA (Di Lorenzo and Mantua, 2016; Hermann et al., 2016).

Analysis of a 40-year time series of temperature and salinity (Campbell, this issue) showed a long-term warming trend in PWS at most depths ( $\sim 0.2^\circ\text{C decade}^{-1}$ , with considerable interannual variability), which may indicate that the thermal habitat for warm water associated species is becoming more widespread over time. The PWS winter-indicative copepods *Mesocalanus tenuicornis*, *Corycaeus anglicus*, and *Calanus pacificus* and the autumn-indicative *Paracalanus parvus* are typically dominant in off-shelf waters from California to Oregon late in the production season (Fleminger, 1967; Mackas and Galbraith, 2002; Morgan et al., 2003; Peterson, 1972; Peterson and Keister, 2003). Their populations increase in warm waters particularly during/after ENSO events (Cooney and Coyle, 1985; Coyle and Pinchuk, 2003; Mackas et al., 2001; Peterson and Keister, 2003). The winter-indicative calanoid copepod *Mesocalanus tenuicornis* was first reported in PWS in 1983 (Cooney and Coyle, 1985) and high abundance has been reported in PWS in the following decades (Cooney et al. 2001b). The arrival and proliferation of these warm water species to PWS may be related to the overall warming in the region and the enhanced transport of water onto the shelf and into PWS (discussed in detail by Campbell, this issue) from southern regions. The amplified presence of these warm water copepods in the autumn/winter may be due to a life history strategy not suited for deeper overwintering in the PWS winter environment as compared to resident copepods that disappear from the upper water column during this food limited season (R. Hopcroft, University of Alaska Fairbanks, pers. comm.).

The ecological effects that increased water temperatures from the complex interactions of atmospheric forcing may have on PWS zooplankton communities and zooplankton predators are difficult to forecast. For juvenile herring, the quality of diet is a key factor in growth and survival (Norcross et al., 2001). The timing of larval emergence produces age-0 herring that begin feeding during the summer months in PWS. This timing historically coincides with peak zooplankton abundance mainly consisting of small energy-rich copepods (e.g. *Pseudocalanus* spp.) in the summer. Foy and Norcross (1999) described juvenile herring diet from Zaikof Bay in June of 1995 as having a similar composition to the “Summer” community reported here with small calanoid copepods and cladocerans comprising 80% of the diet. Age-0 herring rely on lipid reserves accumulated from these species to overwinter in PWS when prey is scarce (Foy and Paul, 1999; Norcross et al., 2001). We have shown that the zooplankton cycle from 2010 to 2015 follows this trend of small copepod and overall zooplankton abundance peaks in the summer. The ISA shows evidence of interannual shifts in the species composition of the prey field available to age-0 herring. The “Summer” community (Fig. 5) appears throughout this critical period of herring development in the summer in 2010–2012 then disappears in 2013. The scarce and sporadic reappearance of the “Summer” community in 2014 and 2015 and the dominance of the “Larval Spring” group during this time may have energetic consequences for age-0 herring overwintering success. The nutritional quality of many of these “Larval Spring” species are poorly understood (e.g. larval polychaetes). Future zooplankton research assessing PWS species specific energy density and lipid content would help to better understand the quality of the prey field available to herring and other predators.

#### Acknowledgements

The authors would like to thank Melissa May, Jessica Lueders-Dumont, Kayleen Fulton, and Rachel Ertz for their help in the field and in the lab, and the three anonymous reviewers of this manuscript for their insight and recommendations.

#### Funding

The research described in this paper was supported by the Exxon Valdez Oil Spill Trustee Council [project number: 10100132[TS8201]A]. However, the findings and conclusions presented by the authors are their own and do not necessarily reflect the views or position of the Trustee Council.

#### Appendix A. Supporting information

Supplementary data associated with this article can be found in the online version at <http://dx.doi.org/10.1016/j.dsr2.2017.08.016>.

#### References

- Abramova, E., Tuschling, K., 2005. A 12-year study of the seasonal and interannual dynamics of mesozooplankton in the Laptev Sea: significance of salinity regime and life cycle patterns. *Glob. Planet. Change* 48, 141–164.
- Batten, S.D., Raitos, D.E., Danielson, S., Hopcroft, R., Coyle, K., McQuatter-Gollop, A., 2017. Interannual variability in lower trophic levels on the Alaskan Shelf. *Deep-Sea Res. II*. <http://dx.doi.org/10.1016/j.dsr2.2017.04.023>.
- Bond, N.A., Cronin, M.F., Freeland, H., Mantua, N., 2015. Causes and impacts of the 2014 warm anomaly in the NE Pacific. *Geophys. Res. Lett.* 42, 3414–3420.
- Boufadel, M.C., Geng, X., Short, J., 2016. Bioremediation of the Exxon Valdez oil in Prince William Sound beaches. *Mar. Pollut. Bull.* 113, 158–164.
- Campbell, R.W., Hydrographic trends in Prince William Sound, Alaska, 1960–2013, *Deep-Sea Res. II* In Press, 10.1016/j.dsr2.2017.08.014.
- Clarke, K.R., Ainsworth, M., 1993. A method of linking multivariate community structure to environmental variables. *Mar. Ecol. Prog. Ser.* 92, 205–219.
- Cooney, R.T., 1986. The seasonal occurrence of *Neocalanus cristatus*, *Neocalanus plum-chirus*, and *Eucalanus bungii* over the northern Gulf of Alaska. *Cont. Shelf Res.* 5, 541–553.
- Cooney, R.T., Coyle, K.O., 1985. The occurrence of the subtropical copepod, *Mesocalanus tenuicornis*, in Columbia Bay, Prince William Sound, Alaska. *Crustaceana*. 49, 310–313.
- Cooney, R.T., Allen, J.R., Bishop, M.A., Eslinger, D.L., Kline, T., Norcross, B.L., McRoy, C.P., Milton, J., Olsen, J., Patrick, V., Paul, A.J., Salmon, D., Scheel, D., Thomas, G.L., Vaughn, S.L., Willette, T.M., 2001a. Ecosystem control of pink salmon (*Oncorhynchus gorbuscha*) and Pacific herring (*Clupea pallasii*) populations in Prince William Sound AK. *Fish. Oceanogr.* 10 (Suppl. 1), S1–S13.
- Cooney, R.T., Coyle, K.O., Stockmar, E., Stark, C., 2001b. Seasonality in surface-layer net zooplankton communities in Prince William Sound, Alaska. *Fish. Oceanogr.* 10 (Suppl. 1), S97–S109.
- Coyle, K.O., Pinchuk, A.I., 2003. Annual cycle of zooplankton abundance, biomass, and production on the northern Gulf of Alaska shelf, October 1997 through October 2000. *Fish. Oceanogr.* 12, 327–338.
- Coyle, K.O., Pinchuk, A.I., 2005. Seasonal cross-shelf distribution of major zooplankton taxa on the northern Gulf of Alaska shelf relative to water mass properties, species depth preferences and vertical migration behavior. *Deep-Sea Res. II* 52, 217–245.
- Coyle, K.O., Gibson, G.A., Hedstrom, K., Hermann, A.J., Hopcroft, R.R., 2013. Zooplankton biomass, advection, and production on the northern Gulf of Alaska shelf from simulations and field observations. *J. Mar. Syst.* 128, 185–207.
- Damkaer, D.M., 1977. Initial zooplankton investigations in Prince William Sound, Gulf of Alaska, and lower Cook Inlet. Environmental Assessment of the Alaska Continental Shelf. Annual Reports of the Principal Investigators, for the year ending 1997. Receptors – Fish, Littoral, Benthos, 137–274. U.S. Dept. of Commerce, Washington D.C.
- De Caceres, M., 2013. How to Use Indicspecies Package. R Package Version 1.7.1. <https://cran.r-project.org/web/packages/indicspecies/vignettes/indicspeciesTutorial.pdf>.
- De Caceres, M., Legendre, P., 2009. Associations between species and groups of sites: indices and statistical inference. *Ecology*. <http://sites.google.com/site/miqueldecaceres/>.
- Di Lorenzo, E., Mantua, N., 2016. Multi-year persistence of the 2014/15 North Pacific marine heatwave. *Nat. Clim. Change* 6, 1042–1048.
- Doubleday, A.J., Hopcroft, R.R., 2015. Interannual patterns during spring and late summer of larvaceans and pteropods in the coastal Gulf of Alaska, and their relationship to pink salmon survival. *J. Plankton Res.* 37, 134–150.
- Dufrene, M., Legendre, P., 1997. Species assemblages and indicator species: the need for a flexible asymmetrical approach. *Ecol. Monogr.* 67, 345–366.
- Eslinger, D.L., Cooney, R.T., McRoy, C.P., Ward, A., Kline, T.C., Simpson, E.P., Wang, J., Allen, J.R., 2001. Plankton dynamics: observed and modeled responses to physical conditions in Prince William Sound, Alaska. *Fish. Oceanogr.* 10 (Suppl. 1), S81–S96.
- Fleminger, A., 1967. Distributional atlas of calanoid copepods in the California current region, Part II. *CalCOFI Atlas* 7, 213.
- Foy, R.J., Norcross, B.L., 1999. Spatial and temporal variability in the diet of juvenile Pacific herring (*Clupea pallasii*) in Prince William Sound, Alaska. *Can. J. Zool.* 77, 697–706.
- Foy, R.J., Paul, A.J., 1999. Winter feeding and changes in somatic energy content of age-0 Pacific herring in Prince William Sound, Alaska. *Trans. Am. Fish. Soc.* 128, 1193–1200.

## Appendix B

Open Access manuscript available at <https://doi.org/10.1016/j.dsr2.2017.08.016>

C.A.E. McKinstry, R.W. Campbell

Deep-Sea Research Part II 147 (2018) 69–78

- Frost, B.W., 1993. A modelling study of processes regulating plankton standing stock and production in the open subarctic Pacific Ocean. *Prog. Oceanogr.* 32, 17–56.
- Grant, U.S., Higgins, D.F., 1910. Reconnaissance of the geology and mineral resources of Prince William Sound, Alaska. *Bull. US Geol. Surv.* 443, 1–89.
- Halverson, M.J., Bélanger, C., Gay, S.M., 2012. Season transport variations in the straits connecting Prince William Sound to the Gulf of Alaska. *Cont. Shelf Res.* 63, S63–S78. <http://dx.doi.org/10.1016/j.csr.2012.06.017>.
- Hastie, T., Tibshirani, R., 1986. Generalized additive models. *Stat. Sci.* 1, 297–318.
- Henson, S.A., 2007. Water column stability and spring bloom dynamics in the Gulf of Alaska. *J. Mar. Res.* 65, 715–736.
- Hermann, A.J., Ladd, C., Cheng, W., Curchitser, E.N., Hedstrom, K., 2016. A model-based examination of multivariate physical modes in the Gulf of Alaska. *Deep-Sea Res. II* 132 (2016), 68–89.
- Integrated Taxonomic Information System, 1996. <http://www.itis.gov> (Accessed 27 July 2016).
- Keister, J.E., Peterson, W.T., 2003. Zonal and seasonal variations in zooplankton community structure off the central Oregon coast, 1998–2000. *Prog. Oceanogr.* 57, 341–361.
- Keister, J.E., Peterson, W.T., Pierce, S.D., 2009. Zooplankton distribution and cross-shelf transfer of carbon in an area of complex mesoscale circulation in the northern California Current. *Deep-Sea Res. I* 56, 212–231.
- Keister, J.E., Di Lorenzo, E., Morgan, C.A., Combes, V., Peterson, W.T., 2011. Zooplankton species composition is linked to ocean transport in the Northern California Current. *Glob. Change Biol.* 17, 2498–2511.
- Legendre, P., Legendre, L., 2012. 3rd ed. *Numerical Ecology* 513. Elsevier, Amsterdam, The Netherlands, pp. 599–604 (pp).
- Mantua, N.J., Hare, S.R., Zhang, Y., Wallace, J.M., Francis, R.C., 1997. A Pacific inter-decadal climate oscillation with impacts on salmon production. *Bull. Am. Meteorol. Soc.* 78, 1069–1079.
- Mackas, D.L., Sefton, H., Miller, C.B., Raich, A., 1993. Vertical habitat partitioning by large calanoid copepods in the oceanic subarctic Pacific during Spring. *Prog. Oceanogr.* 32, 259–294.
- Mackas, D.L., Thomson, R.E., Galbraith, M., 2001. Changes in the zooplankton community of the British Columbia continental margin, 1985–1999, and their covariation with oceanographic conditions. *Can. J. Fish. Aquat. Sci.* 58, 685–702.
- Mackas, D.L., Galbraith, M.D., 2002. Zooplankton distribution and dynamics in a North Pacific eddy of coastal origin: 1. Transport and loss of continental margin species. *J. Oceanogr.* 58, 725–738.
- Manley, B.F.J., 1994. *Multivariate Statistical Methods*, 2nd ed. Chapman & Hall, London, pp. 215.
- McEwen, G.F., Johnson, M.W., Folsom, T.R., 1954. A statistical analysis of the performance of the Folsom plankton sample splitter, based upon test observations. *Arch. Met. Geoph. Biokl. A.* 7, 502.
- Morgan, C.A., Peterson, W.T., Emmett, R.L., 2003. Onshore-offshore variations in copepod community structure off the Oregon coast during the summer upwelling season. *Mar. Ecol. Prog. Ser.* 249, 223–236.
- Niebauer, H.J., Royer, T.C., Weingartner, T.J., 1994. Circulation of Prince William Sound, Alaska. *J. Geophys. Res.* 99, 14113–14126.
- NOAA NWFS, 2015. *Annual summary of ocean ecosystem indicators for 2015 and pre-season outlook for 2016*. <https://www.nwfsc.noaa.gov/research/divisions/te/estuarine/oelp/b/latest-updates.cfm>.
- Oksanen, J., Blanchet, F.G., Friendly, M., Kindt, R., Legendre, P., McGinn, D., Minchin, P.R., O'Hara, R.B., Simpson, G.L., Solymos, P., Henry, M., Stevens, H., Szocs, E., Wagner, H., 2016. *Vegan: Community Ecology Package*. R package version 2.4-0. <https://CRAN.R-project.org/package=vegan>.
- Peterson, W.T., 1972. Distribution of pelagic Copepoda off the coasts of Washington and Oregon during 1961 and 1962. In: Alverson, D.L. (Ed.), *The Columbia River Estuary and Adjacent Ocean Waters*. University of Washington Press, Seattle, pp. 313–343.
- Peterson, W.T., Keister, J.E., 2003. Interannual variability in copepod community composition at a coastal station in the northern California current: a multivariate approach. *Deep-Sea Res. II* 50, 2499–2517.
- Purcell, J.E., Sturdevant, M.V., 2001. Prey selection and dietary overlap among zooplanktivorous jellyfish and juvenile fishes in Prince William Sound, Alaska. *Mar. Ecol. Prog. Ser.* 210, 67–83.
- R Development Core Team, 2005. *A Language and Environment for Statistical Computing*. R Foundation for Statistical Computing, Vienna, Austria. <https://www.R-project.org/>.
- Sousa, L., Coyle, K.O., Bary, R.P., Weingartner, T.J., Hopcroft, R.R., 2017. Climate-related variability in abundance of mesozooplankton in the northern Gulf of Alaska 1998–2009. *Deep-Sea Res. II* 132, 122–135.
- Swain, D.L., 2015. A tale of two California droughts: Lessons amidst record warmth and dryness in a region of complex physical and human geography. *Geophys. Res. Lett.* 42, 9999–10003.
- Thomson, R.E., Pine, I.V., 2003. Estimating mixed layer depth from oceanic profile data. *J. Atmos. Ocean. Tech.* 20 (319), 329.
- Willette, T.M., 2001. Foraging behavior of juvenile pink salmon (*Oncorhynchus gorbuscha*) and size-dependent predation risk. *Fish. Oceanogr.* 10, 97–109.
- Wood, S.N., 2004. Stable and efficient multiple smoothing parameter estimation for generalized additive models. *J. Am. Stat. Assoc.* 99, 673–686.